

# ICE, CLOUD, and Land Elevation Satellite (ICESat-2) Project:

## Algorithm Theoretical Basis Document (ATBD) for ATL02 (Level 1B) Data Product Processing

**Prepared By:**

|                      |             |          |
|----------------------|-------------|----------|
| Anthony J. Martino   | NASA GSFC   | Code 615 |
| Megan R. Bock        | ADNET       | Code 615 |
| Catherine Gosmeyer   | ADNET       | Code 615 |
| Christopher Field    | Sigma Space | Code 615 |
| Thomas A. Neumann    | NASA GSFC   | Code 615 |
| David W. Hancock III | SGT         | Code 615 |
| Robert L. Jones III  | Sigma Space | Code 615 |
| Philip W. Dabney     | NASA GSFC   | Code 694 |
| Charles E. Webb      | SGT         | Code 615 |
| Jeff Lee             | SGT         | Code 615 |

**Document #: ICESat-2-SIPS-SPEC-0150 (alt: ICESat-2-SIPS-SPEC-1610)**

**Applicable Software Release: 005**

**Document Version Date: November 16, 2021**

## Abstract

This Algorithm Theoretical Basis Document, or ATBD, describes the methodology used to convert the Level 1A (L1A) parsed, partially reformatted, time ordered telemetry data into the Level 1B (L1B) science unit converted time ordered telemetry, along with some preliminary products corrected for known system calibrations and environmental effects that will be used in the derivation of the next level of data products. These data are intended to be an end product for system level quality control analysis. They are also a source file for use in the Level 2 products and the Precise Pointing Determination (PPD) and Precise Orbit Determination (POD) solutions.

The list of L1B products includes, but is not limited to: all data, including house-keeping and ancillary data, converted to scientific units; reconstructed absolute time-bias corrected Time of Day (TOD) for all laser fire times and time tagged data; Time of Flight (TOF) for each photon event corrected for known system time biases and time base errors derived from the GPS 1 PPS and PCE self-calibration channels assuming a constant speed of light (ignoring atmospheric effects, for the moment); raw histogram atmospheric profiles range corrected to height and aggregated to 25-Hz frames; and the approximate location of each beam footprint on the WGS84 reference surface using the Spacecraft GPS position and Spacecraft pointing control data to allow for quick searching of data based on footprints on the ground.

All data are stored in NCSA HDF5 formatted files.

CHECK TDMS / NSIDC TO VERIFY THAT THIS IS THE CORRECT VERSION PRIOR TO USE.

## Preface

This document is the Algorithm Theoretical Basis Document for the Level 1B processing to be implemented at the ICESat-2 Science Investigator-led Processing System (SIPS). The SIPS supports the ATLAS (Advanced Topographic Laser Altimeter System) instrument on the Ice, Cloud, and Land Elevation (ICESat-2) Spacecraft and encompasses the ATLAS Science Algorithm Software (ASAS) and the Scheduling and Data Management System (SDMS). The science algorithm software will produce Level-0 through Level-4 standard data products as well as the associated product quality assessments and metadata information.

In this document, a requirement is identified by “shall,” a good practice by “should,” permission by “may” or “can,” expectation by “will,” and descriptive material by “is.”

The ICESat-2 Project Science Office (PSO), assumes responsibility for control of this document and updates it, as required, as algorithms are refined or to meet the needs of the ICESat-2 SIPS. Reviews of this document are performed when appropriate and as needed updates to this document are made. Changes to this document will be made by complete revision.

Changes to this document require prior approval of the Change Authority listed on the signature page. Proposed changes shall be submitted to the ICESat-2 PSO, along with supportive material justifying the proposed change.

Questions or comments concerning this document should be addressed to:

Thomas Neumann, ICESat-2 Project Scientist  
Mail Stop 615  
Goddard Space Flight Center  
Greenbelt, Maryland 20771

## List of Open TBDs/TBRs

| Item No.     | Location | Summary  |
|--------------|----------|--|
| <b>TBR-2</b> | 3.10     | Expansion/definition of QA metrics and monitoring is needed. |
|              |          |  |
|              |          |  |
|              |          |  |
|              |          |  |
|              |          |  |

# Table of Contents

|  |           |
|--|-----------|
| <b>ABSTRACT</b> .....  | <b>2</b>  |
| <b>PREFACE</b> .....   | <b>3</b>  |
| <b>LIST OF OPEN TBDS/TBRS</b> .....  | <b>4</b>  |
| <b>TABLE OF CONTENTS</b> .....   | <b>5</b>  |
| <b>LIST OF FIGURES</b> .....   | <b>8</b>  |
| <b>LIST OF TABLES</b> .....  | <b>9</b>  |
| <b>ACRONYMS AND TERMINOLOGY</b> .....  | <b>11</b> |
| <b>1 INTRODUCTION</b> .....  | <b>13</b> |
| 1.1 BACKGROUND.....  | 13        |
| 1.2 TERMINOLOGY, NOTATION, AND CONVENTIONS .....   | 15        |
| 1.3 DESCRIPTION OF RELEVANT HARDWARE INTERACTIONS .....  | 17        |
| 1.4 INSTRUMENT DATA.....   | 25        |
| 1.4.1 <i>Data Products</i> .....   | 25        |
| 1.5 ATL02 SPECIFIC INFORMATION.....  | 26        |
| 1.5.1 <i>Knowledge of Instrument Configuration</i> .....   | 26        |
| 1.5.2 <i>Control File &amp; Overrides</i> .....  | 28        |
| 1.5.3 <i>Relevant Calibrations</i> .....   | 28        |
| 1.5.4 <i>General Data QA Philosophy</i> .....  | 29        |
| <b>2 TIME OF DAY (TOD) CALCULATION</b> .....   | <b>30</b> |
| 2.1 CLOCKS AND TIMING RELATIONSHIPS .....  | 30        |
| 2.2 GROUND RULES & ASSUMPTIONS .....   | 31        |
| 2.3 VARIABLE DEFINITIONS AND NOTATION SYNTAX.....  | 31        |
| 2.4 ESTABLISHING THE USO RULER CLOCK SCALE FACTOR .....  | 33        |
| 2.5 CALCULATION OF EVENT TIME OF DAY .....   | 34        |
| 2.5.1 <i>Constructing AMET Counter Values</i> .....  | 35        |
| 2.5.2 <i>Determination of GPS Time of First T0 in Major Frame</i> .....                                    | 36        |
| 2.5.3 <i>Determining Effective Shot (T0) Count within Major Frame</i> .....                                | 37        |
| 2.5.4 <i>Calculation of GPS Time at T0 of Shot</i> .....   | 38        |
| 2.5.5 <i>Calculation of GPS Time of Leading Lower of Shot and Delta Time</i> .....                         | 38        |
| 2.5.6 <i>An Alternative View: Calculation of GPS Time of Leading Lower of Shot Expressed in AMET</i> ..... | 39        |
| 2.5.7 <i>Time Alignment of PCE Data</i> .....  | 39        |
| 2.6 DEALING WITH MISSING DATA.....   | 41        |
| 2.7 DATA QUALITY MONITORING.....   | 41        |
| 2.7.1 <i>Quality Check of TOD Calculation Inputs</i> .....   | 42        |
| 2.7.2 <i>Confirmation of TOD Calculations and Data Alignment</i> .....                                     | 43        |
| 2.7.3 <i>Data Screening Mechanisms &amp; Associated Responses</i> .....                                    | 44        |
| 2.8 DATA PRODUCTS .....  | 44        |
| <b>3 TIME OF FLIGHT CALCULATION</b> .....  | <b>46</b> |
| 3.1 GROUND RULES & ASSUMPTIONS .....   | 46        |
| 3.2 VARIABLE DEFINITIONS AND NOTATION SYNTAX.....  | 47        |
| 3.3 MAPPING OF TRANSMIT AND RETURN EVENT INFORMATION .....   | 51        |
| 3.3.1 <i>Laser Start Pulse Detector Channels</i> .....   | 51        |
| 3.3.2 <i>Photon Detector Channels</i> .....  | 51        |
| 3.4 CALCULATION OF START TIME .....  | 52        |
| 3.4.1 <i>Calculation of Leading Lower Start Event Coarse Time</i> .....                                    | 53        |
| 3.4.2 <i>Calculation of Other Element Start Event Coarse Time</i> .....                                    | 53        |
| 3.4.3 <i>Calculation of Transmit Event Fine Time</i> .....   | 53        |

|          |   |            |
|----------|---|------------|
| 3.4.4    | <i>Calculation of Precise Start Event Times</i> .....                           | 56         |
| 3.4.5    | <i>Calculation of Precise Start Time &amp; Overall Timing Uncertainty</i> ..... | 57         |
| 3.4.6    | <i>Calculation of Pulse Widths and Start Skews</i> .....                        | 58         |
| 3.5      | CALCULATION OF RECEIVE EVENT TIMES.....   | 59         |
| 3.5.1    | <i>Calculation of Receive Event Coarse Time</i> .....                           | 60         |
| 3.5.2    | <i>Calculation of Receive Event Fine Time</i> .....                             | 60         |
| 3.5.3    | <i>Assigning Range Window Start Value</i> .....                                 | 60         |
| 3.5.4    | <i>Determining Downlink Band Offset</i> .....                                   | 60         |
| 3.5.5    | <i>Calculation of Precise Event Times</i> .....                                 | 61         |
| 3.6      | CALCULATION OF NOMINAL TIME OF FLIGHT (TOF).....                                | 62         |
| 3.7      | IDENTIFICATION OF DUPLICATE RETURN-EVENT TIME TAGS.....                         | 63         |
| 3.8      | DETERMINING TIMES OF RANGE WINDOW AND DOWNLINK BAND FEATURES.....               | 64         |
| 3.8.1    | <i>Calculation of Range Window Start Time</i> .....                             | 64         |
| 3.8.2    | <i>Calculation of Range Window Width in Units of Time</i> .....                 | 64         |
| 3.8.3    | <i>Calculation of Downlink Band Start Time</i> .....                            | 64         |
| 3.8.4    | <i>Calculation of Downlink Band Width in Units of Time</i> .....                | 65         |
| 3.8.5    | <i>Times of Flight Outside of DLB limits</i> .....                              | 65         |
| 3.9      | A WORD ON ZERO RANGE POINT.....   | 65         |
| 3.10     | DATA SCREENING MECHANISMS & ASSOCIATED RESPONSES.....                           | 66         |
| 3.11     | TOF-RELATED PARAMETERS INCLUDED IN ATL02 OUTPUT FILE.....                       | 68         |
| <b>4</b> | <b>TRANSMITTER ECHO PATH</b> .....  | <b>70</b>  |
| 4.1      | GROUND RULES AND ASSUMPTIONS.....   | 70         |
| 4.2      | VARIABLE DEFINITIONS AND NOTATION SYNTAX.....                                   | 71         |
| 4.3      | DETERMINING IF THE TE IS CAPTURED BY A DLB.....                                 | 73         |
| 4.4      | CALCULATION OF TEP TIME OF FLIGHT (TE_TOF).....                                 | 74         |
| 4.5      | FLAGGING OF TEP PHOTONS.....  | 75         |
| 4.6      | DATA SCREENING MECHANISMS & ASSOCIATED RESPONSES.....                           | 76         |
| 4.7      | DATA PRODUCTS.....  | 76         |
| <b>5</b> | <b>RADIOMETRY</b> .....   | <b>78</b>  |
| 5.1      | DATA PRODUCTS.....  | 78         |
| 5.2      | TRANSMITTED ENERGY.....   | 78         |
| 5.2.1    | <i>Total Transmitted Energy</i> .....   | 79         |
| 5.2.2    | <i>Individual Transmitted Beam Energies</i> .....                               | 82         |
| 5.3      | SMALL-SIGNAL RECEIVER SENSITIVITY.....  | 83         |
| 5.3.1    | <i>Maximum Sensitivity</i> .....  | 84         |
| 5.3.2    | <i>Background Sensitivity</i> .....   | 88         |
| 5.3.3    | <i>Return Sensitivity</i> .....   | 88         |
| 5.4      | DEAD TIME EFFECTS ON RADIOMETRY.....  | 93         |
| 5.5      | DATA SCREENING MECHANISMS & ASSOCIATED RESPONSES.....                           | 93         |
| <b>6</b> | <b>POINTING AND GEOLOCATION</b> .....   | <b>96</b>  |
| <b>7</b> | <b>ATMOSPHERIC HISTOGRAMS</b> .....   | <b>97</b>  |
| 7.1      | ATMOSPHERIC HISTOGRAM NOMINAL CALCULATIONS.....                                 | 97         |
| 7.2      | CONSTRUCTION OF THE ATMOSPHERIC HISTOGRAM.....                                  | 98         |
| 7.3      | ATMOSPHERIC HISTOGRAM PARAMETERS INCLUDED IN ATL02 OUTPUT FILE.....             | 99         |
| 7.4      | DATA SCREENING MECHANISMS & ASSOCIATED RESPONSES.....                           | 100        |
| <b>8</b> | <b>OTHER DATA &amp; DATA PASS-THROUGHS</b> .....                                | <b>101</b> |
| 8.1      | ASSIGNMENT OF <i>DELTA_TIME</i> FOR NON-ALTIMETRIC SCIENCE DATA.....            | 101        |
| 8.1.1    | <i>Determining delta_time for Packets without a 1 PPS Reference</i> .....       | 101        |
| 8.2      | ANCILLARY DATA (/ANCILLARY_DATA).....   | 103        |
| 8.3      | STATUS HKT DATA (/ATLAS/HOUSEKEEPING/STATUS).....                               | 103        |
| 8.4      | THERMAL & ELECTRICAL HKT DATA (/ATLAS/HOUSEKEEPING/MEB, PDU, THERMAL).....      | 103        |

|      |   |     |
|------|---|-----|
| 8.5  | MCE HKT DATA (/ATLAS/HOUSEKEEPING/MCE_POSITION).....  | 104 |
| 8.6  | RADIOMETRY HKT DATA (/ATLAS/HOUSEKEEPING/LASER_ENERGY_*) .....                                  | 104 |
| 8.7  | POINTING, POSITION, & VELOCITY HKT DATA (/ATLAS/HOUSEKEEPING/POINTING, POSITION_VELOCITY) ..... | 104 |
| 8.8  | TIME AT THE TONE (/ATLAS/HOUSEKEEPING/TIME_AT_THE_TONE/).....                                   | 105 |
| 8.9  | ALGORITHM SCIENCE DATA (/ATLAS/PCEX/ALGORITHM_SCIENCE/).....                                    | 105 |
| 8.10 | PCE BACKGROUND DATA (/ATLAS/PCEX/BACKGROUND).....   | 105 |
| 8.11 | SBC EXTRAPOLATION TASK TELEMETRY (/ATLAS/PCEX/SXP_SSR_*).....                                   | 106 |
| 8.12 | LRS DATA (/LRS) .....   | 106 |
| 8.13 | SPACECRAFT DATA (/GPSR/*, /ORBIT_INFO, /SC/*).....  | 107 |
| 8.14 | QUALITY ASSESSMENT (/QUALITY_ASSESSMENT) .....  | 107 |

## List of Figures

|  |    |
|--|----|
| FIGURE 1: THE PRIMARY MEASUREMENTS OF THE ATLAS INSTRUMENT .....                                       | 13 |
| FIGURE 2: ATLAS IDEALIZED BEAM AND FOOTPRINT .....   | 14 |
| FIGURE 3: ATLAS SYSTEM-LEVEL COMPONENTS RELEVANT TO THE COMPUTATIONS DESCRIBED IN THE ATLO2 ATBD ..... | 18 |
| FIGURE 4: TIMING APPARATUS USES HIERARCHICALLY NESTED, MULTI-RESOLUTION TIME SCALES .....              | 19 |
| FIGURE 5: BLOCK DIAGRAM OF ATLAS TIMEKEEPERS .....   | 21 |
| FIGURE 6: PCE ARCHITECTURE BLOCK DIAGRAM.....  | 22 |
| <b>FIGURE 7: PCE COARSE AND FINE TIME</b> .....  | 24 |
| FIGURE 8: ICESAT-2 DATA PROCESSING FLOW OF ICESAT-2 DATA.....  | 26 |
| FIGURE 9: PROGRESSION OF TIME OF DAY CALCULATION.....  | 35 |
| FIGURE 10 : LASER PULSE IS DETECTED USING .....  | 51 |
| <b>FIGURE 11: SUMMARY OF TOF CALCULATION COMPONENTS</b> .....  | 63 |
| FIGURE 12: SCHEMATIC OF THE DATA FLOW TO DETERMINE BIAS-CORRECTED PHOTON RANGES.....                   | 66 |
| FIGURE 13: POSSIBLE RELATIONSHIPS BETWEEN A TE AND DLB .....   | 73 |
| FIGURE 14: SIMPLIFIED TE_TOF REFERENCES.....   | 75 |
| FIGURE 15: TRANSMITTED ENERGY WORK/DATA FLOW.....  | 78 |
| FIGURE 16: RECEIVER SENSITIVITY WORK/DATA FLOW .....   | 84 |
| FIGURE 17: HISTOGRAM ALIGNMENT TECHNIQUE FOR ATMOSPHERIC HISTOGRAM GENERATION.....                     | 99 |



# List of Tables

|   |     |
|---|-----|
| TABLE 1: PHOTON COUNTING ELECTRONICS TERMINOLOGY .....  | 16  |
| TABLE 2: PRIMARY MEASUREMENTS .....   | 16  |
| TABLE 3: KEY ICESAT-2 / ATLAS PARAMETERS .....  | 17  |
| TABLE 4: KNOWLEDGE OF INSTRUMENT CONFIGURATION .....  | 27  |
| TABLE 5: USEFLAG VALUES.....  | 27  |
| TABLE 6: CAL PRODUCTS USED IN ATLO2 ATBD.....   | 28  |
| TABLE 7: SUMMARY OF SYNCHRONOUS TIME REFERENCES .....   | 30  |
| TABLE 8: GENERALIZED TOD CALCULATION NOTATION .....   | 31  |
| TABLE 9: DICTIONARY OF TOF DERIVATION VARIABLES .....   | 32  |
| TABLE 10: DIRECTIONS FOR SELECTION OF ANC27/CAL-10 VALUE.....   | 34  |
| TABLE 11: MISSING DATA SCENARIOS AND THEIR ASSOCIATED REPERCUSSION + MITIGATION .....   | 41  |
| TABLE 12: TOD DATA QUALITY MONITORING CRITERIA .....  | 44  |
| TABLE 13: <i>DELTA_TIME</i> PARAMETERS WRITTEN TO THE ATLO2 PRODUCT (VARIABLE DATA RATE).....   | 45  |
| TABLE 14: GENERALIZED TOF CALCULATION NOTATION .....  | 47  |
| TABLE 15: DICTIONARY OF TOF DERIVATION VARIABLES .....  | 47  |
| TABLE 16: LOGICAL MAPPING OF RETURN EVENT CHANNELS IDS .....  | 52  |
| TABLE 17: SUPER CHANNEL ASSIGNMENT ALGORITHM.....   | 52  |
| TABLE 18: DIRECTIONS FOR SELECTION OF CAL-17 VALUE .....  | 56  |
| TABLE 19: DIRECTIONS FOR SELECTION OF CAL-44 VALUE .....  | 57  |
| TABLE 20: MAPPING OF CASE, I, ACCORDING TO WHICH THRESHOLD DATA IS MISSING FROM SCIENCE DATA TELEMETRY (X DENOTES MISSING DATA) ..... | 58  |
| TABLE 21: ATLO1 PARAMETERS USED TO DESCRIBE RX TAGS.....  | 59  |
| TABLE 22: DOWNLINK BAND ASSIGNMENT AND IDENTIFICATION.....  | 61  |
| TABLE 23: DIRECTIONS FOR SELECTION OF CAL-49 VALUE .....  | 62  |
| TABLE 24: FILTER ALGORITHM TO REMOVE DUPLICATE RETURN-EVENT TIME TAGS .....   | 64  |
| TABLE 25: TOF DATA QUALITY MONITORING CRITERIA .....  | 66  |
| TABLE 26: TOF-RELATED PARAMETERS INCLUDED IN THE ATLO2 PRODUCT (AT 50HZ/MAJOR FRAME RATE) .....                                       | 69  |
| TABLE 27: TOF-RELATED PARAMETERS INCLUDED IN THE ATLO2 PRODUCT (AT 10KHZ/SHOT RATE) .....   | 69  |
| TABLE 28: TOF-RELATED PARAMETERS INCLUDED IN THE ATLO2 PRODUCT (AT VARIABLE/PHOTON RATE).....   | 69  |
| TABLE 29: GENERALIZED TE-TOF CALCULATION NOTATION .....   | 71  |
| TABLE 30: DICTIONARY OF TE_TOF DERIVATION VARIABLES.....  | 71  |
| TABLE 31: TEP DATA QUALITY MONITORING CRITERIA .....  | 76  |
| TABLE 32: TE-RELATED PARAMETERS INCLUDED IN THE ATLO2 PRODUCT (AT VARIABLE/PHOTON RATE) .....   | 77  |
| TABLE 33: TOTAL TRANSMITTED ENERGY VALUES REPORTED ON THE ATLO2 PRODUCT .....   | 79  |
| TABLE 34: DATA SOURCES FOR THE TOTAL TRANSMITTED ENERGY CALCULATION .....   | 80  |
| TABLE 35: ACCEPTABLE DATA INPUT RANGES FOR TRANSMITTED ENERGY CALCULATION .....   | 81  |
| TABLE 36: EXPECTED OUTPUT RANGES FOR TOTAL TRANSMITTED ENERGY CALCULATION.....  | 82  |
| TABLE 37: INDIVIDUAL TRANSMITTED BEAM ENERGY VALUES REPORTED ON THE ATLO2 PRODUCT.....  | 83  |
| TABLE 38: DATA SOURCES FOR MAXIMUM SENSITIVITY CALCULATION.....   | 87  |
| TABLE 39: INPUT DATA RANGE FOR MAXIMUM SENSITIVITY CALCULATION .....  | 87  |
| TABLE 40: OUTPUT OF BACKGROUND SENSITIVITY CALCULATION.....   | 88  |
| TABLE 41: EXPECTED OUTPUT RANGE FOR BACKGROUND SENSITIVITY CALCULATION.....   | 88  |
| TABLE 42: OUTPUT OF RETURN SENSITIVITY CALCULATION.....   | 90  |
| TABLE 43: DATA SOURCES FOR RETURN SENSITIVITY CALCULATION.....  | 92  |
| TABLE 44: INPUT DATA RANGES FOR RETURN SENSITIVITY CALCULATION .....  | 93  |
| TABLE 45: OUTPUT DATA RANGE FOR RETURN SENSITIVITY CALCULATION.....   | 93  |
| TABLE 46: RADIOMETRY DATA QUALITY MONITORING CRITERIA.....  | 93  |
| TABLE 47: GENERALIZED ATMOSPHERIC HISTOGRAM CALCULATION NOTATION.....   | 97  |
| TABLE 48: DICTIONARY OF ATMOSPHERIC HISTOGRAM DERIVATION VARIABLES .....  | 98  |
| TABLE 49: ATMOSPHERIC HISTOGRAM PARAMETERS ON THE ATLO2 PRODUCT (25HZ DATA RATE) .....  | 100 |
| TABLE 50: ATMOSPHERIC HISTOGRAM QUALITY MONITORING CRITERIA .....   | 100 |
| TABLE 51: HOUSEKEEPING PACKET CONFIGURATIONS.....   | 102 |
| TABLE 52: REFERENCED DOCUMENTIT .....   | 108 |
| TABLE 53: ATLO2 PARAMETERS USED TO PROVIDE UNIQUE PHOTON IDENTIFICATION .....   | 109 |

TABLE 54: MAPPING OF EQUIVALENT DATA PARAMETERS ACROSS ATL01, ATL02, AND ATL03.....109

## Acronyms and Terminology

| Acronym                  | Definition  |
|--------------------------|---|
| <b>AMET</b>              | ATLAS Mission Elapsed Time  |
| <b>AMCS</b>              | Alignment Monitoring Control System   |
| <b>ANC##</b>             | Ancillary Data File   |
| <b>APID</b>              | Application Identifier (ID)   |
| <b>ASAS</b>              | ATLAS Science Algorithm Software  |
| <b>ASC</b>               | ATLAS Serial Card   |
| <b>ATBD</b>              | Algorithm Theoretical Basis Document  |
| <b>ATL##</b>             | ATLAS Science Data Product  |
| <b>ATLAS</b>             | Advanced Topographic Laser Altimeter System   |
| <b>CAL-##</b>            | Calibration Product   |
| <b>CC</b>                | Coarse Clock or Coarse Count  |
| <b>CCSDS</b>             | Consultative Committee for Space Data Systems   |
| <b>DAA</b>               | Detector Array Assembly   |
| <b>DEM</b>               | Detector Electronics Module   |
| <b>DFC</b>               | Data Flow Controller (one of three FPGAs on a PCE card)                                 |
| <b>DLB</b>               | Downlink Band   |
| <b>DLBO</b>              | Downlink Band Offset  |
| <b>DLBW</b>              | Downlink Band Width   |
| <b>DNF</b>               | Did Not Finish  |
| <b>DOM</b>               | Detector Optics Module  |
| <b>DSM</b>               | Detector Select Mechanism   |
| <b>FC</b>                | Fine Count  |
| <b>FPGA</b>              | Field-Programmable Gate Array   |
| <b>FSRA</b>              | Flight Science Receiver Algorithm   |
| <b>FSW</b>               | Flight Software   |
| <b>GLAS</b>              | Geoscience Laser Altimeter System   |
| <b>GMT</b>               | Greenwich Mean Time   |
| <b>GPS</b>               | Global Positioning System   |
| <b>GPSR</b>              | GPS Receiver  |
| <b>Granule</b>           | The smallest unit of subject data processed at any one time at a given level (e.g. L1B) |
| <b>HDF5</b>              | Hierarchical Data Format  |
| <b>HISTO</b>             | Histogrammer FPGA   |
| <b>HKT</b>               | Housekeeping FPGA   |
| <b>ICD</b>               | Interface Control Document  |
| <b>ICESat / ICESat-2</b> | Ice, Cloud, and land Elevation Satellite  |
| <b>IMET</b>              | Instrument Mission Elapsed Time (Maintained on each PCE; 3 values)                      |
| <b>ISF</b>               | Instrument Support Facility   |
| <b>LIDAR</b>             | Light Detection and Ranging System  |
| <b>LL</b>                | Leading Lower (start component)   |

| Acronym      | Definition   |
|--------------|--|
| <b>LRS</b>   | Laser Reference System   |
| <b>LU</b>    | Leading Upper (start component)  |
| <b>MEB</b>   | Main Electronics Box   |
| <b>MF</b>    | Major Frame  |
| <b>MKS</b>   | System of units based on measuring lengths in meters, mass in kilograms, and time in seconds |
| <b>NSIDC</b> | National Snow and Ice Data Center  |
| <b>OFM</b>   | Optical Filter Module  |
| <b>PCE</b>   | Photon Counting Electronics  |
| <b>POD</b>   | Precision Orbit Determination  |
| <b>PPD</b>   | Precision Pointing Determination   |
| <b>PPS</b>   | Pulse Per Second   |
| <b>PSO</b>   | Project Science Office   |
| <b>QA</b>    | Quality Assurance  |
| <b>RSS</b>   | Root Sum Square  |
| <b>RWS</b>   | Range Window Start for altimetry range windowing   |
| <b>RWW</b>   | Range Window Width for altimetry range windowing   |
| <b>RX</b>    | Receive  |
| <b>SBC</b>   | Single Board Computer  |
| <b>SC</b>    | Spacecraft   |
| <b>SCF</b>   | Science Computing Facility   |
| <b>SDP</b>   | Science Data Product   |
| <b>SIPS</b>  | Science Investigator-led Processing System   |
| <b>SNR</b>   | Signal to Noise Ratio  |
| <b>SPD</b>   | Start Pulse Detector   |
| <b>T0</b>    | Represents the time of the laser fire command  |
| <b>TAMS</b>  | Telescope Alignment Monitoring System  |
| <b>TAT</b>   | Time-at-the-Tone-was   |
| <b>TDC</b>   | Time to Digital Conversion   |
| <b>TE</b>    | Transmitter Echo   |
| <b>TEP</b>   | Transmitter Echo Path  |
| <b>TL</b>    | Trailing Lower (start component)   |
| <b>TOD</b>   | Time of Day  |
| <b>TOF</b>   | Time of Flight   |
| <b>TU</b>    | Trailing Upper (start component)   |
| <b>TX</b>    | Transmit   |
| <b>USO</b>   | Ultra-Stable Oscillator  |
| <b>UTC</b>   | Universal Time Coordinated; Coordinated Universal Time                                       |
| <b>WTEM</b>  | Wavelength Tracking Electronics Module   |
| <b>WTOM</b>  | Wavelength Tracking Optics Module  |
| <b>ZRP</b>   | Zero Range Point   |

# 1 Introduction

This section provides an introduction to the ICESat-2 mission, the measurement concept of its sole instrument, the Advanced Topographic Laser Altimeter System, or ATLAS, and the family of ICESat-2 data products.

## 1.1 Background

The ICESat-2 observatory and ATLAS instrument use a photon-counting LIDAR and ancillary systems, including GPS and star cameras, to make three primary measurements. As seen in Figure 1, the measurements are:

- The time of flight of a photon from ATLAS, to the earth, and back to ATLAS;
- The pointing vector at the time a photon is transmitted by ATLAS; and
- The position of ICESat-2 in space at the time a photon is recorded by ATLAS.

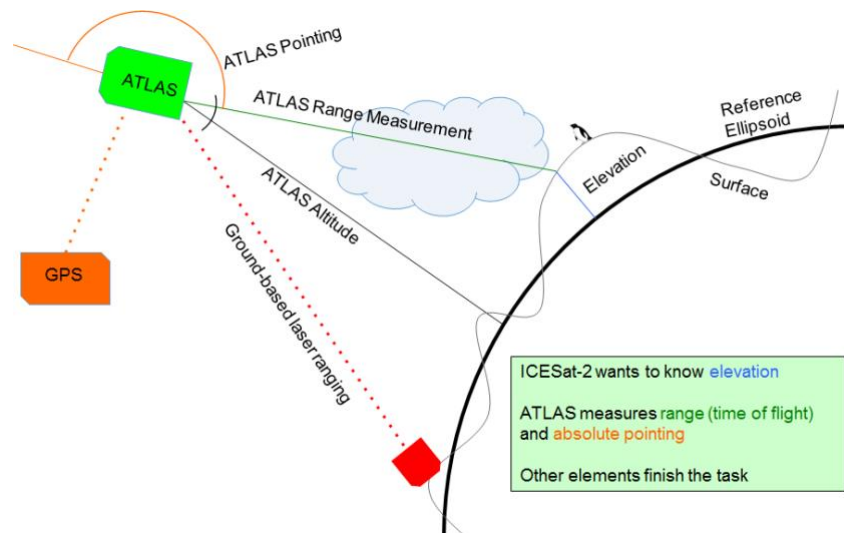


**Figure 1: The Primary Measurements of the ATLAS Instrument**

This measurement approach is fundamentally different than a full-waveform LIDAR system, such as the 1064-nm GLAS instrument on ICESat, in that ATLAS uses statistical analysis to improve the signal-to-noise ratio (SNR) and detect the laser-induced signal arising from return events. In so doing, the ATLAS instrument transmits green (532 nm) laser pulses at 10 kHz from the nominal ICESat-2 ~500 km orbit.

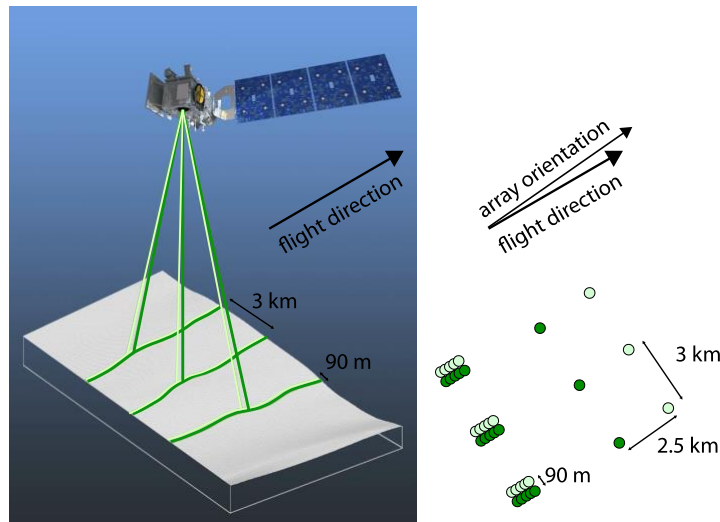


**Figure 2: ATLAS Idealized Beam and Footprint**

One laser pulse is emitted every of  $\sim 0.7$  m in the along-track direction. Following its emission from the laser, each pulse is split by a diffractive optical element to generate three pairs (six total) beams. Each pair of beams along the three tracks have different transmission energies and are referred to as “strong” and “weak”. The strong-to-weak energy ratio is approximately 4:1. The idealized footprint can be seen in Figure 2, where strong and weak beams are denoted by the dark and light green circles respectively. Each pair of beams (strong, weak) are separated by about 90 m in the cross-track direction. The beam pairs are further separated by  $\sim 3.3$  km in the cross-track direction, and the strong and weak beams are separated by  $\sim 2.5$  km in the along-track direction.

A small fraction of the photons transmitted from ATLAS complete the journey through the atmosphere, reflect off the surface of the earth, return through the atmosphere, into the ATLAS telescope, and are recorded by the instrument electronics. For highly reflective surfaces and clear skies, on the order of 10 signal photons from a single strong beam are expected to be recorded by ATLAS for a given transmit laser pulse. At the same time, background photons from sunlight at the same 532 nm wavelength may be arriving at the detector, and some of them will also be recorded by ATLAS.

Upon arrival at ATLAS, photons progress from the point of detection to intermediate data to being recorded as timing information downlinked in telemetry. This processing includes a function to time tag key events, including each laser transmit (TX), return events (RX), and the time of day (TOD) of each event. The number of RX recorded by ATLAS depends on the geometry and reflectance of the Earth’s surface, solar conditions, and on scattering and attenuation in the atmosphere. The instrument thus has to deal with a range of SNR depending on these conditions. Statistical analysis is used to improve SNR, detect the signal, and decide on the signal band to downlink for post processing into geolocated data products.

Each of three Photon Counting Electronics (PCE) cards contains the electronics for a “strong” and “weak” laser spot pair for a single ground track. Although there are actually six total ground spots, the remainder of this document will refer to only two: one strong and one weak. Identical Receiver Algorithms are run concurrently on each PCE card. The sole purpose of the algorithms is to reduce the telemetry data volume to fit within the downlink constraint while maximizing the probability of downlinking surface signal. To that end, these algorithms count the received photon events and generate histograms to aid the statistical signal processing.

The statistical approach inherent to photon counting LIDAR allows for the discrimination of signal from Poisson-distributed background noise. This is the function of the onboard Receiver Algorithms, which identify the data to be downlinked in telemetry. Given the 10 kHz laser pulse repetition rate, transmitted laser pulses are separated in flight by about 30 km in one-way travel, or about 15 km in two-way travel. As such, there is an inherent height ambiguity of about 15 km in received photons and, consequently, ICESat-2 can only characterize the lowest 15 km of the earth's atmosphere.

Among other uses, the Receiver Algorithms utilize these histograms to select the signal location around the ground in real-time and instruct the hardware to telemeter a vertical band of received time-tags about this signal location. To do that, the algorithms set a Range Window (RW) of at 500 m to 6000 m and generate histograms using a much finer 3-m bin size. The width of the range window is primarily dependent on the surface type (e.g. ocean, land ice, land) as well as the topography. This RW remains fixed for a 200-shot interval, or major frame.

Concurrent to the altimetric histograms, atmospheric histograms using 30-m bins are generated that aggregate the number of photon events over 400 consecutive laser shots. These atmospheric histograms are generated every 0.04 seconds and spans 280 m of along-track distance. Atmospheric histograms are downlinked for the three strong ATLAS beams.

While the lower-level data products, such as the ATL02 product described by this ATBD, typically work with individual time tags, higher-level geophysical data products work with aggregations of time tags in order to determine the ellipsoidal height of the earth, canopy height and structure, and other quantities of geophysical interest. More information may be found in the higher level data product ATBDs.

## **1.2 Terminology, Notation, and Conventions**

The relevant acronyms, terminology, and variable shorthand used in this document are listed the tables below.

**Table 1: Photon counting electronics terminology**

| Term                                 | Description  |
|--------------------------------------|--|
| <b>Background photons</b>            | Photons from any source other than the laser that strike the detector.   |
| <b>Background photons per second</b> | Background power divided by energy per photon.   |
| <b>Counting Efficiency</b>           | Combined effect of the detector's efficiency and the throughput of any optics between the input and the detector.  |
| <b>Dark electrons</b>                | All electrons emitted from the detector cathode not due to incident photons.   |
| <b>Energy per photon</b>             | Planck's constant times the speed of light divided by wavelength.  |
| <b>Events (in a time interval)</b>   | Nonlinear function of total electrons in that time interval and earlier; electrons that are emitted within the detector dead time after a previous electron do not result in events. |
| <b>Photoelectrons</b>                | Electrons emitted from the detector cathode in response to photons striking the detector   |
| <b>Receive Events (RX)</b>           | Digital edges coming from the DEM, assumed to be the result of electrons emitted from the detector cathode. May also be referred to as a Return Event.                               |
| <b>Return photons</b>                | Photons emitted by the ATLAS laser that scatter off an object downrange, are collected by the ATLAS receiver, and strike the detector.   |
| <b>Time tags</b>                     | Each time tag corresponds to a particular start or return event and gives the time at which events undergo a time-to-digital conversion (TDC) by a PCE.                              |
| <b>Transmit Events (TX)</b>          | Digital edges coming from the SPD at threshold crossings. May also be referred to as a Start Event.  |

**Table 2: Primary measurements**

| Purpose     | Measurement    | Calculation                                      | Resolution (Units)   |
|-------------|----------------|--|--|
| Elevation   | Time of Flight | Elapsed Time from Transmit Pulse to Return Pulse | <ul style="list-style-type: none"> <li>• USO: Coarse Time (10 ns)</li> <li>• TDC: Fine Time (200 ps)</li> </ul>  |
| Geolocation | Time of Day    | GPS Time Elapsed from 1 PPS to Transmit Pulse    | <ul style="list-style-type: none"> <li>• GPS (100 ns)</li> <li>• IMET (40 ns)</li> <li>• AMET (10 ns)</li> </ul> |
| Geolocation | Pointing       | <i>Responsibility of POD/PPD</i>                 |  |



**Table 3: Key IceSat-2 / ATLAS Parameters**

| Parameter Name   | Value      | Units           | Notes   |
|--|------------|-----------------|---|
| <b>Orbital Altitude</b>  | 481 to 511 | km              |   |
| <b>Laser Firing Rate (nominal)</b>   | 10         | kHz             |   |
| <b>Transmitted Energy (typical strong beam)</b>  | 48 to 172  | $\mu\text{J}$   | Best-estimate actual energies for all beams are in ATL02. See Section 5.2.  |
| <b>Transmitted Energy (typical weak beam)</b>  | 12 to 43   | $\mu\text{J}$   |   |
| <b>Transmitted Wavelength</b>  | 532.272    | nm              |   |
| <b>Transmitted Beam divergence, 85% enclosed energy (typical)</b>  | 21         | $\mu\text{rad}$ | Measured profiles of all beams are in CAL 22  |
| <b>Transmitted Beam Eccentricity</b>   | 0.4        | none            |   |
| <b>Transmitted Beam diameter, 85% enclosed energy (typical)</b>  | 10.5       | m               | At 500 km altitude  |
| <b>Transmitted Beam Angular Spacing (long dimension)</b>   | 6.6        | mrad            | approximately across track  |
| <b>Transmitted Beam Angular Spacing (short dimension)</b>  | 5          | mrad            | approximately along track   |
| <b>Transmitted Beam Spacing (long dimension)</b>   | 3.3        | km              | approximately across track, at 500 km altitude  |
| <b>Transmitted Beam Spacing (short dimension)</b>  | 2.5        | km              | approximately along track, at 500 km altitude   |
| <b>Pointing Direction (nominal)</b>  | N/A        | N/A             | Nadir is along the centerline of cross-track direction of the beam pattern. Position along the centerline varies with roll. |
| <b>Track Pair Spacing (nominal)</b>  | 90         | m               | spacing between weak and strong track in the same pair, at 500 km altitude  |
| <b>Receiver Aperture Diameter</b>  | 0.802      | m               |   |
| <b>Receiver Aperture Effective Area</b>  | 0.41       | $\text{m}^2$    | Less than aperture circular area due to obstruction in telescope  |
| <b>Receiver Field of View Angular Diameter</b>   | 83.5       | $\mu\text{rad}$ |   |
| <b>Receiver Field of View Diameter</b>   | 41.75      | m               | At 500 km altitude  |
| <b>Receiver Optical Throughput (typical at peak wavelength; does not include obstruction in telescope)</b> | .41        | none            | Best-estimate actual products of receiver throughput and efficiency are in ATL02. See Section 5.3.                          |
| <b>Receiver Counting Efficiency (typical)</b>  | 0.15       | none            |   |
| <b>Receiver Effective Optical Bandwidth</b>  | 38         | pm              | Rectangular band at peak wavelength throughput  |
| <b>Event timing precision (typical)</b>  | 200        | ps              | Width of delay-line cell  |
| <b>Single-photon time-of-flight uncertainty (typical standard deviation)</b>                               | 800        | ps              | Best-estimate time-of-flight uncertainties are in ICESat-2-ATSYS-TN-0660.   |

### 1.3 Description of Relevant Hardware Interactions

The ATLAS system-level components shown in Figure 3 are relevant to the scope of the detailed computations presented in this ATBD. This section summarizes how these components are used in photon time tagging and within the timing apparatus presented in the next section and throughout the remainder of this document.

The ATLAS Serial Card (ASC) is housed within the Main Electronics Box (MEB). The ASC has four primary functions:

- 1) house two SpaceWire routers to interface the Single Board Computer (SBC) with the three PCEs and the Spacecraft;
- 2) provide a serial interface to the laser electronics responsible for providing the 10-kHz laser fire command to the laser;
- 3) provide the necessary time indexing to correlate the Spacecraft GPS time reference from the active GPS Receiver (A or B) to an Ultra-Stable Oscillator (USO) used for precise timing; and
- 4) distribute an internal 1 *pulse per second* (1 PPS) signal to the various boards in the MEB that need it.

All timing events recorded by ATLAS can be related to the internal USO clock, referred to hereafter as the “ruler clock.” The ruler clock and other timers have various resolutions that are hierarchically nested. This multi-resolution timing apparatus is portrayed graphically in Figure 4.

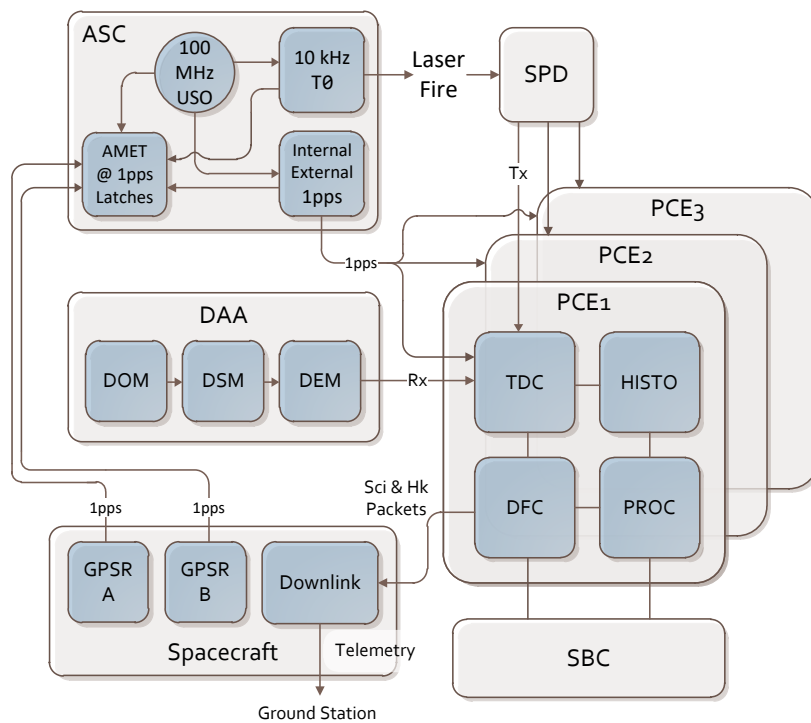


**Figure 3: ATLAS System-Level Components Relevant to the Computations Described in the ATL02 ATBD**

At the lowest resolution, 1-second intervals are counted off both internally in the ASC and externally via the Spacecraft GPS Receivers (GPSR). There are two GPSRs, referred to as GPSR A and GPSR B, according to which receiver is in use. The GPSR provides *about* 100-ns resolution time reference to the instrument via a one pulse per second (1 PPS) signal and a corresponding Time-at-the-Tone-was (TAT) message to the MEB via the ASC. The SBC receives the TAT message and distributes it to the PCE LEON3FT flight software over the SpaceWire link. *Note that the PCE LEON3FT may be referenced, interchangeably, as the PROC or LEON3 card.*

As Figure 4 shows, these nested time-measurement resolutions are used from coarse scale to fine scale for measuring the time of events. At the top, and coarsest resolution, there is the 1 PPS signal. This is the first step in aligning relative time measurements with the GPS time reference via linear interpolation using the

ATLAS Mission Elapsed Time (AMET) counter. The source of the 1 PPS can be either ATLAS *internal* or *external*. For the internal 1 PPS the ASC takes its 100-MHz USO clock and divides it down to 1 Hz. This is the *default* source of the 1 PPS signal and is referred to as the internal 1 PPS or the ASC 1 PPS. Additionally, the external 1 PPS is taken directly from either GPSR A or B time signal received by the ASC. We refer to that source as the external 1 PPS, Spacecraft (SC) 1 PPS, or simply GPS 1 PPS. Whatever the source, the ASC distributes a 1 PPS signal to each PCE card, which then correlates it to its internal time measurements, which includes the Instrument Mission Elapsed Time (IMET), major frames, and minor frames.

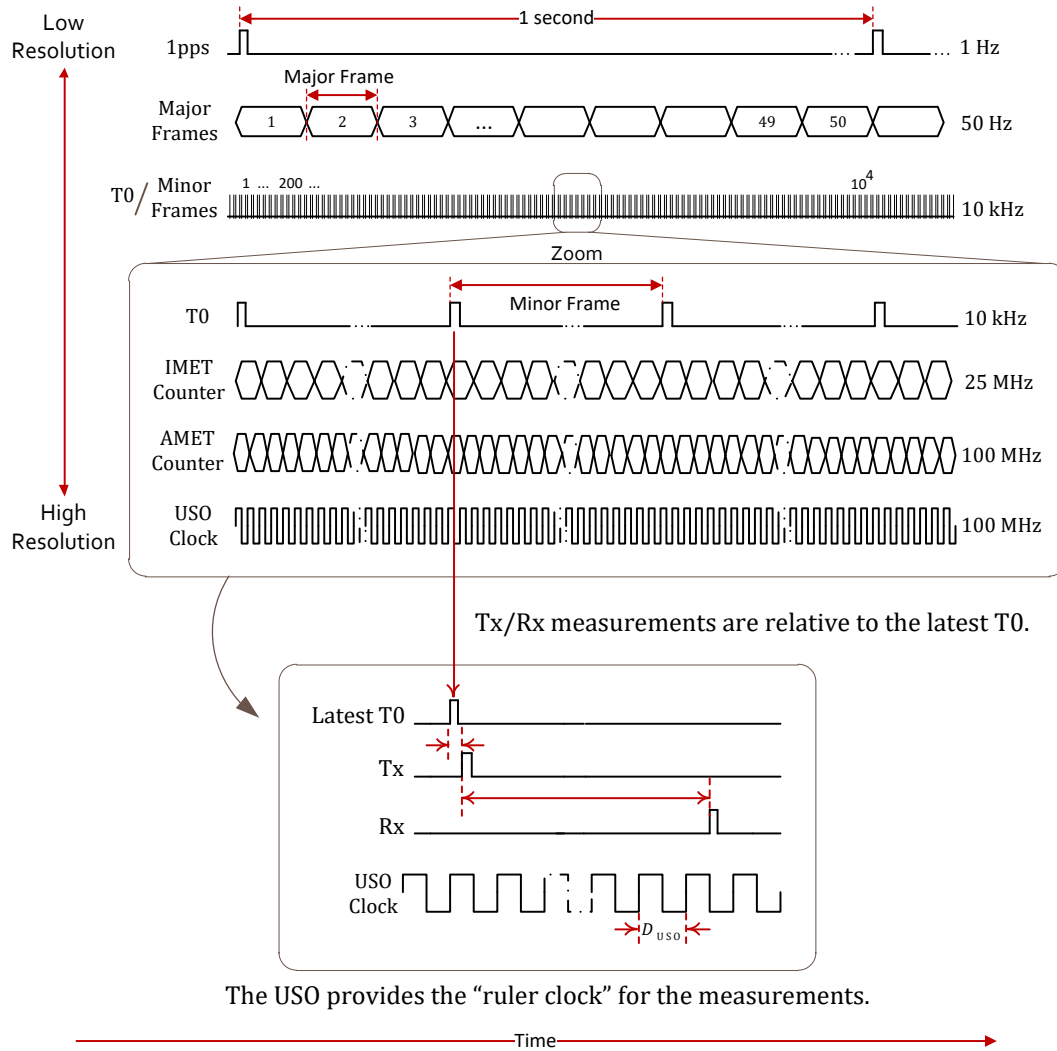


**Figure 4: Timing apparatus uses hierarchically nested, multi-resolution time scales**

At the next level of resolution is the 50-Hz data processing frame, otherwise known as the major frame. Nominally, each major frame is comprised of 200 minor frames consisting of a single laser shot and its associated return event(s). The purpose of the major frames is to granularize the data processing by the flight software for scheduling data processing, data management, operational parameter settings, and housekeeping. The Dataflow Controller (DFC) on each PCE maintains a major frame counter for both the strong and weak beam. These counters are used as the major frame ID. The major frame counters start counting after PCE power-on (or reset) and can count up for about 2.7 years before rolling over. The major frame ID is used to identify individual major-frame dependent data carried by both housekeeping and science telemetry packets to, in part, identify the start/return events and associated time tags.

Because it stems from the internal USO clock we can enjoy clock synchronization across the three Photon Counting Electronics (PCE) cards that also receive the USO clock for internal timing alongside the 1 PPS reference. So, when using internal 1 PPS to define every 1-second period, 10,000 T0 events will always be observed within said period. However, when using the *asynchronous* external 1 PPS, there will be some clock phase skew and, hence, the number of T0 events can differ from 10,000 by either plus or minus one count. It is for that reason that the *internal 1 PPS* source is favored as the *default* source to distribute to each PCE and fall back to the external 1 PPS sources (from either GPSR A or B) only for fault tolerance. This is shown graphically in Figure 5.

Nevertheless, the use of the external 1 PPS source for internal timing is not expected to adversely affect the data processing algorithms beyond what can be corrected by further ground processing. However, testing with the redundant GPSR 1 PPS signals as external sources of 1 PPS for the PCEs will not be tested operationally. Regardless of the 1 PPS source distributed to the PCEs, both the internal and external 1 PPS signals are used concurrently by the ASC to latch the current AMET value every 1 PPS pulse. This latch mechanism is also shown in Figure 5.

The ASC divides down the USO clock to a 10 kHz frequency and uses this to drive the laser fire commands. Each command results in the emission of laser light from one of the two ATLAS lasers. The lasers are redundant units so only one laser is operational at a time. Part of the outgoing laser pulse is picked off and routed to the Start Pulse Detector (SPD). After filtering, the smoothed laser pulse is timed by reporting the time of the leading and trailing edges of the voltage pulse across two adjustable thresholds. Details of this are discussed in future sections. For now, it is sufficient to say that each T0 clock advance (clock tick) is associated (by its trigger) with precisely one laser transmit pulse. The subsequent return events captured by the Detector Array Assembly (DAA) and communicated to the PCEs RX input channels via the Detector Electronics Module (DEM) as electrical pulses. These return events are referred to as RX events. The RX event data is related to the TX event also communicated to the PCEs TX input channels via the SPD. The TX and associated RX events are all collected within the same major frame. The major frame is processed by the on-board signal processing on each PCE card, which is also responsible for start/return time tagging, RX event histogramming, and transmitting of the resulting science data via downlink telemetry.

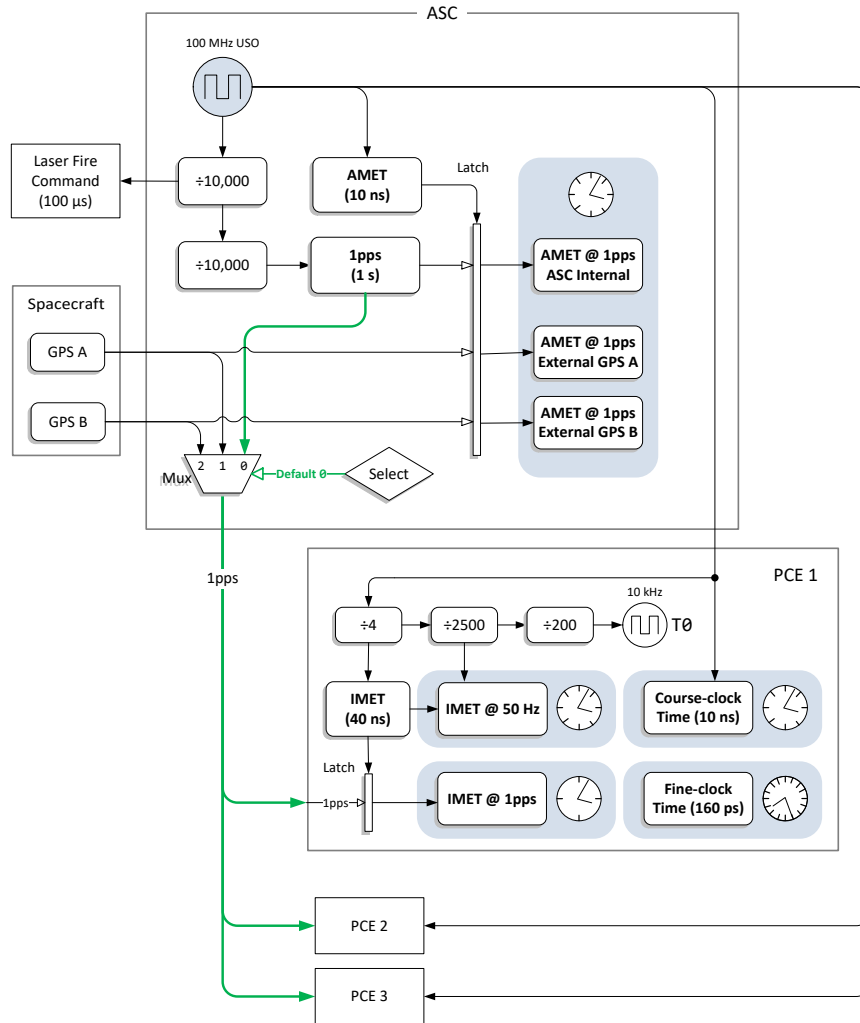


**Figure 5: Block diagram of ATLAS timekeepers**

The flight software uses the notion of “major frames” to organize the low-level data processing and storage. A 50-Hz interrupt to the LEON3FT microprocessor is used to delineate major frame boundaries, which are then used to synchronize all flight software operations on each PCE. Even though the major frame counter is unique within the scope of an individual PCE, the counter value is not consistently the same across all three PCEs. In other words, for the same T0 event, the major frame counter of any two PCEs will not necessarily be the same. But this is of no consequence in the time management scheme presented in this chapter, as it uses other auxiliary counters and time relationships.

As pictured Figure 5, each of the three PCE cards makes use of its own clocks. Part of the PCE runs at 100 MHz and, on each PCE card, is driven by the 100-MHz USO on the ASC. All logic related to transmit and receive event tag logic – including start pulse detection, range window generation, and T0 signal generation – uses this 100-MHz clock. Yet another clock domain runs at 25 MHz, which is divided internally within the FPGA of each PCE. It is used for the Instrument Mission Elapsed Time (IMET) functions, thereby maintaining an IMET with a resolution of 40 ns. Logic running at 25 MHz includes time tagging the internal 1 PPS signal, the time of the first T0 after the 1 PPS, the 50-Hz major frame interrupt, latching the major frame counter, and latching the T0 counter. It is also used in the calibration request logic pulse generation. There is a requirement for the IMET to be reported at the receipt of the ASC/internal 1 PPS to a minimum accuracy of 50 ns. As such, the IMET is used to time stamp the GPS/external 1 PPS and T0, the difference of which correlates all USO timestamps to the GPS time.

Figure 6 shows the four main components of a PCE. Three of the main components are FPGAs; the fourth is the Signal Processor (PROC or LEON3), which is a LEON3FT microprocessor. The first FPGA is the Time-to-Digital Converter (TDC), which performs the precise time tagging function. As will be shown later in this document, the time conversion is performed in two scales of resolution by using a coarse clock and a fine clock. The second FPGA is a Dataflow Controller (DFC), which controls the TDC FPGA and performs the time keeping, data management, and serves as the primary interface for the downlink telemetry. The DFC data management oversees all the critical information and control parameters on the PCE. The data management also includes the collection and storage of start/return event time tags that flow from the TDC and manages the high throughput via flow control and queuing. The time tags are managed with a special data structure for efficient storage and retrieval by the large on-board memory. The DFC timekeeping and control parameters include the 10 kHz T0 clock, 50 Hz major frame counter, 25 MHz Instrument Mission Elapsed Time (IMET) counter for the internal time reference, Range Window Start (RWS), Range Window Width (RWW), and Downlink Band Offset (DLBO). The latter three parameters are settable before each major frame by the *Flight Science Receiver Algorithm* (FSRA) running on the LEON3FT and subsequently used to search for and select the signal data. The data collected within the downlink signal bands are transmitted via science telemetry packets for data processing on the ground. Finally, the third FPGA is the Histogrammer (HISTO), which is the “statistics offload engine,” or coprocessor, for the flight software on the Signal Processor.

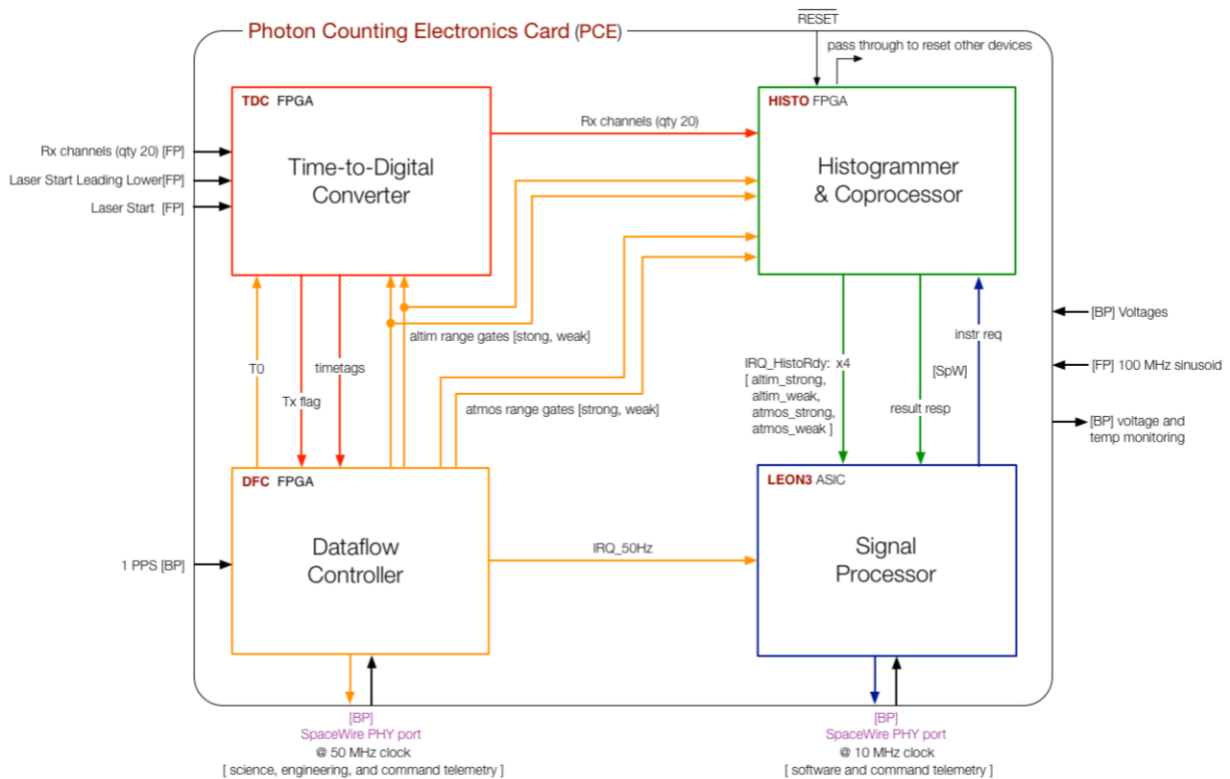


**Figure 6: PCE Architecture Block Diagram**

The DFC takes the 1 PPS and 100 MHz USO as input and derives its own local T0 clock correlated to its internal IMET reference. The T0 events reset the coarse clock used to time tag laser start (shot) and return events. These events are time tagged by the TDC in full resolution of coarse-clock and fine-clock scales. Ensuing start/return events flow directly into the TDC, and the associated time-tag measurements are passed to the DFC. Asserting the TX flag conveys to the DFC that the event is a start event; otherwise it is considered a return event. The RX channels into the TDC are also passed through to the HISTO. While the DFC is storing

the return events (for each start event) for later retrieval, the HISTO is counting and binning the return events. The Signal Processor uses the histograms to perform statistical analysis as part of the Altimetry/Atmospheric Receiver Algorithms. The Receiver Algorithms control the range windows that collect the return events and associated time tags via control parameters it updates in the DFC via the SpaceWire datalink. The range window gates (defining range window start and width) are applied as input to both the TDC and HISTO for the altimetry data, but only to the HISTO for atmospheric histogramming purposes. As a hardware co-processor, the HISTO interrupts the main Signal Processor whenever a certain set of histograms (altimetry/atmospheric, strong/weak beams) are ready for analysis by the Signal Processor software implementing the Receiver Algorithms. This processor is partitioned into consecutive major frames of 200 TX shots each for altimetry histograms with the smallest (3 m range) bins. The DFC (being the time manager) notifies the Signal Processor with a 50 Hz interrupt signal to delineate major frame boundaries. Meanwhile, atmospheric histograms are integrated over 400 TX shots into coarser (30 m) bins. Ultimately, the Receiver Algorithms determine which signal downlink bands to send to the ground station via telemetry. This decision is communicated to the DFC, at which time it retrieves the start/return time tags from its large memory store (not shown), and packages the data for CCSDS telemetry. These data products include both the start/return time tags and the atmospheric histograms, which are downlinked inside altimetry science packets and (separate) atmospheric science packets, respectively.

The two-scale time measurement apparatus is pictured in Figure 7 by using the USO ruler clock. That is, the *coarse-clock* time resolution stems from the USO clock input to each PCE, thus providing 10-ns time resolution. Harder to achieve is the fine-clock time resolution. This fine resolution is accomplished by using a carefully designed logic gate/cell delay line within the TDC FPGA consisting of 75 gates (cells) in serial chain (see the gate delay chain in Figure 7). A pulse input to the front of the chain can be observed as it propagates from one cell to the next by latching the input/output of each cell by a designated clock edge to a synchronous circuit. In this way, the number of cells a pulse can transit in a coarse clock period may be measured. Doing so establishes a highly precise timing apparatus for making measurements in fine-clock resolution much smaller than the 10-ns period of the USO clock. Each cell represents approximately 180 ps of time resolution on average with a standard deviation of about 60 ps. There is some variability to this resolution according to temperature and the card in use when collecting the data; this is accounted for in several calibrations. The TDC is thus able to provide the requisite fine-clock time of the TOF measurement, which meets the ATLAS time precision requirement.



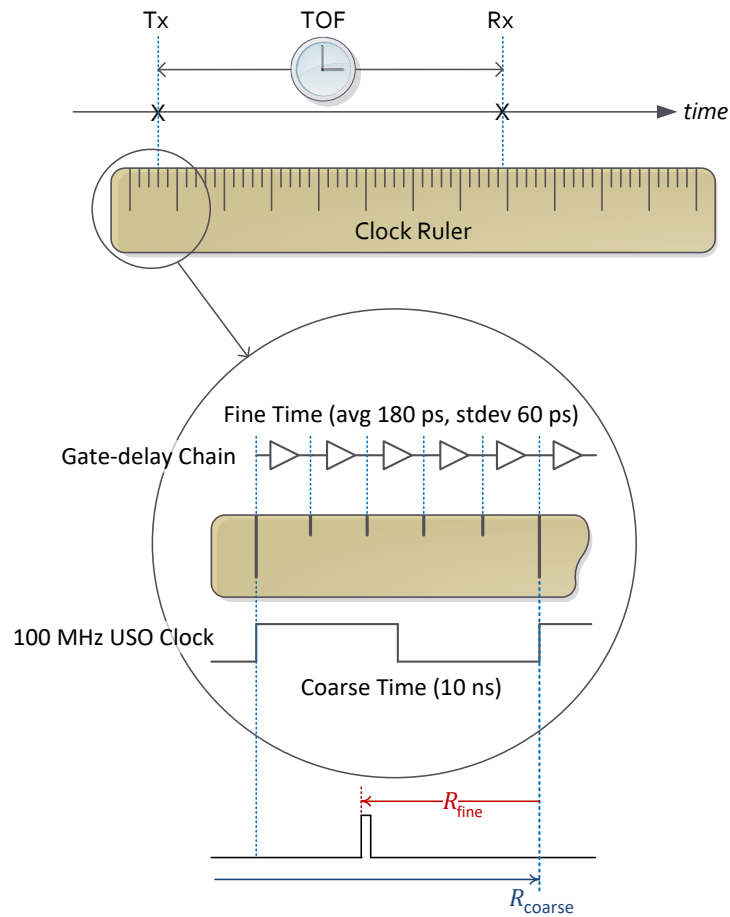


**Figure 7: PCE Coarse and Fine Time**

To relate return times to start times, and start times to *absolute time* of day (TOD) for the purpose of geolocating (geo-referencing) the return bounce points, additional timers must be introduced. The additional timers are correlated in a concerted fashion back to the Spacecraft GPS 1 PPS signal. That never-ending sequence of 1-second intervals will become the definitive time line to which the altimetry science data, including TOFs, will be referenced. That process is presented in Section 2 for the TOD calculations.



## 1.4 Instrument Data

The data telemetered by ATLAS and its subsequent products are listed below. It is important to note that all of these items are generated at different rates and may not be present in telemetry at the same time:

- Time-tag measurements that are converted to altimetry time-of-flight (TOF) and time-of-day (TOD) using GPS time. The calculated TOF values are computed for each return event measured relative to the transmit pulse centroid.
- Data to determine the pointing direction of the transmitted beam with respect to the instrument coordinate system.
- Data to determine the direction to known stars with respect to the instrument coordinate system.
- Atmospheric histograms.
- Housekeeping data consisting of routine telemetry of the state of instrument components.
- Diagnostic data which contains more detailed telemetry pertaining to the state of instrument components (as needed).
- Calibration data consisting of time tags and histograms recorded during instrument calibration procedures.

Note that in the ATL02 product, ATL01 (L1A) telemetry packets are converted from native, raw data form to engineering data in engineering units (MKS, joules, volts, radians, degrees C, etc.).

Additionally, data from packets with checksum flag set as failed will not be placed on ATL02. In the QA summary there will be a count of packets deleted by packet type. The following sections discuss data processing and resulting output of ATL02 data products.

### 1.4.1 Data Products

This ATBD covers the data processing steps to generate the ATL02/L1B data product from the ATL01/L1A data product including the derivation of several key parameters using pre- and post-launch calibration data, housekeeping data, and system models. Throughout this document, ATL02 and L1B are frequently used interchangeably, as are ATL01 and L1A.

The goal of the ATL02 data product is to support the Precise Pointing Determination (PPD) and the Precise Orbit Determination (POD) processing, as well as the ATL03 (global geolocated photons). The full complement of ICESat-2 mission data products and the connections between them are shown in Figure 8.

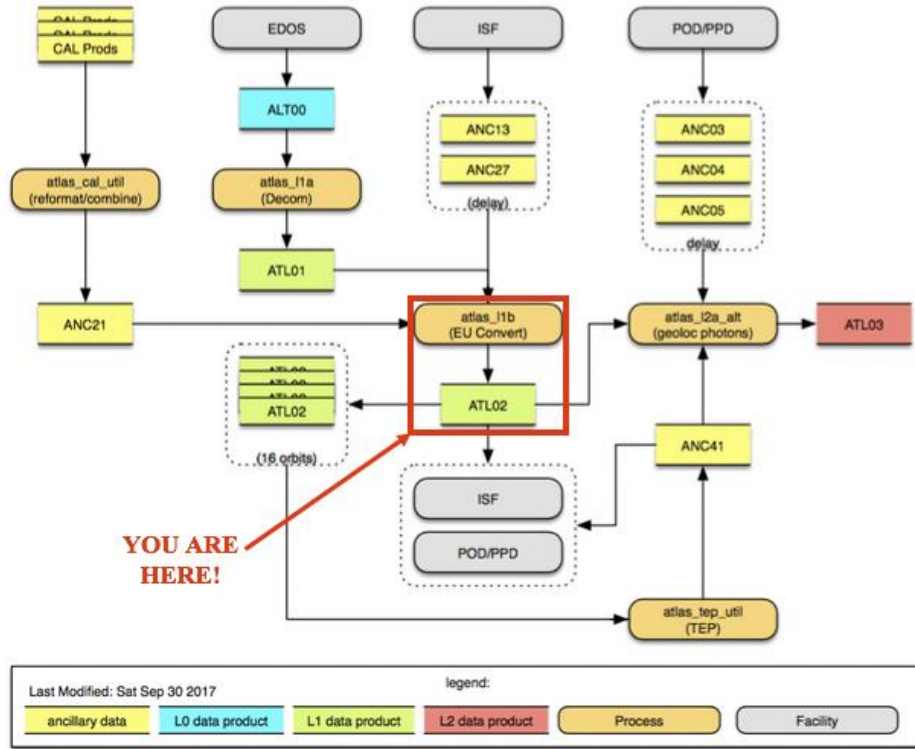


**Figure 8: ICESat-2 Data Processing Flow of ICESat-2 Data**

POD and PPD take the unit converted data provided by ATL02 as the analysis input. The outputs of the POD, PPD and ATL02 data products are combined in ATL03 to produce a Level-2 product containing geolocated ellipsoidal heights for each time-tagged photon event downlinked from ATLAS. These heights are corrected for several geophysical phenomena (e.g. atmospheric refraction, tides) and are classified as likely signal photons (ground or TEP) or likely background photons.

The ATL02 L1B product is delivered in a granule whose bounds are set by the geographic regions defined by the ICESat-2 mission. ATL02 products are delivered in HDF5 format and are accompanied by a QA file which summarizes the basic statistics of all parameters written on the product.

## 1.5 ATL02 Specific Information

### 1.5.1 Knowledge of Instrument Configuration

Knowledge of the instrument configuration, relevant calibrations, and USO behavior are captured in the ANC13 and ANC27 products. These products are delivered by the ISF to SIPS. ASAS compares these ANC files to the information contained in the HKT packets. If the configuration information matches, it then utilizes the information to determine the calibration values and other, configuration-specific assumptions which go into the calculations outlined in this document. In the event of a conflict, the HKT packet governs and ASAS will note the discrepancy. Detailed information on these products may be found in ICESat-2-ISF-IFACE-1639. Instrument configurations as well as ISF/ANC27 supplied constants and calibrations are captured on the ATL02 data product; this information is stored in the `/ancillary_data/housekeeping/` and `/ancillary_data/isf/` groups on the ATL02 product, respectively. The description of instrument configuration can be found at the following location on the ATL02 product:

**Table 4: Knowledge of Instrument Configuration**

| ATL02 Parameter Path<br><i>/ancillary_data/housekeeping/</i> | Description           |
|--|-----------------------|
| <i>det_ab_flag</i>   | Detector Side, A or B |
| <i>hvpc_ab_flag</i>  | HVPC Side, A or B     |
| <i>laser_12_flag</i>   | Laser 1 or Laser 2    |
| <i>lrs_ab_flag</i>   | LRS Side A or B       |
| <i>pdu_ab_flag</i>   | PDU Side A or B       |
| <i>spd_ab_flag</i>   | SPD A or B            |
| <i>tams_ab_flag</i>  | TAMS Side A or B      |

Additionally, the ATL02 product contains "useflag" parameters that indicate whether ATLAS was in "normal science mode" when the associated data were recorded. This flag is merely a label provided as a service for ATL03 processing; no data are removed or changed in ATL02 processing as a result of this flag's state. A "useflag" parameter is stored within each of the following ATL02 groups at that group's data rate:

- */atlas/pcex/algorithm\_science*
- */atlas/pcex/altimetry*
- */atlas/pcex/atmosphere\_sw*
- */atlas/pcex/background*

The input ATL01 data used to determine the useflag are the (1) *amcs\_mode* and *delta\_time* fields within */atlas/a\_sbs\_hk\_1030* and (2) the *PMF mode* and the *delta\_time* fields within */atlas/pcex/a\_pce\_pmf\_hk*. The values of the time target arrays should be ATL02-computed Time of Day timestamps to ensure accuracy in aligning the data between different packet types.

If the ATL01 data does not indicate that ATLAS is in a valid mode, then PCE processing is skipped.

Useflag is initially set to 1, indicating science mode with the AMCS functioning normally, at the data rate (length) of the target group. Then, PMF and AMCS data are evaluated for mode transitions. For any period where the PMF and/or AMCS data indicate a non-science mode, the useflag within the corresponding target time interval is set to a value as given in Table 5. Since the target data may be at a different rate than the 1-second rate of the PMF and AMCS data, a 1-second pad is added at the end of the time interval to account for any sampling ambiguity and to allow for the instrument state to 'settle' during the transition.

The only useflag value that signifies "normal science mode" is 1. ATL03 intends to only process data where the corresponding useflag = 1. Instrument mode transitions are tracked by the ISF and all transitions are recorded in the associated ISF log files.

**Table 5: Useflag Values**

| PMF Mode       | Useflag Value, AMCS Normal | Useflag Value, AMCS Not Normal |
|----------------|----------------------------|--------------------------------|
| <b>Standby</b> | 0                          | 10                             |
| <b>Science</b> | 1                          | 11                             |
| <b>Test</b>    | 2                          | 12                             |
| <b>Manual</b>  | 3                          | 13                             |
| <b>Radio</b>   | 4                          | 14                             |
| <b>Unknown</b> | 5                          | 15                             |
| <b>Unused</b>  | 6-9                        | >15                            |

When ATLAS transitions from another mode to Science Mode, a 15-second buffer is now added, so the useflag retains the previous value until 15 seconds after the transition.

## 1.5.2 Control File & Overrides

As a good practice, data analysis tools provide provisions to modify constants, equations, or flag values used during future analysis. In the case the ATL02 L1B software, the mechanism to enact such overrides is via manipulation of the ATL02 control file.

Often, these control files are written to accommodate parameters which may change along with operational situations, aging, or similar influences. In the case of the ATL02 L1B control file, the parameters contained in the file are all artifacts of the physical hardware configuration itself – and were initially implemented to accommodate hardware modification during integration and testing of the ATLAS instrument. Since the instrument has launched, no future modifications to the hardware, and thus these parameters, is anticipated. Additional information about the ATL02 control file may be found in the ASAS L1B software description document (ICESat-2-SIPS-SPEC-2325).

## 1.5.3 Relevant Calibrations

The calibration products listed in Table 6 are used within the context of this ATBD. Specific direction for selecting these values, including how to recover related information from the appropriate ANC or CAL file, is provided in context of the section or chapter where they are applied.

**Table 6: CAL Products Used in ATL02 ATBD**

| CAL Product | Title  | Use Described in... | Expected Frequency of CAL Product Update               | Value(s) Vary Within Granule? |
|-------------|--|---------------------|--|-------------------------------|
| 10          | USO (A & B) Frequency Deviation  | Table 10            | Superseded by ANC-27 after launch; updated as required | No                            |
| 17          | PCE Effective Cell Delay   | Table 18            | No post-launch updates planned                         | Yes (@ Major frame rate)      |
| 30          | Nominal Receiver Sensitivity   | 5.3.1.1             | No post-launch updates planned                         | No                            |
| 44          | Start Timing Skews   | Table 19            | No post-launch updates planned                         | No                            |
| 45          | Transmit Energy Fraction per Beam  | 5.2.2.1             | No post-launch updates planned                         | No                            |
| 46          | Receiver Sensitivity as a Function of PMT High Voltage                           | 5.3.1.3             | No post-launch updates planned                         | No                            |
| 47          | Receiver Sensitivity as a Function of Transmitter-to-Receiver Beam Misalignments | 5.3.3.1             | No post-launch updates planned                         | No                            |
| 49          | Receiver Channel Skews   | Table 23            | At least one update after launch                       | No                            |
| 54          | Absolute, Energy Monitor Product   | 5.2.1.1             | No post-launch updates planned                         | No                            |
| 61          | Receiver Sensitivity Using WTEM  | 5.3.3.2             | At least one update after launch                       | No                            |

## 1.5.4 General Data QA Philosophy

To ensure that the ATL02 data product is generated appropriately and its contents are legitimate, a multi-faceted data quality assurance process is planned. The following utilities will be used to accomplish this task:

- Custom Python scripts developed by the ATL02 ATBD team – These scripts will be used primarily for pre-launch validation of ATBD algorithm implementations, telemetry conversions, etc. in the ASAS code. They will be run on key test data sets with each new release of the ATL02 software.
- ASAS QA Scripts – This code is integrated directly into the utilities which create the ATL02 data products. These scripts will be used to screen for catastrophic errors in the product. If errors are found, further processing of the granule will be halted. These scripts will be used both during pre-launch and post-launch validation efforts and will be executed each time an ATL02 data product is created.
- SCF Limit Checking Scripts – The ICESat-2 SCF has the ability to perform rote limit checks on parameters contained in the ATL02 HDF5 data products. These scripts will check the values contained in the ATL02 products and alert the responsible parties when something is out of bounds. In the case of the SCF limit checking, the utility will be used to flag issues that warrant additional investigation but are not severe enough to halt the processing of the granule. These scripts will be used both during pre-launch and post-launch validation efforts and will be executed each time an ATL02 data product is created.
- ISF Trending – The ISF has the ability to trend overall behavior of the results reported out in the ATL02 HDF5 data products. The trending capability of the ISF will be used to evaluate the long-term stability of the ATLAS instrument as well as key parameters used when producing the ATL02 HDF5 data products. The ISF trends will need to be monitored within the context of operations and engineering judgement. These trends will then be used to help identify areas where additional investigation may be needed but a halt in ATL02 product creation isn't necessary.

## 2 Time of Day (TOD) Calculation

The TOD calculation is used to assign a GPS time to each laser shot (TX) for the purposes of geolocation of laser fires as well as for correlating shot information among the three PCE cards. The approach outlined in this section takes the GPS time distributed by the spacecraft and proceeds through the various internal time references established (latched) by ATLAS until reaching the time of a laser fire. It also details how to recover an AMET counter value, which may be used to correlate laser fire data among the three PCE cards.

### 2.1 Clocks and Timing Relationships

In order to properly assign a time of day to a laser fire, as recorded by a PCE, the relationship between the clocks and GPS signals used onboard the spacecraft must first be established. A summary of the synchronous time references used in ATL02 processing is seen in Table 7 and described in detail below.

**Table 7: Summary of synchronous time references**

| Time Reference                         | Rate    | Purpose  |
|--|---------|--|
| Coarse Time (“Ruler Clock”)            | 100 MHz | <ul style="list-style-type: none"> <li>Used to time stamp the transmit pulse and return pulses, the difference of which provides a coarse time of flight.</li> <li>Used to time the start and stop of the range window.</li> <li>Used to time the period of each histogram bin.</li> </ul> |
| ATLAS Mission Elapsed Time (AMET)      | 100 MHz | <ul style="list-style-type: none"> <li>Used to resolve the differences between the Spacecraft GPS/external 1 PPS signal and the ASC/internal 1 PPS signals by calculating the respective time differences.</li> </ul>  |
| Instrument Mission Elapsed Time (IMET) | 25 MHz  | <ul style="list-style-type: none"> <li>Used to time stamp the ATLAS Internal PPS and the first T0 of each major frame, which makes part of the chain connecting the shot times to GPS</li> </ul>   |
| Time-Zero (T0)                         | 10 KHz  | <ul style="list-style-type: none"> <li>Used to reset the coarse-count time of the start pulse to zero. All start pulse timestamps are relative to the most recent T0. (Note, return pulse times are relative to the start of their corresponding downlink band.)</li> </ul>                |
| Major Frame (MF)                       | 50 Hz   | <ul style="list-style-type: none"> <li>Used to latch new range window values.</li> <li>Used to signal to the LEON3FT processor.</li> </ul>   |

Each PCE has two internal clocks that can be used to time laser fire events: a high-resolution time of flight clock and a low-resolution time of day clock. The high-resolution clock, referred to as the ruler clock, is a copy of the 100 MHz USO and provides 10 ns resolution. Samples from this clock are generally addressed as events measured in coarse counts. Combined with the fine counts, which are fractions of the coarse clock interval, the high-resolution clock can time tag laser fire and return events to a resolution of approximately 200 ps for the TOF calculation.

The ASC counts cycles of the 100 MHz clock in a 32 bit counter to generate the ATLAS Mission Elapsed Time (AMET). The AMET counter rolls over every 42.9 seconds, but the flight software tracks the rollovers to generate a 64 bit version of the AMET that won’t rollover during the life of the mission. The spacecraft distributes a 1 PPS from the GPS receiver that goes to the ASC. Upon receipt of the spacecraft PPS, the ASC latches the current AMET value. Every 100 MHz oscillator cycles, the ASC generates an Internal 1 PPS and, when generated, latches in a different register the current AMET. The AMET internal PPS is distributed to the PCEs/DFC where it is used to time stamp the altimetric science packets.

It should be noted that each PCE divides the ruler clock to 25 MHz, the IMET clock, which is used to time tag the internal (ASC)1 PPS and the first T0 after the internal 1 PPS with a 40 ns resolution. While this can be used to compute the time of day of each laser to a resolution of 40 ns it is not used for the TOD specified in this ATBD. Note because the PCE uses IMET there is a basic limitation of 40 ns to the resolution of TOD and that because each PCE generates its own IMET, the three PCEs are likely to assign different IMET times to a given laser fire. A depiction of these relationships may be seen in Figure 5.

## 2.2 Ground Rules & Assumptions

The following “ground rules” and assumptions apply to the calculations outlined in this chapter:

- Only the leading lower time of a laser fire (see Section 3.4 for a description of laser fire timing) is used when calculating its GPS time, as this is sufficient for meeting the GPS timing requirements as will be discussed later in this section.
- The analysis outlined in this chapter relies on contiguous major frame data. If a packet or segment is missing, it is impossible to interpolate across the missed data. Thus, each “block” of contiguous data within the granule, beginning with its first full and properly formed major frame, must be processed as its own group of data. Note that the case of missing data differs from the case where the PCE does not finish (DNF) transferring data. In the case of a DNF, the information needed to time align the data is present.
- In the case of a major frame which is missing segment(s), the major frame is considered to be invalid as it is impossible to interpolate the data needed to assign a time of day. This major frame should be discarded and not written to the ATL02 product.

## 2.3 Variable Definitions and Notation Syntax

Before deriving the equations for determining the TOD of a TX and using this information to align data across the three PCEs, shorthand notations and symbols must be established. These will be used for expressing the generalized form of equations. Notation syntax is as follows:

$$\mathbf{Parameter}^{\mathbf{Hardware Identifier(s)}}_{\mathbf{Telemetry Type(s)}}$$

- Bolded parameters are values expressed in seconds
- Non-bolded parameters are dimensionless (i.e. clock cycles or ratios)
- Lower case parameters are uncalibrated
- Upper case parameters are calibrated
- Hardware identifiers include Hardware sides (SPD A or B), PCE Identifiers (1, 2, or 3)
- Telemetry Types include: High or low bits for counter values

**Table 8: Generalized TOD Calculation Notation**

| Symbol   | Parameter               | Super or Subscript | Valid Values  |
|----------|-------------------------|--------------------|---------------|
| $\alpha$ | Hardware Side           | Superscript        | A, B          |
| $\beta$  | PCE Identifier          | Superscript        | 1, 2, 3       |
| $\delta$ | Leading Start Component | Subscript          | LL1, LL2, LL3 |



Because of the great degree of variety of notation in this document, a dictionary of utilized terms follows (in order of appearance):

**Table 9: Dictionary of TOF Derivation Variables**

| Uncalibrated Notation              | Calibrated Notation        | Description   | Units              | Source  |
|------------------------------------|----------------------------|---|--------------------|---|
| $d_{\text{USO}}$                   | n/a                        | Nominal USO period (10ns)   | Seconds            | DFC FPGA Spec   |
| $\tilde{d}_{\text{USO}}$           | n/a                        | Observed USO period   | Seconds            | Equation 2-4  |
| n/a                                | $f_{\text{cal}}^{\alpha}$  | USO frequency deviation   | Hz                 | ANC27   |
| n/a                                | $SF_{\text{USO}}^{\alpha}$ | USO scale factor  | Dimensionless      | Calculated value per Equation 2-4   |
| $simhk_{\text{amet}_{64\_high}}$   | n/a                        | Highest 32 bits of 64 bit AMET counter, generated by Flight Software at the time of packet generation   | Ruler clock cycles | ATL01 parameter: <i>/atlas/a_sim_hk_1026/raw_amet_64_bit_hi</i>               |
| $simhk_{\text{amet}_{64\_low}}$    | n/a                        | Lowest 32 bits of 64 bit AMET counter, generated by Flight Software at the time of packet generation  | Ruler clock cycles | ATL01 parameter: <i>/atlas/a_sim_hk_1026/raw_amet_64_bit_lo</i>               |
| $simhk_{\text{amet}_{sc\_1PPS}}$   | n/a                        | Lowest 32 bits of 64 bit AMET counter, latched at the time when the ASC receives the spacecraft 1 PPS. Note that depending on which GPS receiver is active, only one of the A/B latches will be active and the other will remain static.<br>Note: computations outlined in this chapter rely on the active counter. | Ruler clock cycles | ATL01 parameter: <i>/atlas/a_sim_hk_1026/raw_amet_at_sc_{a/b}_1PPS</i>        |
| $gps\_sec_{sc\_1PPS}$              | n/a                        | Latched Value - The GPS time for the 1 PPS provided by the spacecraft. This value is latched at the same time as the <i>amet_at_sc_a b_1PPS</i> fields and represents the last time at tone message used by the flight software to propagate time on board the instrument.  | Seconds            | ATL01 parameter: <i>/atlas/a_sim_hk_1026/raw_gps_of_used_sc_1PPS_secs</i>     |
| $gps_{subsec}_{sc\_1PPS}$          | n/a                        | The corresponding subseconds to the above <i>gps_of_used_sc_1PPS_secs</i> field. The subseconds are converted to seconds by dividing the value by 4294967296.0 (which is the max 32 bit integer value).   | Seconds            | ATL01 parameter: <i>/atlas/a_sim_hk_1026/raw_gps_of_used_sc_1PPS_sub_secs</i> |
| $mf_{\text{amet}_{upper}}^{\beta}$ | n/a                        | Highest 32 bits of 64 bit AMET counter, generated by Flight Software at time of the first T0 in the major frame.  | Ruler clock cycles | ATL01 parameter: <i>/atlas/pcex/a_alt_science/raw_pce_amet_mframe_hi</i>      |



| Uncalibrated Notation       | Calibrated Notation     | Description  | Units              | Source   |
|-----------------------------|-------------------------|--|--------------------|--|
| $mf_{amet}^{\beta}_{lower}$ | n/a                     | Lowest 32 bits of 64 bit AMET counter, generated by Flight Software at time of the first T0 in the major frame.  | Ruler clock cycles | ATL01 parameter: <i>/atlas/pcex/a_alt_science/raw_pce_amet_mframe_lo</i>   |
| $tx_{cc\delta}^{\beta}$     | $TX_{cc\delta}^{\beta}$ | Leading lower element coarse counts  | Ruler clock cycles | ATL01 parameter: <i>/atlas/pcex/a_alt_science/ph/raw_tx_leading_coarse</i> |
| $GPSTime_{Epoch}$           | n/a                     | Number of GPS seconds between the GPS epoch (1980-01-06T00:00:00.000000Z UTC) and the ATLAS Standard Data Product (SDP) epoch (2018-01-01:T00.00.00.000000 UTC).<br><br><b>Note:</b> $GPSTime_{Epoch}$ is stored as the GPS representation of the ATLAS SDP epoch. | Seconds            | ATL01 parameter: <i>/ancillary_data/atlas_sdp_gps_epoch</i>                |

## 2.4 Establishing the USO Ruler Clock Scale Factor

This section shows the conversion from clock cycles to calibrated time in seconds. First, derive the scale factor to adjust for variation in USO frequency (or period):

|                     |   |                     |
|---------------------|---|---------------------|
| $d_{USO}$           | $\stackrel{\text{def}}{=} \text{The nominal period of the USO clock period (10ns).}$  | <b>Equation 2-1</b> |
| $\tilde{d}_{USO}$   | $\stackrel{\text{def}}{=} \text{The as-measured value of the USO clock period.}$  | <b>Equation 2-2</b> |
| $f_{cal}^{\alpha}$  | $\stackrel{\text{def}}{=} \text{Frequency deviation (Hz), as reported by ANC-27/CAL-10.}$   | <b>Equation 2-3</b> |
| $SF_{USO}^{\alpha}$ | $\stackrel{\text{def}}{=} \frac{\tilde{d}_{USO}}{d_{USO}} \cong \frac{\left(\frac{1}{d_{USO}}\right)}{\left(\frac{1}{d_{USO}}\right) + f_{cal}^{\alpha}}$ | <b>Equation 2-4</b> |

**Table 10: Directions for Selection of ANC27/CAL-10 Value**

| CAL-10: USO Frequency Deviation                   |  |
|---|--|
| <b>Description</b>                                | Over defined time intervals, values for the USO frequency deviation from nominal 100-MHz value.  |
| <b>Dependencies</b>                               | Date, Instrument Side  |
| <b>How to Select Value</b>                        | <ul style="list-style-type: none"> <li>Determine date and time of data being evaluated</li> <li>Recover the appropriate ANC-27 value provided by the ISF.</li> <li>Use this information to find the “USO_FREQ” line in ANC-27 whose date occurs most recently with respect to the time of the data being evaluated. Note that the date is provided in the 3<sup>rd</sup> field of the comma separated line.</li> <li>Recover value from “Offset” field of the same line in ANC-27. This data is provided in the 2<sup>nd</sup> field of the comma separated line and should be used in Equation 2-3.</li> <li>Note: Because the instrument only operates on one side or the other, the Instrument Side can be deduced from the Date. Therefore, in some sense, the SF depends only on date.</li> </ul> |
| <b>Telemetry Point Used to Select Calibration</b> | <ul style="list-style-type: none"> <li>To determine which USO is in use, consult the 4<sup>th</sup> field in the ANC-13 file.</li> </ul>   |

The value of  $SF_{USO}^\alpha$  may be used to convert values expressed in clock cycles to units of seconds. To do so, the value in clock cycles,  $t$ , is multiplied by the nominal USO period and the USO scale factor. This yields a time,  $T$ , in units of seconds:

|          |                                   |                     |
|----------|-----------------------------------|---------------------|
| <b>T</b> | $= t * d_{USO} * SF_{USO}^\alpha$ | <b>Equation 2-5</b> |
|----------|-----------------------------------|---------------------|

A caveat to this calculation is that it only applies to time references established solely within the context of a single granule. This is due to the fact that the value of  $SF_{USO}^\alpha$  will likely drift over the lifetime of the mission. (i.e. this approach cannot be used to convert AMET values to seconds since the value of the scale factor will have varied within the counter interval).

## 2.5 Calculation of Event Time of Day

In order to determine the time of day (and *delta\_time*) of the leading lower threshold crossing of a laser fire, it must be related back to a known AMET counter value. By way of the SIM\_HK timekeeping packet which distributes the spacecraft 1 PPS and corresponding GPS time, this AMET value can in turn be associated to a known GPS time. The progression of establishing these relationships can be seen in Figure 9 and is detailed in the following sections. The calculation is performed on a per-PCE basis.

It is important to note that the ability to establish the event time of day is predicated on contiguous major frame data. If data are missing within a major frame due to dropped segments, the frame is invalid and should be discarded. This and related scenarios are summarized further in Section 2.6.

If a major frame contains fewer than 199 TX values, it is excluded from further processing unless the DNF flag is raised on that major frame. If the DNF flag is raised, it is assumed that the missing TX values are from the end of the major frame, and times for the TX events that are present are calculated on that basis.

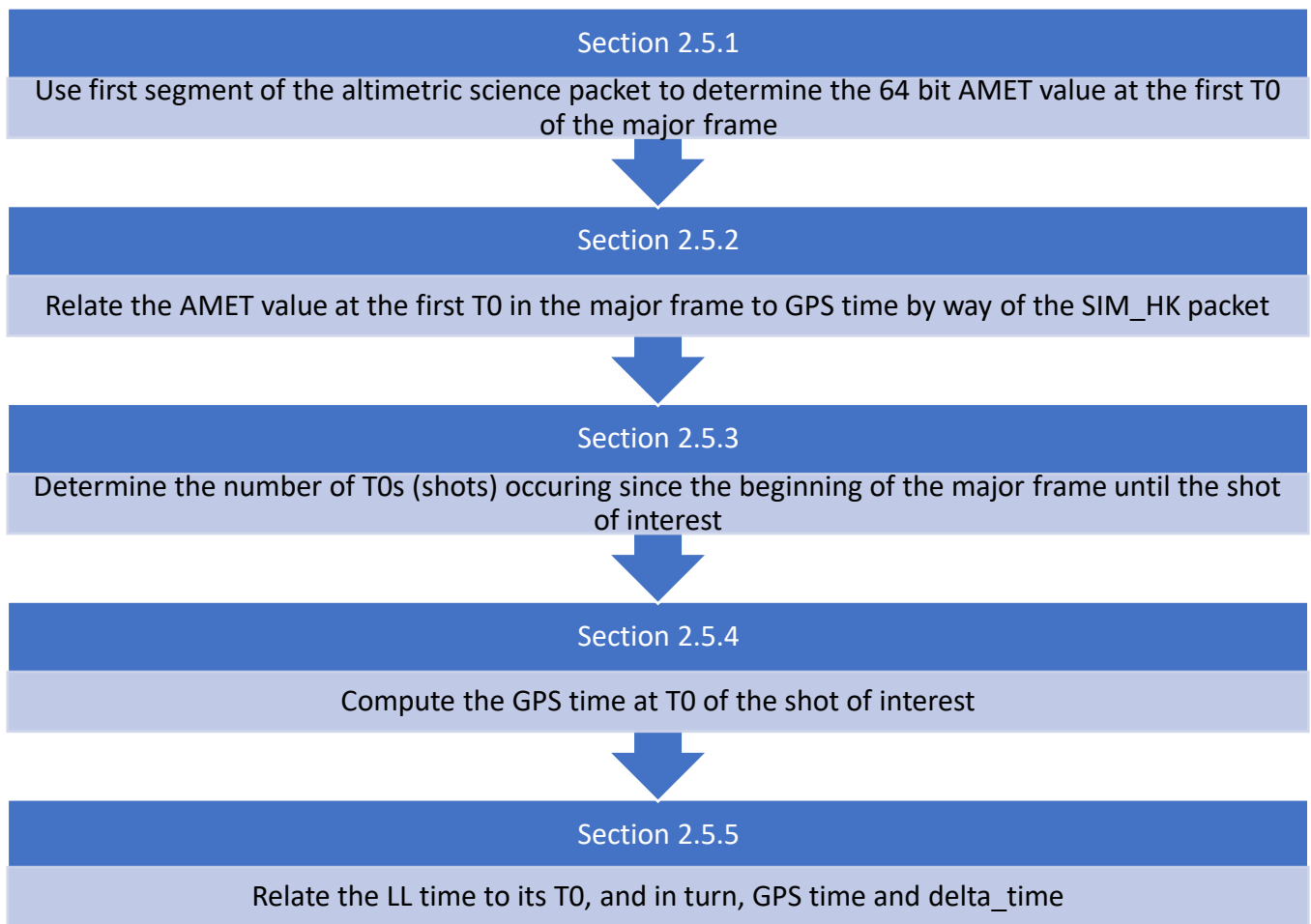


**Figure 9: Progression of Time of Day Calculation**

## 2.5.1 Constructing AMET Counter Values

The SIM\_HK packet reports out several different AMET counter values. The ones relevant to the TOD calculation are:

- A counter value whose value is based on the time of the SIM\_HK packet generation (expressed as a 32 bit `amet_64_bit_hi` and a 32 bit `amet_64_bit_low` value) Note that this time should always be the largest time in the 1024 packet because it represents the time the ASC times were read by the SBC.
- A counter which latches upon receipt at the spacecraft 1 PPS, one each for the A and B side external PPS (expressed as a 32 bit `amet_at_sc_a_1 PPS`, `amet_at_sc_b_1 PPS` value, representing the least significant bits, LSBs, of a 64 bit expression)

The 64 bit AMET counter value is free running + will generate whenever the SIM\_HK packet is created, regardless of whether or not the internal or external PPS values are updating. Note that:

- For the `amet_at_sc_a_1 PPS` and `amet_at_sc_b_1 PPS` values, only one of these fields will be incrementing at a time, according to which spacecraft GPS is in use. One of these values will latch upon receipt of the spacecraft 1 PPS and will not update in the case of a lost GPS signal.
- If a packet's value for `gps_secsc_1PPS` and/or `simhkametsc_1PPS` is found to be unchanged since the last SIM\_HK packet, then the packet containing the static value is likely stale and should not be used.

It is important to realize that only the SIM\_HK packet AMET counter value is expressed as a 64 bit value (split into 32 high + 32 low bits). The remaining AMET counters only represent the 32 LSBs of their respective AMET counters. To reconstitute the 64 bit representation of the  $amet\_at\_sc\_a|b\_1PPS$  values, the  $amet\_64\_bit\_hi$  value may be used. However, as these AMET references are not generated simultaneously, care must be taken to address the idea that the LSBs will roll over (and in turn increment the upper 32 bits of the AMET counter seen in the  $amet\_64\_bit\_hi$  field) at different times. This 64 bit expression of the latched AMET at spacecraft 1 PPS may therefore be nominally found as follows:

|                 |  |                         |
|-----------------|--|-------------------------|
| $amet_{SC1PPS}$ | $= \left( 256^4 * simhk_{amet_{64\_high}} \right) + simhk_{amet_{sc\_1PPS}}$ | <b>Equation<br/>2-6</b> |
|-----------------|--|-------------------------|

As alluded to previously, the value of  $simhk_{amet_{64\_high}}$  may need to be reduced by one count before evaluating Equation 2-6. This reduction is needed **only** when the following criterion is true:

|  |  |                         |
|--|--|-------------------------|
|  | If $simhk_{amet_{64\_low}} < simhk_{amet_{sc\_1PPS}}$ , then $simhk_{amet_{64\_high}} - 1$ | <b>Equation<br/>2-7</b> |
|--|--|-------------------------|

Similarly, the DFC altimetric science packets also contain a 64 bit expression of the AMET counter value, again expressed in two, 32 bit packet fields. These values are contained in the first (start) segment of the DFC altimetric science packets and are generated at the first T0 occurring within a major frame. It is important to note that as the T0s are free running and independent across the three PCEs, the AMET counter values reported in the first segment of each PCE’s altimetric science packet are *not* expected to align in the majority of circumstances. The value of a given PCE’s first T0 in a major frame may be constructed as follows:

|                                    |  |                         |
|------------------------------------|--|-------------------------|
| $amet_{FirstT0MajorFrame}^{\beta}$ | $= \left( 256^4 * mf_{amet_{upper}}^{\beta} \right) + mf_{amet_{lower}}^{\beta}$ | <b>Equation<br/>2-8</b> |
|------------------------------------|--|-------------------------|

### 2.5.2 Determination of GPS Time of First T0 in Major Frame

With the latched AMET counter values determined in the previous section, the process of determining the GPS time of the first T0 in a major frame can then be undertaken. Recall the following distribution of timing information:

- The spacecraft (on side A or B) distributes a GPS time as seconds and subseconds at the spacecraft 1 PPS to the SBC via the time at tone (TAT) message.
- The spacecraft (on side A or B) distributes a simultaneous electronic tick to the ASC card. This causes the latch of the AMET counter at the GPS 1 PPS time.
- The ASC also latches the AMET when it generates the internal ASC 1 PPS.
- The internal ASC 1 PPS is distributed to the DFC.
- The DFC uses this ASC 1 PPS in conjunction with the 10ns ruler clock to record an AMET value (via FSW) for the first T0 in the major frame. This value is reported in the first segment of the DFC altimetric science packet with a 40 ns resolution.

Based on this, the GPS time of the first T0 in each major frame can be found as follows. Note that the values of  $gps\_sec_{sc\_1PPS}$ ,  $gps\_subsec_{sc\_1PPS}$ , and  $amet_{SC1PPS}$  used in Equation 2-9 should be selected based on the value of  $amet_{SC1PPS}$  which is the nearest neighbor to each  $amet_{FirstT0MajorFrame}^\beta$  value.

|                                     |  |                     |
|-------------------------------------|--|---------------------|
| $GPSTime_{FirstT0MajorFrame}^\beta$ | $= \left( gps\_sec_{sc\_1PPS} + gps\_subsec_{sc\_1PPS} \right) + \left\{ \left( amet_{FirstT0MajorFrame}^\beta - amet_{SC1PPS} \right) * d_{USO} * SF_{USO}^\alpha \right\}$ | <b>Equation 2-9</b> |
|-------------------------------------|--|---------------------|

### 2.5.3 Determining Effective Shot (T0) Count within Major Frame

In order to establish a GPS time for every transmit tag present in the altimetric science data, the GPS time for the T0 from which every shot is referenced must first be established. Unfortunately, this process is not particularly straight-forward; the phase relationship between the T0 marked by the respective PCE and when the laser actually fires is randomly established according to the time at which the PCE board is powered up. This is a critical nuance to the ATLAS timing scheme. Because each TX tag will be referenced from the T0 immediately preceding it, simply assuming that the first shot is referenced to the first T0, the second shot to the second T0, etc., is not practical nor advisable.

It is helpful to understand the relationship between laser fire commands, laser fires, and T0 before describing the details of how to match laser first to T0s. Each PCE generates its T0s by dividing the USO by 10,000. The ASC generates the laser fire command by dividing the USO by 10,000. Because the four dividers (three PCEs and one ASC) start asynchronously, the initial time difference between any pair is an arbitrary number. But once established, that time difference is fixed until a PCE(s) is reset or ATLAS is power cycled.

The ASC fire command is sent to the laser, but does not directly trigger the fire. The laser synchronizes the received fire to its own internal clock (~30 MHz), which operates asynchronously from the USO and ASC fire command. The result is a slow drift of the time between the ASC fire command and the laser actual fire until the fire command catches a different edge of the laser’s internal oscillator where upon the laser period experiences a 30 ns jump. The result is the time between the laser fire command (and the three PCE T0s) follows a saw tooth, slowly increasing (or decreasing), followed by a 30 ns jump. Once the lasers are warmed up, the saw tooth has a period of about 30 shots (3 ms). This document refers to the time variations between the fire command (and T0s) and the actual laser light as “jitter” although it is not a random process and will happen six or seven times during each major frame.

When the ASC fire command is very close to a PCE’s T0, it is possible for the laser fire jitter to cross the T0, sometimes triggering the laser before and sometime after the T0. The result is a given T0 may have zero, one, or two laser fires associated with it. This scenario creates a number of complications and thus is to be avoided. An operational constraint of performing a “soft reset” of the symptomatic PCE card has been adopted to mitigate this scenario.

**Caution:** A “soft reset” of a PCE will lead to a reset of its major frame counter value as well as create a temporary discontinuity in the data generated by the PCE being reset. This information should be considered when attempting to uniquely identify photon data via its major frame counter and pulse ID, as it will potentially introduce conflicting information across data sets. As always, the data may instead be uniquely identified via its time of day.

Should a PCE “soft reset” *not* be advisable for some reason, additional mathematics can be used in order to determine the effective T0 of each laser fire. This math can be seen in ICESat-2-SIPS-TN-0957. Otherwise, in the nominal scenario, the effective T0 for shot,  $n$ , is equal to its index within the major frame. Note that T0 indexes from  $n = 0$ , not 1, as the AMET value reported at the start of the major frame is based on the first T0.

|                            |       |                      |
|----------------------------|-------|----------------------|
| $T0_{effective,n}^{\beta}$ | $= n$ | <b>Equation 2-10</b> |
|----------------------------|-------|----------------------|

## 2.5.4 Calculation of GPS Time at T0 of Shot

Once each shot’s effective T0 is found, the calculation of its GPS time may be calculated as follows:

|                         |   |                      |
|-------------------------|---|----------------------|
| $GPSTime_{T0n}^{\beta}$ | $= GPSTime_{FirstT0MajorFrame}^{\beta} + \{T0_{effective,n}^{\beta} * 10,000 * d_{USO} * SF_{USO}^{\alpha}\}$ | <b>Equation 2-11</b> |
|-------------------------|---|----------------------|

## 2.5.5 Calculation of GPS Time of Leading Lower of Shot and Delta Time

Once each shot’s effective T0 GPS is found, its LL GPS time may be determined. First, the coarse count must be calibrated as follows.

|                               |   |                      |
|-------------------------------|---|----------------------|
| $tx_{cc\delta}^{\beta}$       | $\stackrel{\text{def}}{=} \text{Start event } LL_{\beta} \text{ value in units of USO coarse-clock cycles (counter) input from ATL01.}$   | <b>Equation 2-12</b> |
| $tx_{cal_{ccoffset}}^{\beta}$ | $\stackrel{\text{def}}{=} \text{Start time offset is an integer-valued correction to the coarse-clock counter to account for the difference between the reported number and the actual number. This offset can be unique for each PCE, } \beta, \text{ but is nominally set to } -1. \text{ This is a calibration value defined by the DFC FPGA spec.}$ | <b>Equation 2-13</b> |
| $TX_{CC\delta}^{\beta}$       | $= tx_{cc\delta}^{\beta} + tx_{cal_{ccoffset}}^{\beta}$   | <b>Equation 2-14</b> |

The GPS time of an individual laser fire is calculated by adding the GPS time of its associated T0 to the scale factor corrected leading lower course count as:

|                         |   |                      |
|-------------------------|---|----------------------|
| $GPSTime_{LLn}^{\beta}$ | $= GPSTime_{T0n}^{\beta} + \{TX_{CC\delta}^{\beta} * d_{USO} * SF_{USO}^{\alpha}\}$ | <b>Equation 2-15</b> |
|-------------------------|---|----------------------|

To conserve bits in the final data product, GPS time will be established relative to the ATLAS standard data product (SDP) GPS Epoch. The SDP epoch is recorded in the ancillary data portion of the ATL02 data product. Therefore, this delta\_time can be found as:

|                           |   |                      |
|---------------------------|---|----------------------|
| $DeltaTime_{LLn}^{\beta}$ | $= GPSTime_{LLn}^{\beta} - GPSTime_{Epoch}$ | <b>Equation 2-16</b> |
|---------------------------|---|----------------------|

**Note:  $DeltaTime_{LLn}^{\beta}$  is in GPS seconds.**

## 2.5.6 An Alternative View: Calculation of GPS Time of Leading Lower of Shot Expressed in AMET

Should it be desired that as much of the calculation be performed in integer math as is practical, the equations shown in the previous sections may be combined and reduced as follows:

|                       |  |                      |
|-----------------------|--|----------------------|
| $GPSTime_{LLn}^\beta$ | $= \left( gps\_sec_{sc\_IPPS} + gps\_subsec_{sc\_IPPS} \right) + \left\{ \left( amet_{FirstTOMajorFrame}^\beta - amet_{SC1PPS} \right) * d_{USO} * SF_{USO}^\alpha \right\} + \left\{ T0_{effective,n}^\beta * 10,000 * d_{USO} * SF_{USO}^\alpha \right\} + \left\{ TX_{CC\delta}^\beta * d_{USO} * SF_{USO}^\alpha \right\}$ | <b>Equation 2-17</b> |
|                       | $= \left( gps\_sec_{sc\_IPPS} + gps\_subsec_{sc\_IPPS} \right) + \left\{ \left( amet_{FirstTOMajorFrame}^\beta - amet_{SC1PPS} + \left[ T0_{effective,n}^\beta * 10,000 \right] + TX_{CC\delta}^\beta \right) * d_{USO} * SF_{USO}^\alpha \right\}$  | <i>Simplified</i>    |

By ignoring both the conversion to seconds and the addition of GPS time, the AMET counter value at leading lower can thus be found:

|                    |   |                      |
|--------------------|---|----------------------|
| $AMET_{LLn}^\beta$ | $= amet_{FirstTOMajorFrame}^\beta + \left[ T0_{effective,n}^\beta * 10,000 \right] + TX_{CC\delta}^\beta$ | <b>Equation 2-18</b> |
|--------------------|---|----------------------|

## 2.5.7 Time Alignment of PCE Data

Because the Time of Flight Data recorded by the PCEs is split amongst three cards, and thus three asynchronous APIDs, an effort to align the data among these sources must be made. The approach considers the idealized case where no data has been lost; additional discussion of how to address various circumstances which lead to data dropouts is discussed further in Section 2.6.

### 2.5.7.1 Aligning PCE Data Via Time of Day or *delta\_time*

The PCE data is aligned using the TOD or *delta\_time* assigned to each laser shot via the following method:

1. Identify the PCE whose first value of  $GPSTime_{LLn}^\beta$  (or  $DeltaTime_{LLn}^\beta$ ) is the largest. This will become the point to which the remaining two PCEs are aligned.
2. Recover the array of  $GPSTime_{LLn}^\beta$  (or  $DeltaTime_{LLn}^\beta$ ) values for the remaining two PCEs. Find the value in each array which is the nearest neighbor to the  $GPSTime_{LLn}^\beta$  (or  $DeltaTime_{LLn}^\beta$ ) value found in the previous step. This is the point at which the three PCEs are aligned to the same event.

A nearest neighbor is considered to be a good match if the AMET counters are aligned to +/- 150 ns (+/- 15 coarse counts). The reasons for this are as follows:

- The flight software uses IMET to assign an AMET to the first T0 of each major frame. While the AMET has a resolution of 10 ns, IMET has a 40 ns resolution. Therefore, times cannot be expected to match between PCEs to better than 40 ns, or 4 AMET counter intervals.



- If the PPS arrives at a PCE within one or two IMET cycles of the start of a MF, there is an 80 ns (eight USO cycle) ambiguity in the time provided by the instrument for the AMET at major frame.

Thus, a +/- 150 ns (+/- 15 coarse counts) tolerance is suggested as it gives nearly 2x margin on this 80 ns ambiguity.

Further, because of the way that the ground system parses data into granules, it is possible that the time of the first packet on each of the three PCEs will be sufficiently far apart that a triad of nearest neighbor values will not exist. In these cases, only the remaining PCEs (one or two total) will be able to be aligned to one another. This will have additional implications when calculating the start centroid time later on in this document.

**2.5.7.2 Aligning PCE data to non-PCE Data using *delta\_time***

In the case of other, non-altimetric science data packets, *delta\_times* are determined in a slightly different manner. The methodology used to assign a *delta\_time* to these data products is outlined in Section 8.1. These non-PCE values of *delta\_time* are used to align non-PCE to PCE data.

**2.5.7.3 Dealing with transmit/receive slips**

Under certain conditions, the transmit event data from one laser shot can be lost from the sequence on a PCE. This results in receive events for that and subsequent laser shots being associated with the wrong transmit event. This error is called a “TX/RX slip”. TX/RX slips are detected and corrected by the following process:

First, calculate the sequence of time differences between transmit leading-lower times for each PCE:

|                        |   |                      |
|------------------------|---|----------------------|
| $\Delta T_{LLn}^\beta$ | $= \mathit{DeltaTime}_{LLn+1}^\beta - \mathit{DeltaTime}_{LLn}^\beta$ | <b>Equation 2-19</b> |
|------------------------|---|----------------------|

Then count the number of instances in the granule, for each PCE, in which  $\Delta T_{LLn}^\beta$  differs from the corresponding values for both of the other PCEs by more than 10 ns, producing three values  $N\Delta T^\beta$ , and record the major frame counter values of the first and last of occurrences. Finally, compute a confidence for each PCE:

|                  |   |                      |
|------------------|---|----------------------|
| $C_{TXRX}^\beta$ | $= 100 \frac{N\Delta T^\beta}{n_{aligned_{tx}}/75}$ | <b>Equation 2-20</b> |
|------------------|---|----------------------|

Where  $n_{aligned_{tx}}$  is the number of instances in which the TX values are aligned across all three PCEs (ideally equal to the number of TX events in the granule).

A nonzero value of  $N\Delta T^\beta$  indicates a TX/RX slip. In that case, correct the data in the affected major frames for the PCE with the highest confidence value as follows:

1. Discard event data from the first major frame containing a TX/RX slip



2. If there is no (n+1)th transmit event, discard receive data associated with the nth transmit event; else shift receive events from the (n+1)th transmit event to the nth transmit event.

This repairs most of the corrupted data, but one major frame is lost at the beginning of the TX/RX slip, and the last shot of each repaired major frame is lost. This method works only if the TX/RX slip occurs on only one PCE at a time.

## 2.6 Dealing with Missing Data

There are several circumstances which would prevent the time alignment technique outlined above from being performed as designed. Table 11 outlines the various scenarios, their potential repercussions, and mitigation strategies.

**Table 11: Missing Data Scenarios and Their Associated Repercussion + Mitigation**

| Scenario  | Repercussion + Mitigation   |
|---|---|
| <b>All APIDs are present but begin at markedly different CCSDS timestamps</b> | Provided all packet segments are available (i.e. data is contiguous), the calculations proceed as outlined above, with the warning that some TOFs may not have a full complement of three PCE's worth of data aligned at a given AMET time. This will occur at the very beginning and end of a granule. The implication of this is that the start centroid calculation will lose some precision; aside from that, all other calculations may be performed as written. |
| <b>Missing first segment of a major frame packet</b>                          | If the first segment of a major frame is missing, this eliminates the ability to align any data within the remainder of the frame to its appropriate T0 value. The code should simply skip the remainder of the frame missing its first segment. Remaining contiguous data should be aligned and evaluated from the start of the next available major frame.  |
| <b>Missing segment between 2<sup>nd</sup> and end of a major frame packet</b> | If any continuation segments of a major frame are missing, this eliminates the ability to align any data from that point forward (within the frame) to its appropriate T0 value. The code should simply skip the remainder of the frame missing its first segment. Remaining contiguous data should be aligned and evaluated from the start of the next available major frame.  |
| <b>Missing a SIM_HK packet</b>  | The 64 bit AMET rolls once every ~5800 years (unless there is a board level reset), so the calculation can simply use the nearest available SIM_HK packets. Even if only 1 SIM_HK packet is present in a 10 minute granule, the timing knowledge will be less than 100 ns. If no SIM_HK packets are present in any of the granule, the telemetry should be called into question and no further processing should be performed.  |
| <b>If AMET hi + low bytes are both 0</b>                                      | Check for non-zero value of Range Window Start + Range Window Width Parameters. If all are found to be 0, then the AMET counter has not yet initialized. The major frame should be discarded and analysis should begin with the first major frame with a non-zero AMET counter value.   |

## 2.7 Data Quality Monitoring

The data quality monitoring of TOD data should undertake a two-fold check. First, to check the inputs to the TOD calculations and secondly to confirm that the output of the calculations, including alignment of data, is reasonable.

## 2.7.1 Quality Check of TOD Calculation Inputs

In order to ensure that the TOD calculations are likely to yield reasonable results, the input values must be checked for their own integrity. What follows is a suggested quality check of the fields within the SIM\_HK packet, which is the backbone not only for spacecraft GPS time references, but also the flight software calculated AMET values supplied in the DFC.ALT\_SCI packets.

To begin, compute the available times of the spacecraft GPS:

|                         |  |                          |
|-------------------------|--|--------------------------|
| $gps_{time_{sc\_1PPS}}$ | $= gps_{sec_{sc\_1PPS}} + gps_{subsec_{sc\_1PPS}}$ | <b>Equation<br/>2-21</b> |
|-------------------------|--|--------------------------|

Next, calculate the time interval between the GPS PPS values:

|                                |   |                          |
|--------------------------------|---|--------------------------|
| $\delta gps_{time_{sc\_1PPS}}$ | $= gps_{time_{sc\_1PPS,j+1}} - gps_{time_{sc\_1PPS,j}}$ | <b>Equation<br/>2-22</b> |
|--------------------------------|---|--------------------------|

Then calculate the AMET counter interval between the GPS PPS values. The 64 bit AMET value should be used.

|                        |   |                          |
|------------------------|---|--------------------------|
| $\delta amet_{SC1PPS}$ | $= amet_{SC1PPS,j+1} - amet_{SC1PPS,j}$ | <b>Equation<br/>2-23</b> |
|------------------------|---|--------------------------|

Finally, compute the time between the ASC internal PPS values. Note that this value is not used directly by any of the calculations outlined in this section; however, it is used by the flight software when assigning an AMET value to the first T0 in each major frame. The 64 bit AMET value should be used.

|                              |   |                          |
|------------------------------|---|--------------------------|
| $\delta amet_{Internal1PPS}$ | $= amet_{Internal1PPS,j+1} - amet_{Internal1PPS,j}$ | <b>Equation<br/>2-24</b> |
|------------------------------|---|--------------------------|

The data from the SIM\_HK packet is likely good if the following criteria are met:

- All values of  $\delta gps_{time_{sc\_1PPS}}$  are approximately 1 second (which matches the expected rate of the packet)
- All values of  $\delta amet_{SC1PPS}$  and  $\delta amet_{Internal1PPS}$  are approximately 100e6, which matches the expected roll of 10,000 amet counts per shot \* 10,000 shots/sec
- By element comparison of the values of  $\delta amet_{SC1PPS}$  and  $\delta amet_{Internal1PPS}$  show that the approximate AMET roll between the receipt of the spacecraft 1 PPS and the generation of the internal 1 PPS is consistent

If one or more of the above criteria is *not* met, this suggests that the SBC is either uncertain about some information being received via the spacecraft 1 PPS or that the values are not updating as they should. In either event, the data should be flagged for additional inspection.

If all of the above criteria are met, this indicates that the data is flowing into the SBC appropriately. However, the relative behavior of all of the time references should also be compared. To do so, compute the following ratios:

|      |   |                          |
|------|---|--------------------------|
| $R1$ | $= \frac{\delta amet_{SC1PPS} * d_{USO} * SF_{USO}^\alpha}{\delta gps_{time_{sc\_1PPS}}}$ | <b>Equation<br/>2-25</b> |
| $R2$ | $= \frac{\delta amet_{Internal1PPS}}{round(\delta gps_{time_{sc\_1PPS}})}$                | <b>Equation<br/>2-26</b> |

If:

- $R1 \approx 1$ , this indicates that the time stamps are likely reasonable and the scale factor is accurate. Otherwise, this indicates a problem with one or both of these.
- $R2 \approx 100e6$ , this indicates that the time stamps are likely reasonable. Otherwise, this indicates a problem with the time stamps.

Should either of the criteria for  $R1$  or  $R2$  not be met, this is indicative of a problem with the GPS time stamps and/or the scale factor. In these cases, additional investigation will be necessary.

### 2.7.2 Confirmation of TOD Calculations and Data Alignment

The individual TODs assigned to a shot must be evaluated to see if they are reasonable. To do so, the time elapsed between adjacent shots should be calculated per Equation 2-27. If time delta within the data being examined outside of the expected jitter (100usec +/- 30ns), the time assignments are questionable and warrant additional investigation. This may also be an indication of missing time data.

|                                  |   |                          |
|----------------------------------|---|--------------------------|
| $\delta GPSTime_{LLn,n+1}^\beta$ | $= GPSTime_{LLn+1}^\beta - GPSTime_{LLn}^\beta$ | <b>Equation<br/>2-27</b> |
|----------------------------------|---|--------------------------|

If all of the individual time deltas are found to be reasonable within the context of a given PCE, the time series of deltas from each PCE should be correlated to one another, with the data aligned according to section 2.5.7.

|                    |  |                          |
|--------------------|--|--------------------------|
| $\rho_{PCE1,PCE2}$ | $= CORR(\delta GPSTime_{LL}^{PCE1}, \delta GPSTime_{LL}^{PCE2})$ | <b>Equation<br/>2-28</b> |
| $\rho_{PCE1,PCE3}$ | $= CORR(\delta GPSTime_{LL}^{PCE1}, \delta GPSTime_{LL}^{PCE3})$ | <b>Equation<br/>2-29</b> |
| $\rho_{PCE2,PCE3}$ | $= CORR(\delta GPSTime_{LL}^{PCE2}, \delta GPSTime_{LL}^{PCE3})$ | <b>Equation<br/>2-30</b> |

If the data from the three PCE cards is properly aligned, the values for  $\rho_{PCE1,PCE2}$ ,  $\rho_{PCE1,PCE3}$ ,  $\rho_{PCE2,PCE3}$  will result in a strong correlation. For the purposes of this document, a strong correlation is defined

as a  $\rho > 0.9$ . In the event that a sufficiently strong correlation is not identified in all three possible correlation combinations, this is suggestive of a questionable data association and additional investigation may be needed.

### 2.7.3 Data Screening Mechanisms & Associated Responses

The computations outlined in this chapter will be assessed via the quality assessment parameters included in Table 12 below.

**Table 12: TOD Data Quality Monitoring Criteria**

| Check                                     | Pass Criteria                     | ATL02 Screening Parameter                                       | Method  | Failure Response   |
|---|-----------------------------------|---|---|--|
| <b>Time elapsed per shot</b>              | Within 100 $\mu$ s +/- 40 ns      | <i>/quality_assessment/summary/pce/qa_s_tod_alt</i>             | By PCE, compare delta_time intervals. If time is out of tolerance, this suggests that a shot has an improper TOD value. | Alert via digest email. Additional investigation of granule may be needed if this behavior is observed outside of a DNF or similar warning where a skipped shot is expected. |
| <b>Shot time delta correlation</b>        | $\rho > 0.9$ for all combinations | <i>/quality_assessment/summary/qa_time_corr</i>                 | After aligning data by delta_time, compute correlation per section 2.7.2.   | Data is poorly aligned. Stop processing of granule + investigate further.  |
| <b>AMET Counter Increments Per Second</b> | $R1 \approx 1$<br>$R2 = 100e6$    | <i>/quality_assessment/summary/qa_amet_r1 &amp; /qa_amet_r2</i> | Compute values of $R1$ and $R2$ . If out of tolerance, suggests issue with scale factor and/or time stamps.             | AMET references may be poorly conditioned. Stop processing of granule + investigate further.   |
| <b>Freewheel Flag Is Non-Zero</b>         | Flag = 0                          | <i>/quality_assessment/summary/qa_fw_flag</i>                   | Evaluate if instrument ever entered a freewheel state by checking the value of A_PCEx_PMF.TIMEKEEPING.                  | Alert via digest email. If flag is non-zero, this indicates that the instrument was projecting AMET/GPS times. Data is likely still valid, but should be viewed accordingly. |

## 2.8 Data Products

The following values, as related to TOF calculations, are written to the ATL02 output file. Anywhere shot-wise data is stored within the ATL02 standard data product, the following time-of-data reference will also be stored:

**Table 13: *delta\_time* Parameters Written to the ATL02 Product (variable data rate)**

| Parameter Path                                      | Equation      | Description   |
|---|---------------|---|
| <i>/atlas/pcex/altimetry/s_w/photons/delta_time</i> | Equation 2-16 | The Time of Day associated with the Transmit (TX) pulse, relative to the ATLAS SDP GPS Epoch. Units are in seconds. Data rate is equal to the return event rate (variable).   |
| <i>/atlas/pcex/tep/delta_time</i>                   | Equation 2-16 | The Time of Day associated with the Transmit (TX) pulse, relative to the ATLAS SDP GPS Epoch. Units are in seconds and are based on the <i>delta_time</i> of the shot that the RX should have been associated with. Data rate is equal to the return event rate (variable). |

***Note: Since the groups above write out data on the basis of received events, *delta\_time* information is repeated for every photon which originated from a given shot.***

***Note: Each PCE will have a different *delta\_time* for a given shot, but will be within 40ns across all three PCEs.***

## 3 Time of Flight Calculation

Time of Flight (TOF) is one of the fundamental and crucially important measurements made by the ATLAS instrument. This section presents the algorithms used to compute TOF *relative* to the centroid of the detected laser start pulse. The calculation will also be corrected with calibration data as defined throughout this derivation.

Physically, TOF is the time difference between the detection of a transmitted light pulse by the Start Pulse Detector (SPD) and the detection of a photon from that pulse, by a photon-counting detector, after returning from the target or traversing the Transmitter Echo path. The detection of a pulse by the ATLAS Start Pulse Detector (SPD) is referred to as a “start event”, denoted as TX. The detection of each received photon results in a pulse transmitted to the PCE by the Detector Electronics Module (DEM) within the Detector Array Assembly (DAA). This occurrence is referred to as a “return event” and is denoted as RX. The process of measuring the precise times of the TX and RX events, and the TOF value resulting from them, are described in detail below.

### 3.1 Ground Rules & Assumptions

The following “ground rules” and assumptions apply to the calculations outlined in this chapter:

- PCE power-up and reset sequences are not held to a common pattern. Due to the internal nature of PCE time references and an externally assigned AMET, assigned times may disagree by up to 4 clock cycles or 40 ns.
- Because of this, all calculations will be performed with the assumption that the PCEs all detect the LL threshold crossing simultaneously. Given this, it can be assumed that the LL value of each PCE can be used as a common origin point for all calculations on data collected by that PCE.
- Calibration application should be consistent with what is presented in the calibration documentation .
- In the event of a conflict between what is shown in this document and the calibration documents, the calibration documents will govern. The following calibrations are applied within the context of this chapter: CAL-10 / ANC27, 17, 44, 49.
- The phrases “coarse time”, “coarse counts”, and “coarse clocks” will be used to refer to a ruler clock derived time, nominally expressed as an integer multiple of the ~10ns USO period. Coarse times may be expressed as integers (in units of coarse clock period) or in seconds.
- The phrase “fine time” and “fine counts” will be used to refer to a TDC delay chain derived time, nominally expressed as a *fractional* portion of the ~10ns USO period. Fine times may be expressed as fractions of coarse clock periods or in seconds.
- The phrase “precise time” will refer to a calculated time which is derived from a coarse time, fine time, and all applicable calibrations (skews, scale factors, etc.).
- The precise start time will be calculated using three pairs of threshold crossing values, all corresponding to the same laser fire. Each PCE will report the time of the leading lower threshold crossing and one other crossings. In this document, “leading” and “other” are the terms used to generalize this description.
- Because of the asynchronous nature of PCE operation, it is possible that the streams of data from one PCE versus another may be several shots out of phase. This data must be aligned prior to beginning any precise start center calculations. Alignment techniques are discussed in detail in Chapter 2.5.7. For the purpose of the equations outlined in this chapter, it is assumed that the data across the three PCEs have been synchronized.
- ATL02 reports times of flight. Geometric interpretation of times of flight occurs in subsequent science data products.

### 3.2 Variable Definitions and Notation Syntax

Before deriving the equations for TOF, shorthand notations and symbols for use in expressing generalized equations are established. Notation syntax is as follows:

$$\mathbf{Parameter}^{\mathbf{Hardware Identifier(s)}}_{\mathbf{Telemetry Type(s)}}$$

- Bolded parameters are values expressed in seconds
- Non-bolded parameters are dimensionless (i.e. clock cycles, channel, or ratios)
- Lower case parameters are uncalibrated
- Upper case parameters are calibrated
- Hardware identifiers include Hardware sides (A or B), PCE Identifiers (1, 2, or 3)
- Telemetry Types include Toggle values, Start Components, Downlink Band, Spot Type, Channels (Return Events)

**Table 14: Generalized TOF Calculation Notation**

| Symbol     | Parameter               | Super or Subscript | Valid Values    |
|------------|-------------------------|--------------------|-----------------|
| $\alpha$   | Hardware Side           | Superscript        | A, B            |
| $\beta$    | PCE Identifier          | Superscript        | 1, 2, 3         |
| $\gamma$   | Toggle Value            | Subscript          | Rising, Falling |
| $\delta$   | Leading Start Component | Subscript          | LL1, LL2, LL3   |
| $\tau$     | Other Component         | Subscript          | LU, TU, TL      |
| $\xi$      | Spot Type               | Subscript          | Strong, Weak    |
| $\zeta$    | Downlink Band           | Subscript          | 1, 2, 3, 4      |
| $\epsilon$ | Channel                 | Subscript          | 1, 2, ..., 20   |

Because of the great degree of variety of notation in this document, a dictionary of utilized terms follows (in approximate order of appearance):

**Table 15: Dictionary of TOF Derivation Variables**

| Uncalibrated Notation | Calibrated Notation   | Description  | Units         | Source   |
|-----------------------|-----------------------|--|---------------|--|
| $rx\_ch$              | n/a                   | Receive PCE channel ID (range [1,20]).   | dimensionless | ATL01 parameter: <i>/atlas/pcex/a_alt_science/raw_rx_channel_id</i>                                |
| $rx\_tog$             | n/a                   | Flag to indicate whether received time tag toggle is rising or falling edge detection (1 = rising, 0 = falling). | dimensionless | ATL01 parameter: <i>/atlas/pcex/a_alt_science/raw_rx_toggle_flg</i>                                |
| $d_{USO}$             | n/a                   | Nominal USO period (10ns).   | seconds       | Value defined per the DFC FPGA specification   |
| n/a                   | $SF_{USO}^\alpha$     | USO scale factor.  | dimensionless | Calculated value per Equation 2-4  |
| $tx_{cc\delta}^\beta$ | $TX_{CC\delta}^\beta$ | Leading lower element coarse counts.   | clock cycles  | $tx_{cc\delta}^\beta$ : ATL01 parameter: <i>/atlas/pcex/a_alt_science_ph/raw_tx_leading_coarse</i> |



| Uncalibrated Notation                | Calibrated Notation    | Description  | Units            | Source   |
|--------------------------------------|------------------------|--|------------------|--|
|                                      |                        |  |                  | $TX_{CC\delta}^\beta$ : Calculated value per Equation 3-4  |
| $tx_{cal}^\beta$ <sub>ccoffset</sub> | n/a                    | Integer correction to coarse count values to TX.   | clock cycles     | Value defined per the DFC FPGA specification and documented in Equation 3-3  |
| $tx_{smbit}^\beta$                   | n/a                    | Start marker bit for “other” start element.  | clock cycles     | ATL01 parameter:<br><i>/atlas/pcex/a_alt_science_ph/raw_tx_start_marker</i>  |
| n/a                                  | $TX_{CC\tau}^\beta$    | “Other” start element.   | clock cycles     | Calculated value per Equation 3-6  |
| $fc_{TDC\gamma}^\beta$               | n/a                    | Sum of 256 estimates of the number of delay line cells per USO, or coarse, clock cycle.  | delay line cells | ATL01 parameter:<br><i>/atlas/pcex/a_alt_science/raw_alt_cal_{rise/fall}</i>   |
| n/a                                  | $FC_{TDC\gamma}^\beta$ | Averaged and smoothed value representing the number of delay line cells expected per USO cycle.  | delay line cells | Calculated value per Equation 3-9  |
| n/a                                  | $FC_{TDC\gamma}^\beta$ | Averaged and smoothed value representing the elapsed time per delay line cell.   | seconds          | Calculated value per Equation 3-10   |
| $tx_{fc\delta}^\beta$                | $TX_{FC\delta}^\beta$  | Fine count value for leading start element. Calibrated (or effective) value found via CAL-17.  | delay line cells | $tx_{fc\delta}^\beta$ : ATL01 parameter:<br><i>/atlas/pcex/a_alt_science_ph/raw_tx_leading_fine</i><br><br>$TX_{FC\delta}^\beta$ : Value selected per Table 18 |
| $tx_{fc\tau}^\beta$                  | $TX_{FC\tau}^\beta$    | Fine count value for other start element. Calibrated (or effective) value found via CAL-17.  | delay line cells | $tx_{fc\tau}^\beta$ : ATL01 parameter:<br><i>/atlas/pcex/a_alt_science_ph/raw_tx_trailing_fine</i><br><br>$TX_{FC\tau}^\beta$ : Value selected per Table 18    |
| $tx_{t\delta}^\beta$                 | n/a                    | Precise time of leading start element relative to T0.  | clock cycles     | Calculated value per Equation 3-17   |
| $tx_{t\tau}^\beta$                   | n/a                    | Precise time of other start element relative to T0.  | clock cycles     | Calculated value per Equation 3-18   |
| $spd_{cal\tau}^\alpha$               | n/a                    | Calibrated offset to correct for the SPD path delay between the leading and other transmit pulse threshold crossing. Found via CAL-44. | seconds          | Value selected per Table 19  |
| n/a                                  | $TX_{T\tau}$           | Time elapsed between the leading and other transmit pulse threshold crossing.  | seconds          | Calculated value per Equation 3-20   |
| $\frac{n}{a}$                        | $TX_{T\delta}^\beta$   | Time elapsed between T0 and LL for a given PCE and laser fire.   | seconds          | Calculated value per Equation 3-21   |



| Uncalibrated Notation | Calibrated Notation        | Description   | Units         | Source  |
|-----------------------|----------------------------|---|---------------|---|
| n/a                   | $T_{center}$               | Time elapsed between LL and the precise start time (centroid).  | seconds       | Calculated value per Equation 3-22  |
| $k_{\#,i}$            | n/a                        | Coefficient for computation of precise start time.  | dimensionless | Calculated value per ICESat-2-ISF-ANYS-0209 and delivered via ANC27               |
| n/a                   | $pulse_{width_{lower}}$    | The distance between the lower threshold crossing times measured by the start pulse detector.   | seconds       | Calculated value per Equation 3-23  |
| n/a                   | $pulse_{width_{upper}}$    | The distance between the upper threshold crossing times measured by the start pulse detector.   | seconds       | Calculated value per Equation 3-24  |
| n/a                   | $pulse_{skew}$             | The difference between the averages of the lower and upper threshold crossing times.  | seconds       | Calculated value per Equation 3-25  |
| n/a                   | $RWS_{\xi}^{\beta}$        | Range window start value, expressed relative to leading lower.<br><b>Note:</b> Value is corrected/calibrated by FSW and 1 coarse count does <b>not</b> need to be deducted.   | clock cycles  | ATL01 parameter:<br><code>/atlas/pcex/a_alt_science/raw_alt_rw_start_{s/w}</code> |
| n/a                   | $RWS_T_{\xi}^{\beta}$      | Time elapsed between LL and Range Window Start.   | seconds       | Calculated value per Equation 3-37  |
| n/a                   | $RWW_{\xi}^{\beta}$        | Range window width value.<br><b>Note:</b> Value is corrected/calibrated by FSW and does <b>not</b> need to be adjusted.   | clock cycles  | ATL01 parameter:<br><code>/atlas/pcex/a_alt_science/raw_alt_rw_width_{s/w}</code> |
| n/a                   | $RWW_T_{\xi}^{\beta}$      | Time elapsed between the start and end of the Range Window.   | seconds       | Calculated value per Equation 3-38  |
| n/a                   | $DLBO_{\xi,\zeta}^{\beta}$ | Downlink band offset value, expressed relative to range window start.<br><b>Note:</b> The appropriate $DLBO_{\xi,\zeta}^{\beta}$ is selected from the array of 4 values appearing in the ATL01 product. This is done per Section 3.5.4. The values on the ATL01 product are corrected/calibrated by FSW prior to packetization and are used in the TE_TOF calculation as telemetered. | clock cycles  | ATL01 parameter:<br><code>/atlas/pcex/a_alt_science/raw_alt_band_offset</code>    |

| Uncalibrated Notation                | Calibrated Notation     | Description  | Units            | Source  |
|--------------------------------------|-------------------------|--|------------------|---|
| n/a                                  | $DLBO_{T\zeta}^{\beta}$ | Time elapsed between the RWS and the beginning of the downlink band. Precision is in units of coarse clocks.<br><br><b>Note:</b> Calculation removes the FSW correction incorporated for TOF computation. See section 3.8.3 for more information.  | seconds          | Calculated value per Equation 3-39  |
| n/a                                  | $DLBW_{\zeta}^{\beta}$  | Downlink band width value.<br><br><b>Note:</b> The appropriate $DLBW_{\zeta}^{\beta}$ is selected from the array of 4 values appearing in the ATL01 product. This is done per Section 3.5.4. The values on the ATL01 product are corrected/calibrated by FSW prior to packetization and are used in the TE_TOF calculation as telemetered. | clock cycles     | ATL01 parameter:<br><i>/atlas/pcex/a_alt_science/raw_alt_band_width</i>   |
| n/a                                  | $DLBW_{T\zeta}^{\beta}$ | Time elapsed between the start and end of the DLBand.<br><br><b>Note:</b> Calculation removes the FSW correction incorporated for TOF computation. See section 3.8.4 for more information.   | seconds          | Calculated value per Equation 3-40  |
| $rx_{cc}^{\beta}$                    | $RX_{CC}^{\beta}$       | Receive event coarse counts.   | clock cycles     | $rx_{cc}^{\beta}$ : ATL01 parameter:<br><i>/atlas/pcex/a_alt_science_ph/raw_rx_leading_coarse</i><br><br>$RX_{CC}^{\beta}$ : Calculated value per Equation 3-28 |
| $rx_{cal}^{\beta}_{ccoffset}$        | n/a                     | Integer correction to coarse count values.   | clock cycles     | Value defined per the DFC FPGA specification and documented in Equation 3-27  |
| $rx_{fc}^{\beta}$                    | $RX_{FC}^{\beta}$       | Receive event fine counts. Calibrated (effective) value found via CAL-17.  | delay line cells | $rx_{fc}^{\beta}$ : ATL01 parameter:<br><i>/atlas/pcex/a_alt_science_ph/raw_rx_leading_fine</i><br><br>$RX_{FC}^{\beta}$ : Value selected per Table 18          |
| $rx_t^{\beta}$                       | n/a                     | Precise time elapsed between LL and the receive event.   | clock cycles     | Calculated value per Equation 3-32  |
| $ch_{cal_{\epsilon}}^{\alpha,\beta}$ | n/a                     | Receiver channel skew correction found via CAL-49.   | seconds          | Value selected per Table 23   |

| Uncalibrated Notation | Calibrated Notation         | Description  | Units   | Source                             |
|-----------------------|-----------------------------|--|---------|------------------------------------|
| n/a                   | $RX_{T_{\epsilon}}^{\beta}$ | Time elapsed between LL and the receive event.                             | seconds | Calculated value per Equation 3-34 |
| n/a                   | $TX_{T_{fine}}^{\beta}$     | Time elapsed between LL and the following coarse clock.                    | seconds | Calculated value per Equation 3-35 |
| n/a                   | $TOF_{\epsilon}^{\beta}$    | Time of flight, as measured from the precise start centroid to the return. | seconds | Calculated value per Equation 3-36 |

### 3.3 Mapping of Transmit and Return Event Information

#### 3.3.1 Laser Start Pulse Detector Channels

The TOF calculation makes use of three pairs of start event time measurements. The TDC FPGA in each of the three PCEs records the time that the leading edge of the outgoing laser pulse crosses the "lower" threshold, and the time of one of the "other" threshold crossing times. As shown in Figure 10, these threshold crossing times are referred to as TX leading-lower (LL), leading-upper (LU), trailing-upper (TU), and trailing-lower (TL).

For each PCE  $\beta = 1, 2, 3$ , two threshold measurements and their associated calibrations are allocated on two start channels to each PCE according to this mapping:

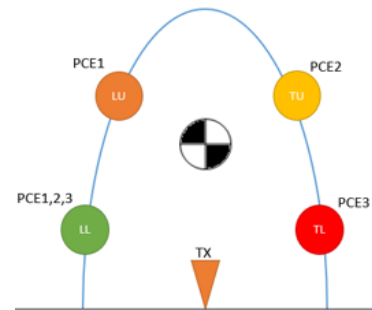


**Figure 10 : Laser pulse is detected using adjustable upper and lower thresholds that are crossed by the leading and trailing edges.**

|             |   |                     |
|-------------|---|---------------------|
| PCE $\beta$ | $= \begin{cases} \{LL_1, LU\}, & \beta = 1 \\ \{LL_2, TU\}, & \beta = 2 \\ \{LL_3, TL\}, & \beta = 3 \end{cases}$ | <b>Equation 3-1</b> |
|-------------|---|---------------------|

#### 3.3.2 Photon Detector Channels

It is necessary to briefly describe the electrical chain between the detector and the PCEs. The photomultiplier tube converts photons into pulses of electrons. This electrical signal passes through an amplifier to a constant-fraction discriminator which generates a digital pulse for as long as the detector output is above a given threshold. From the discriminator, the signal goes to a monostable multivibrator ("one-shot") that generates a fixed-length pulse. The pulse length of the one-shot determines the system dead time, the minimum time between events on each channel. Next the signal goes to the clock input of a toggle flip-flop which changes output state in response to each detected event. This flip-flop is what generates the PCE rising and falling edges. Rising and falling edges are identified in the telemetry because the PCE responds to the two edges slightly differently.

The path described above is duplicated for each of the PCE *physical return channel inputs*. For each PCE, the inputs are numbered 1 to 20 and identify the specific input such that channels 1 through 16 correspond to channels mapped to the *strong* spot detector and channels 17 through 20 correspond to channels mapped to the *weak* spot detector.

For data telemetry and processing with software, a different mapping is defined. This mapping includes a total of 120 *logical return channel IDs*, which convey information about the PCE, channel, and *rising/falling edge* values. The physical return channel IDs are obtained from ATL01 data from the altimetry science packet telemetry and are written to the ATL02 data product. This logical return channel mapping is defined in Table 16.

**Table 16: Logical mapping of return event channels IDs**

| PCE | Physical Channel | Logical Return Channel Ids (ph_id_channel) |                           |
|-----|------------------|--|---------------------------|
|     |                  | Rising Edge (rx_tog = 1)                   | Falling Edge (rx_tog = 0) |
| 1   | 1-20             | 061 – 080                                  | 001 – 020                 |
| 2   | 1-20             | 081 – 100                                  | 021 – 040                 |
| 3   | 1-20             | 101 - 120                                  | 041 - 060                 |

It is important to note that an alternative convention for mapping logical return channels was developed by the ATLAS calibration team. This convention, referred to as “super channels”, seeks to uniquely describe a channel and toggle combination for a PCE. This convention may occasionally be seen in calibration data products but does not appear on the ATL02 product itself. This information is used in conjunction with the instrument side to select the appropriate calibration data. Super channels are determined by PCE via the methodology outlined in Table 17.

**Table 17: Super Channel Assignment Algorithm**

| Event Type                      | Super Channel Value   |
|---------------------------------|---|
| <b>Start Leading Lower (TX)</b> | 0<br><i>Always rising edge</i>  |
| <b>Start Other (TX)</b>         | 1<br><i>Always rising edge</i>  |
| <b>Return Event (RX)</b>        | $(2 * rx\_ch) + rx\_tog$<br><i>Valid values: 2-41</i><br><i>Incorporates rising + falling edge values</i> |

Note that in cases of weak return with low background, it is possible to have transmits which do not yield any returns. In this case, a “return” photon will still be listed in the data, but will have a channel number of 0. The transmit data in these entries are valid, but the return information is filler and should thus be discarded.

### 3.4 Calculation of Start Time

The precise start time of the TOF calculation is found via a centroid calculation which considers six measurements of the start pulse’s threshold crossings. Each PCE characterizes the time of the Leading Lower (LL) threshold plus one “other” threshold element: PCE1, Leading Upper (LU); PCE2, Trailing Upper (TU); or PCE3, Trailing Lower (TL). In order to determine the start time, the precise time of each of these threshold crossings must be determined. All precise times recorded by the ATLAS instrument include a coarse time (maps to 10ns ruler clock) and a fine time (fractional expression of one ruler clock interval as measured via the TDC delay chain).

### 3.4.1 Calculation of Leading Lower Start Event Coarse Time

As was seen in section 2.5.5, the coarse time of a LL event relative to its T0 may be calculated as follows. Units are in clock cycles:

|                               |  |                     |
|-------------------------------|--|---------------------|
| $tx_{cc\delta}^{\beta}$       | $\stackrel{\text{def}}{=} \text{Start event } LL_{\beta} \text{ value in units of USO coarse-clock cycles (counter) input from ATL01.}$  | <b>Equation 3-2</b> |
| $tx_{cal_{ccoffset}}^{\beta}$ | $\stackrel{\text{def}}{=} \text{Start time offset is an integer-valued correction to the coarse-clock counter to account for the difference between the reported number and the actual number. This offset can be unique for each PCE, } \beta, \text{ but is nominally set to } -1. \text{ This is a calibration value defined by the DFC spec.}$ | <b>Equation 3-3</b> |
| $TX_{CC\delta}^{\beta}$       | $= tx_{cc\delta}^{\beta} + tx_{cal_{ccoffset}}^{\beta}$  | <b>Equation 3-4</b> |

### 3.4.2 Calculation of Other Element Start Event Coarse Time

As a bit saving measure, “other” element coarse times are referenced via a start marker bit (“smbit”) relative to the value of  $tx_{cc\delta}^{\beta}$ . Based on this, the coarse time of “other” events may be calculated relative to its T0 as follows. Units are in clock cycles:

|                       |   |                     |
|-----------------------|---|---------------------|
| $tx_{smbit}^{\beta}$  | $\stackrel{\text{def}}{=} \begin{cases} 0, & \text{if measured from the same coarse-clock edge as the } LL_{\beta} \text{ threshold crossing.} \\ 1, & \text{if trailing threshold crossing } x \text{ is measured from the next coarse-clock edge.} \end{cases}$ | <b>Equation 3-5</b> |
| $TX_{CC\tau}^{\beta}$ | $= tx_{cc\delta}^{\beta} + tx_{cal_{ccoffset}}^{\beta} + tx_{smbit}^{\beta}$  | <b>Equation 3-6</b> |

### 3.4.3 Calculation of Transmit Event Fine Time

In order to meet the instrument’s precise timing requirements, all event tags include a fine-clock time. This fine clock time represents a fraction of the 10ns USO ruler clock.

A rare anomalous condition has occurred in which the leading lower fine count value for a PCE,  $tx_{fc\delta}^{\beta}$ , is switched in the telemetry with the other fine count value for the same PCE,  $tx_{fc\tau}^{\beta}$ , and the leading lower coarse count value,  $tx_{cc\delta}^{\beta}$ , is replaced with the other coarse count value for that PCE. In this condition, the start marker bit is correct. Under normal conditions, the start marker and fine count values for a PCE satisfy this condition:

|                         |  |                     |
|-------------------------|--|---------------------|
| $tx_{fc\delta}^{\beta}$ | $\begin{cases} > tx_{fc\tau}^{\beta} & \text{if } tx_{smbit}^{\beta} = 0 \\ < tx_{fc\tau}^{\beta} & \text{if } tx_{smbit}^{\beta} = 1 \end{cases}$ | <b>Equation 3-7</b> |
|-------------------------|--|---------------------|

Under the anomalous condition, the inequalities are reversed. Before start pulse count values are used in any calculation, the fine count and start marker are checked against this condition; if they fail, the fine counts are switched and the start marker is subtracted from the leading lower coarse count. The quality assurance

parameter *qa\_s\_n\_swapped\_txfine* contains the number of shots for each PCE in which the anomalous condition occurred.

Each PCE has 22 delay chains, two for the transmitter and one for each of the 20 receiver channels. A twenty-third delay chain, the calibration channel, is used to characterize the transmitter and receiver delay chains. In the case of the transmit-event tags, fine clock times are only recorded via rising edge delay chain appropriate for the PCE and instrument side in use. Conversely, the return and calibration delay chains consider both the rising and falling edge. The speed of an edge down the delay chain, hence the number of delay units per USO clock cycle, is a weak function of the PCE environment and is different for the input rising and falling edges.

Once per major frame (50Hz), each PCE reports the number of delay chain units per USO cycle for both the rising and falling edge. These values are referred to as calibration words. The *actual* fine components of event times –fractions of a USO or coarse clock period -- are calculated using maps of the delay chain cell widths. As described in Table 18, the maps are selected using these calibration words. Because there is noise in the calibration words, their values are smoothed using a boxcar of 120 seconds (6000 major frames) before use. Note that this series of equations is presented within the context of transmit event time calculations, but it applies to other times recorded by the instrument as well (i.e. receive events).

To begin, the number of delay-line cells per USO clock cycle is computed:

|                          |  |                     |
|--------------------------|--|---------------------|
| $fc_{TDC\gamma}^{\beta}$ | $\stackrel{\text{def}}{=} \text{total number of delay-line cells (fine-clock counts) per coarse clock period for 256 consecutive periods. Value is reported in the first segment of the major frame.}$   | <b>Equation 3-8</b> |
| $FC_{TDC\gamma}^{\beta}$ | $\stackrel{\text{def}}{=} \text{number of delay-line cells (fine-clock counts) per USO clock cycle.}$<br>$= \text{smoothed} \left( \frac{fc_{TDC\gamma}^{\beta}}{256} \right)$<br><i>Note that the smooth function is executed over 6000 samples</i> | <b>Equation 3-9</b> |

Expressed in units of seconds, the mean time elapsed per delay line cell can be found as:

|                          |  |                      |
|--------------------------|--|----------------------|
| $FC_{TDC\gamma}^{\beta}$ | $= \frac{d_{USO} * SF_{USO}^{\alpha}}{FC_{TDC\gamma}^{\beta}}$ | <b>Equation 3-10</b> |
|--------------------------|--|----------------------|

Once the number of fine counts per USO clock cycle is determined, it can be used in conjunction with the event’s fine count (as reported in telemetry) to calculate the fine time expressed as fractional coarse clock cycles. This approach is applicable to both the leading lower and other element event times. Ideally, all delay chain elements, fine counts, are the same. However, they each differ by small amounts and each chain contains one element that is nearly twice as long as the others. CAL-17 converts the integer fine counts, that assume identical delay elements, into effective delays, non-integer delays that account for element to element variations. The calculation for the leading lower component fine time, expressed in units of ruler clocks, is as follows:

|   |   |                          |
|---|---|--------------------------|
| $tx_{fc_{\delta}}^{\beta}$  | $\stackrel{\text{def}}{=} \equiv$ Telemetered fine count value for leading lower start element.   | <b>Equation<br/>3-11</b> |
| $TX_{FC_{\delta}}^{\beta}$  | $\stackrel{\text{def}}{=} \equiv$ Value corresponding to $tx_{fc_{\delta}}^{\beta}$ as recovered from CAL- 17. Directions for selecting the appropriate calibration value are provided in Table 18.                           | <b>Equation<br/>3-12</b> |
| $\frac{TX_{FC_{\delta}}^{\beta}}{FC_{\text{TDC Rising}}^{\beta}}$ | $\stackrel{\text{def}}{=} \equiv$ The calibrated measure of <i>fractional</i> ruler clock cycles for a LL event without regard to the actual clock frequency.<br><i>Note that start channels only see rising edge events.</i> | <b>Equation<br/>3-13</b> |

**Table 18: Directions for Selection of CAL-17 Value**

| CAL-17: PCE Effective Cell Delay                  |   |
|---|---|
| <b>Description</b>                                | Calibration product for PCE Unit Cell Delay; a matrix of effective fine counts for each fine count reading as reported in telemetry.  |
| <b>Dependencies</b>                               | CAL-17 contains tables of effective delay, in units of cells (fractional fine counts), for rising and falling edges for each cell of each channel of each PCE, indexed by the rising-edge and falling-edge cal words for each PCE that are reported in the first segment of each major frame. The value of the cal word varies with temperature, voltage, and possibly other phenomena, but no attempt is made to separate these dependencies. The cal word itself represents their aggregate effect.   |
| <b>How to Select Value</b>                        | <ul style="list-style-type: none"> <li>• Take cal rising and cal falling values from first segment of major frame.</li> <li>• Select the rising-edge and falling-edge delay line maps corresponding to the cal word values closest to the reported values.                             <ul style="list-style-type: none"> <li>○ Report the calculated values of the rising and falling cal words.</li> </ul> </li> <li>• Select the effective delay value for the cell, channel, PCE, and direction. Use this for fine count value in the appropriate equations.</li> <li>• Start pulse channels are labeled as "LL" for the leading lower and "LU", "TU", or "TL" for the "other". All of these start pulse channels are rising-edge.</li> </ul> |
| <b>Telemetry Point Used to Select Calibration</b> | Taken from ATL01, for: <ul style="list-style-type: none"> <li>• PCE1, Rising Edge: /atlas/pce1/a_alt_science/raw_alt_cal_rise</li> <li>• PCE1, Falling Edge: /atlas/pce1/a_alt_science/raw_alt_cal_fall</li> <li>• PCE2, Rising Edge: /atlas/pce2/a_alt_science/raw_alt_cal_rise</li> <li>• PCE2, Falling Edge: /atlas/pce2/a_alt_science/raw_alt_cal_fall</li> <li>• PCE3, Rising Edge: /atlas/pce3/a_alt_science/raw_alt_cal_rise</li> <li>• PCE3, Falling Edge: /atlas/pce3/a_alt_science/raw_alt_cal_fall</li> </ul>  |

Similarly, the other element fine time can be found via:

|  |  |                      |
|--|--|----------------------|
| $tx_{fc_\tau}^\beta$                                       | $\stackrel{\text{def}}{=} \text{Telemetered fine count value for other start element.}$  | <b>Equation 3-14</b> |
| $TX_{FC_\tau}^\beta$                                       | $\stackrel{\text{def}}{=} \text{Value corresponding to } tx_{fc_\tau}^\beta \text{ as recovered from CAL - 17. Directions for selecting the appropriate calibration value are provided in Table 18.}$                    | <b>Equation 3-15</b> |
| $\frac{TX_{FC_\tau}^\beta}{FC_{TDC \text{ Rising}}^\beta}$ | $\stackrel{\text{def}}{=} \text{The calibrated measure of fractional ruler clock cycles for an "other" start event without regard to the actual clock frequency. Note that start channels only see rising edge events.}$ | <b>Equation 3-16</b> |

### 3.4.4 Calculation of Precise Start Event Times

Once the coarse and fine time of the start event are understood, the precise time of the LL event in ruler clock cycles may be calculated as follows:

|                       |  |                      |
|-----------------------|--|----------------------|
| $tx_{t_\delta}^\beta$ | $= \left( TX_{CC_\delta}^\beta - \frac{TX_{FC_\delta}^\beta}{FC_{TDC \text{ Rising}}^\beta} \right)$ | <b>Equation 3-17</b> |
|-----------------------|--|----------------------|

Similarly, the precise start time of the "other" time in ruler clock cycles may be found as follows:



|                      |  |                      |
|----------------------|--|----------------------|
| $tx_{t\tau}^{\beta}$ | $= \left( TX_{CC\tau}^{\beta} - \frac{TX_{FC\tau}^{\beta}}{FC_{TDC \text{ Rising}}^{\beta}} \right)$ | <b>Equation 3-18</b> |
|----------------------|--|----------------------|

To compute the time (in seconds) between the leading + other elements:

|                          |   |                      |
|--------------------------|---|----------------------|
| $spd_{cal\tau}^{\alpha}$ | <sup>def</sup> Calibrated offset to correct for the SPD path delay for the other transmit pulse threshold crossing on PCE $\beta$ . (CAL-44) Directions for selecting the appropriate calibration value are provided in Table 19. | <b>Equation 3-19</b> |
| $TX_{T\tau}$             | $= \left( tx_{t\tau}^{\beta} - tx_{t\delta}^{\beta} \right) \cdot d_{USO} * SF_{USO}^{\alpha} + spd_{cal\tau}^{\alpha,\beta}$   | <b>Equation 3-20</b> |

**Table 19: Directions for Selection of CAL-44 Value**

| CAL-44: Start Timing Skews                        |   |
|---|---|
| <b>Description</b>                                | Produces start pulse timing skews within and among PCEs to properly align all start pulse timing channels.  |
| <b>Dependencies</b>                               | Start Pulse Detector Side, Temperature  |
| <b>How to Select Value</b>                        | <ul style="list-style-type: none"> <li>Recover CAL-44 via ISF</li> <li>Select values based on start pulse detector in use + nearest neighbor temperature (use reported SPD temperature at granule start)</li> </ul>                                   |
| <b>Telemetry Point Used to Select Calibration</b> | Taken from ATL01: <ul style="list-style-type: none"> <li>To determine which SPD is in use: <code>/ancillary_data/housekeeping/spd_ab_flag</code></li> <li>To determine SPD temperature: <code>/atlas/housekeeping/thermal/hkt_spd_t</code></li> </ul> |

### 3.4.5 Calculation of Precise Start Time & Overall Timing Uncertainty

In order to calculate a precise start time, each PCE's LL time must be corrected such that the start time reference is instead reported relative to its start center. To accomplish this, the start data must be first aligned per section 2.5.7.

All PCEs' measurements of LL are assumed to occur simultaneously. (Note that because of the resolution of the 25 MHz IMET clock, the actual LL assigned times may differ up to 40 ns, as described in section 2.5.7.1) To calculate the time of LL of a given PCE relative to its T0:

|                        |  |                      |
|------------------------|--|----------------------|
| $TX_{T\delta}^{\beta}$ | $= tx_{t\delta}^{\beta} \cdot d_{USO} * SF_{USO}^{\alpha}$ | <b>Equation 3-21</b> |
|------------------------|--|----------------------|

The centroid of the transmit must be computed relative to LL, since the reported LL-to-T0 position may vary across the PCEs due to the free-running nature of T0. This is computed in Equation 3-22 and is applied to the TOF computation seen in Equation 3-36. Expressed in seconds, the centroid position relative to LL of any PCE may be found as:

|              |   |                      |
|--------------|---|----------------------|
| $T_{center}$ | $= k_{0,i} + k_{1,i}TX_{TLU} + k_{2,i}TX_{TTU} + k_{3,i}TX_{TTL}$ | <b>Equation 3-22</b> |
|--------------|---|----------------------|

The values of the coefficients,  $k$ , are calculated by the ISF via the method described in ICESat-2-ISF-ANYS-5400. Values of  $k$  are selected based on which, if any, threshold-crossing times are missing. These values are updated as the laser thresholds and/or energy levels are adjusted throughout the life of the mission and are delivered via ANC27. A threshold-crossing time can be missing in one or more of the following circumstances:

1. PCE data absent from telemetry (i.e. when a PCE is not in science mode)
2. PCE skips a frame (i.e. there is a downlink error and the frame is missing from telemetered data)
3. PCE throws a did not finish message (i.e. the PCE ran out of time before being able to completely report out the photon data for a specific frame and was forced to move onto the next frame)
4. The leading and trailing start information (uncalibrated) is identical (i.e. when upper threshold fails to trigger)
5. At the beginning or end of a granule when fewer than 3 PCEs datasets are available.

A summary of the eight possible scenarios is shown in Table 20. Note that the scenario number, corresponding to the TX scenario used when computing the start component of an individual event's fully corrected and calibrated TOF, is preserved in the event's *tof\_flag* parameter.

**Table 20: Mapping of case,  $i$ , according to which threshold data is missing from science data telemetry ( $x$  denotes missing data)**

| Scenario<br>(i) | PCE1 |    | PCE2 |    | PCE3 |    |
|-----------------|------|----|------|----|------|----|
|                 | LL   | LU | LL   | TU | LL   | TL |
| 1               |      |    |      |    |      |    |
| 2               |      | X  |      |    |      |    |
| 3               |      |    |      | X  |      |    |
| 4               |      |    |      |    |      | X  |
| 5               |      | X  |      | X  |      |    |
| 6               |      | X  |      |    |      | X  |
| 7               |      |    |      | X  |      | X  |
| 8               |      | X  |      | X  |      | X  |

It is important to note that the scenarios outlined above will each result in a different level of uncertainty in the  $T_{center}$  calculation. This is not something that is considered within the context of the ATL02 data product, but rather is important when determining the overall TOF (or TEP TOF) uncertainty in ATL03G/POD. Each scenario's uncertainty is calculated by the ISF and provided in ANC27. This uncertainty can, in turn, be RSS'ed on a by-shot basis with the standard deviation of the TEP return histogram computed by ANC41. This RSS'ed value represents the overall TOF uncertainty for all returns associated with that particular shot.

### 3.4.6 Calculation of Pulse Widths and Start Skews

Though not required for calculating TOF, higher level data products may require knowledge of a shot-wise skew value. To compute this, the following equations may be used once data has been aligned by TOD across the PCEs.

To determine the lower and upper widths, expressed in seconds, use the value of  $TX_T$  calculated per Equation 3-20:

|                         |                      |               |
|-------------------------|----------------------|---------------|
| $pulse_{width_{lower}}$ | $=TX_{TL}$           | Equation 3-23 |
| $pulse_{width_{upper}}$ | $=TX_{TU} - TX_{LU}$ | Equation 3-24 |

To compute the pulse skew, relative to LL, expressed in seconds:

|                |  |               |
|----------------|--|---------------|
| $pulse_{skew}$ | $=\frac{TX_{TU}+TX_{LU}}{2} - \frac{TX_{TL}}{2}$ | Equation 3-25 |
|----------------|--|---------------|

Values of  $pulse_{width_{lower}}$ ,  $pulse_{width_{upper}}$ , and  $pulse_{skew}$  are computed at 10kHz and are assigned a  $delta\_time$  based on PCE1’s recording of  $delta\_time$  for the laser fire. However, due to the nature of the alignment of PCE data, it is possible that one or more of the above  $TX\_T$  values will be unavailable. In these cases, the computation of pulse width and skew is not performed and instead a known invalid value (in the form of the maximum possible value for the data type) will be written to the product. The returned time series of  $delta\_time$ ,  $pulse_{width_{lower}}$ ,  $pulse_{width_{upper}}$ , and  $pulse_{skew}$  values reported in the final ATL02 data product should span the full range of available PCE data.

### 3.5 Calculation of Receive Event Times

Receive events (RX), like TX events, are recorded using a fine and a coarse time component. However, unlike TX events, they are expressed relative to the coarse clock occurring *after* the LL of the start rather than to T0. RX events are parameterized via the characteristics summarized in Table 21. The following sections describe how to calculate the time of the RX relative to LL.

**Table 21: ATL01 Parameters Used to Describe RX Tags**

| Parameter                  | Description   | Parameter Path<br><i>/atlas/pcex/a_alt_science_ph/</i> |
|----------------------------|---|--|
| <b>Channel ID</b>          | Channel number that received photon event (as from Telemetry).  | <i>raw_rx_channel_id</i>                               |
| <b>Downlink Band (DLB)</b> | Flag to indicate downlink band id associated with the received time tag.  | <i>raw_rx_band_id</i>                                  |
| <b>Toggle Flag</b>         | Flag to indicate received time tag toggle is rising or falling edge detection. Toggle Flag = 1 indicates a rising edge time tag, and Toggle Flag = 0 indicates a falling edge time tag. | <i>raw_rx_toggle_flg</i>                               |
| <b>Event Coarse Count</b>  | Received time tag leading edge coarse time in counts. Established relative to the downlink band start.  | <i>raw_rx_leading_coarse</i>                           |
| <b>Event Fine</b>          | Received time tag leading edge fine time in counts.   | <i>raw_rx_leading_fine</i>                             |

### 3.5.1 Calculation of Receive Event Coarse Time

To calculate the coarse time of a receive event, expressed in clock cycles and relative to the start of its downlink band:

|                               |   |                      |
|-------------------------------|---|----------------------|
| $rx_{cc}^{\beta}$             | $\stackrel{\text{def}}{=}$ List of receive event values in units of USO coarse clock cycles (counter) input from ATL01.   | <b>Equation 3-26</b> |
| $rx_{cal_{ccoffset}}^{\beta}$ | $\stackrel{\text{def}}{=}$ Start time offset is an integer-valued correction to the coarse-clock counter to account for the difference between the reported number and the actual number. This offset can be unique for each PCE, $\beta$ , but is <b>nominally set to <math>-1</math></b> . This is a calibration value defined by the DFC spec. | <b>Equation 3-27</b> |
| $RX_{CC}^{\beta}$             | $= rx_{cc}^{\beta} + rx_{cal_{ccoffset}}^{\beta}$   | <b>Equation 3-28</b> |

### 3.5.2 Calculation of Receive Event Fine Time

To calculate the fine time of a receive event, expressed in clock cycles:

|  |  |                      |
|--|--|----------------------|
| $rx_{fc}^{\beta}$                                | $\stackrel{\text{def}}{=}$ List of telemetered fine count values for receive event.  | <b>Equation 3-29</b> |
| $RX_{FC}^{\beta}$                                | $\stackrel{\text{def}}{=}$ Value corresponding to $rx_{fc}^{\beta}$ as recovered from CAL-17. Directions for selecting the appropriate calibration value are provided in Table 18.   | <b>Equation 3-30</b> |
| $\frac{RX_{FC}^{\beta}}{FC_{TDC\gamma}^{\beta}}$ | $\stackrel{\text{def}}{=}$ The calibrated measure of <i>fractional</i> clock cycles for a receive event without regard to the actual clock frequency. See derivation of $FC_{TDC\gamma}^{\beta}$ term in section 3.4.3. Note that each element must be divided by the appropriate value of $FC_{TDC\gamma}^{\beta}$ according to if it has a rising or falling toggle. | <b>Equation 3-31</b> |

### 3.5.3 Assigning Range Window Start Value

The Range Window Start ( $RWS_{\xi}^{\beta}$ ) value is a bit-saving measure that is used to describe where the ground returns contained in the altimetric histogram begin. It is expressed once per major frame (200 shots or 50Hz) *per spot* and is reported in the first segment of the major frame packet. The  $RWS_{\xi}^{\beta}$  value is expressed in terms of coarse clocks elapsed since the clock occurring *after* the LL for the shot that generated the returns.

### 3.5.4 Determining Downlink Band Offset

A downlink band (DLB) is a subset of the range window that is identified by the ATLAS flight software to ensure that return events will be in the telemetry packets sent to the ground. Return events are selected for downlink due to the likelihood of originating from a feature of interest, such as the TEP or ground return. Specifically, DLBs are used to prevent the telemetering of extraneous amounts of data and are dynamically positioned once per major frame via onboard algorithms. Per the DFC FPGA spec (ICESat-2-MEB-SPEC-0875), DLBs are characterized by a band number, spot, and DLB ID flag. The bands available for use by each PCE as seen in Table 22 below.

**Table 22: Downlink Band Assignment and Identification**

| Band # | DLB ID Flag |
|--------|-------------|
| 1      | 0           |
| 2      | 1           |
| 3      | 0           |
| 4      | 1           |

Each individual detector has the ability to utilize one, two, or no DLBs to downlink its data. The FSW determines how many bands to use as well as their start and width parameters. The DLB start(s) are expressed in units of coarse clock periods relative to the spot’s RWS and are written as an offset parameter,  $DLBO_{\zeta}^{\beta}$ . The DLB width(s),  $DLBW_{\zeta}^{\beta}$ , are also expressed in units of coarse clock periods.

**Note: The ATL01 product contains a *raw\_alt\_n\_bands* parameter which expresses how many DLBs are in use by each major frame. The value of *raw\_alt\_n\_bands* is equal to the number of bands in use minus 1.**

In addition to describing the offset and width of each DLB, the FSW also supplies a bit mask for each of the 4 DLBs available to each PCE. The information used to describe the 4 possible DLBs is telemetered at the beginning of each major frame, leaving the user to determine which individual returns are assigned to each DLB.

**Warning: Within a major frame, a channel may only be assigned to one DLB with the same DLB ID Flag. If it appears to be assigned to multiple bands with the same DLB ID Flag, the assignment is conflicting and the DLB mask(s) are invalid. The major frame should be discarded.**

Each RX tag contains five parameters which describe it. These can be seen Table 21. The DLB parameter in the RX tag maps to the DLB ID flag seen in Table 22. If the DLB bit is zero, the return came from DLB Band #1 or #3 and if the bit is a one, it came from DLB #2 or #4. Which band the RX came from is determined by testing which of the two possible DLB masks contain its channel. If the mask position which corresponds to a channel is set to 0, the channel is enabled and is thus able to appear in the downlinked telemetry. Otherwise, in the case of the mask being set to 1, the channel is disabled and should not appear.

Once the associated DLB is determined, the value of  $DLBO_{\zeta}^{\beta}$  needed to compute the RX’s TOF can be identified.

### 3.5.5 Calculation of Precise Event Times

Because the time of RX\_CC is expressed relative to the start of the DLB, the RX event time relative to the LL coarse clock, expressed in clock cycles, may be written as:

|                |   |                      |
|----------------|---|----------------------|
| $rx_t^{\beta}$ | $=RWS_{\xi}^{\beta} + DLBO_{\zeta}^{\beta} + RX_{CC_{\epsilon}}^{\beta} - \frac{RX_{FC}^{\beta}}{FC_{TDC\gamma}^{\beta}}$ | <b>Equation 3-32</b> |
|----------------|---|----------------------|

To compute the precise event time (in seconds), the value of  $rx_t^\beta$  computed above may be converted to seconds and then adjusted by the  $ch_{cal_\epsilon}^{\alpha,\beta}$  parameter to account for receiver channel timing skews:

|                                    |  |                      |
|------------------------------------|--|----------------------|
| $ch_{cal_\epsilon}^{\alpha,\beta}$ | $\stackrel{\text{def}}{=} \text{Channel skew correction as recovered from CAL-49. Directions for selecting the appropriate calibration value are provided in Table 23.}$ | <b>Equation 3-33</b> |
| $RX_{T_\epsilon}^\beta$            | $= rx_t^\beta \cdot d_{USO} * SF_{USO}^\alpha + ch_{cal_\epsilon}^{\alpha,\beta}$  | <b>Equation 3-34</b> |

**Table 23: Directions for Selection of CAL-49 Value**

| CAL-49: Receiver Channel Skews                    |   |
|---|---|
| <b>Description</b>                                | Timing skews for every rising/fall channel on ATLAS.  |
| <b>Dependencies</b>                               | Instrument side and temperature   |
| <b>How to Select Value</b>                        | <ul style="list-style-type: none"> <li>Use instrument side (delivered via hk_status packet's detector_bank parameter) and nearest neighbor of the mean temperature (taken over the entire granule) for the point listed below to select the appropriate cal table from the index file. All 3 PCEs use the same temperature telemetry point, converted per Chapter 8.4.</li> <li>Once into cal table, select skew value based on super channel (super channel definition same as seen in CAL-17; combined influence of channel and edge).</li> </ul> |
| <b>Telemetry Point Used to Select Calibration</b> | Taken from ATL01: <ul style="list-style-type: none"> <li>/atlas/a_hkt_c_1061/raw_hkt_dem1_t4_et_t</li> </ul>  |

### 3.6 Calculation of Nominal Time of Flight (TOF)

To calculate the nominal time of flight (TOF), the time elapsed between the RX and precise TX start (centroid) is computed. It must be kept in mind that the RX is established relative to the LL coarse clock boundary occurring after the start centroid, so the value from Equation 3-13 must be added to account for the fine time component of the start. The relationship of all of the telemetry considered when computing nominal TOF can be seen in Figure 11.

Begin by calculating the fine time of the LL event which originated the return being examined:

|                    |  |                      |
|--------------------|--|----------------------|
| $TX_{Tfine}^\beta$ | $= \frac{TX_{FC_\delta}^\beta}{FC_{TDC \text{ Rising}}^\beta} \cdot d_{USO} \cdot SF_{USO}^\alpha$ | <b>Equation 3-35</b> |
|--------------------|--|----------------------|

With this information, the nominal precise TOF for an event, relative to its start centroid, can be calculated as follows:

|                      |   |                      |
|----------------------|---|----------------------|
| $TOF_\epsilon^\beta$ | $= RX_{T_\epsilon}^\beta + TX_{Tfine}^\beta - T_{center}$ | <b>Equation 3-36</b> |
|----------------------|---|----------------------|

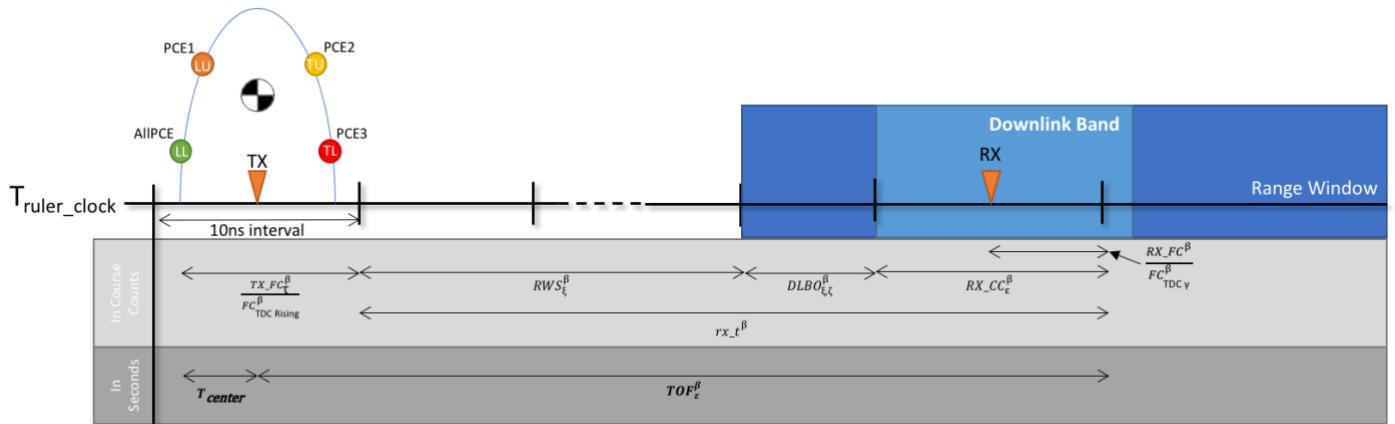


Figure 11: Summary of TOF calculation components

### 3.7 Identification of Duplicate Return-event Time Tags

Duplicate time tags are generated by the TDC FPGA because of the need to ensure that fine timing measurements are made throughout the entire 10 ns clock period. Because of small timing variations due to temperature or voltage, additional resources are incorporated in the TDC to ensure that there will not be missing time tag data. However, the trade-off of ensuring full measurement coverage throughout the clock period is that there will be duplicate time tag data output from the TDC. Upon receipt of the event time tag, if duplicate time tag removal is enabled, the DFC performs a duplicate time tag removal function as described in ICESat-2-MEB-SPEC-0875, Section 5.7.2, which removes many, but not all, duplicates.

Ideally, if the time tag’s fine-count value is greater than the number of delay line cells (fine-clock counts) per USO clock cycle for a given logical channel ID, which accounts for differences in rising and falling events, the time tag can be considered to be a duplicate time tag. The flight software can write to the duplicate margin time tag removal register in the DFC FPGA to provide some extra tolerance for this removal process. This is necessary since the reported calibration value is meant to be averaged and presents a border condition relating to the duplicate cut-off point. The setting also allows for the removal of duplicate time tags at either the beginning or end of the measurement path. Depending on the setting of the +/- bit of the duplicate margin register, the DFC adds or subtracts a value of 0 to 15 to the ideal calculated value. If the DFC considers the time tag to be a duplicate, then it is not stored when duplicate time tag removal is enabled. On board duplicate removal can reduce the duplicate rate from approximately 50% of events having a duplicate to less than 10% of events having duplicates. Unfortunately, complete on board duplicate removal cannot be accomplished without a significant chance of loss of non-duplicate events. Note that duplicate time-tag removal by the DFC FPGA can be disabled for diagnostic use.

Regardless of how aggressive the onboard duplicate removal is, additional removal of duplicate time tags is needed during ground processing. The algorithm presented in Table 24 below is used to perform this removal. Note that the time tags identified as duplicates are removed from the list and are not written to the ATL02 product; all others are saved as output in the ATL02 file.



**Table 24: Filter algorithm to remove duplicate return-event time tags**

Define the tolerance for the number of cells in the delay chain as  $\alpha \equiv 0.8$ .  
 Identify return events coming from the same shot, on the same channel, with the same toggle via `ph_id` count.  
**For** set of returns satisfying this criteria, take difference of coarse counts from *n*th RX vs all others. Repeat for all RX. Note: CC and FC here are *uncalibrated*.  
 $CC_{diff} = CC_n - CC_{other}$   
**if**  $|CC_{diff}| = 1$  **and**  $|FC_n - FC_{other}| > FC_{TDC}^x \cdot \alpha$  then tag pair contains a duplicate.  
     **if**  $CC_{diff} = -1 \rightarrow$  Keep *n*th value. Other value is a duplicate and should be removed.  
     **else** Keep other value being compared. Event *n* is a duplicate and should be removed. (Note: This results in keeping the event with the smaller CC value and removes the other which is a duplicate.)

### 3.8 Determining Times of Range Window and Downlink Band Features

Occasionally, there may be a need to visualize the start and width of the altimetric histogram range window and its associated downlink bands. ATL02 provides this information in units of time, which can in turn be converted to range. The following sections outline the equations for parameterizing the altimetric histogram boundaries.

#### 3.8.1 Calculation of Range Window Start Time

The altimetric range window start (RWS) is reported uniquely for each spot (strong, weak) for each PCE. Therefore, the six RWS times may be calculated as follows. Units are in seconds relative to the coarse clock occurring after the observed PCE LL. The value is reported once per major frame.

|                    |  |                      |
|--------------------|--|----------------------|
| $RWS_{T\xi}^\beta$ | $= RWS_\xi^\beta \cdot d_{USO} \cdot SF_{USO}$ | <b>Equation 3-37</b> |
|--------------------|--|----------------------|

#### 3.8.2 Calculation of Range Window Width in Units of Time

The altimetric range window width (RWW), like the RWS, is reported uniquely for each spot on each PCE. Therefore, the six RWW values may be calculated as follows. Units are in seconds and the value is reported once per major frame.

|                    |  |                      |
|--------------------|--|----------------------|
| $RWW_{T\xi}^\beta$ | $= RWW_\xi^\beta \cdot d_{USO} \cdot SF_{USO}$ | <b>Equation 3-38</b> |
|--------------------|--|----------------------|

#### 3.8.3 Calculation of Downlink Band Start Time

Each of the six spots may utilize 0-2 downlink bands. Each downlink band start time is referenced from the start of the spot’s range window via the DLB offset (DLBO) parameter. The downlink band start time is expressed in seconds and is relative to the RWS. The value is reported once per major frame.



**Note: The DLB offset value obtained from ATL01 and used in the ATL02 time of flight calculation has been adjusted by the Flight Software. The adjustment is in the form of a 2 coarse count increase to the value reported by the hardware. This is done to account for a timing behavior which causes the start of the to be off by 2 clock cycles. The value of  $DLBO_{\xi,\zeta}^{\beta}$  reported out in telemetry, and in ATL01, is the one which has been adjusted to account for this disparity. The correction must therefore be removed from the value when determining the time at which the downlink band actually opens. The time of DLB start reported on the ATL02 product is the output of Equation 3-39.**

|                         |   |                          |
|-------------------------|---|--------------------------|
| $DLBO_{T\zeta}^{\beta}$ | $= \begin{cases} 0, & \text{when } DLBO_{\xi,\zeta}^{\beta} = 0 \\ \left( \{DLBO_{\xi,\zeta}^{\beta} - 2\} \cdot d_{USO} \cdot SF_{USO}^{\alpha} \right), & \text{when } DLBO_{\xi,\zeta}^{\beta} \neq 0 \end{cases}$ | <b>Equation<br/>3-39</b> |
|-------------------------|---|--------------------------|

### 3.8.4 Calculation of Downlink Band Width in Units of Time

The downlink band width (DLBW) is reported uniquely for each of the 1-4 possible DLBs used by a given PCE. Units are in seconds and is reported once per major frame.

**Note: The DLB width value obtained from ATL01 and used in onboard algorithms has been adjusted by the Flight Software. The adjustment is in the form of a 1 coarse count reduction to the DLB width value reported by the hardware. This is done to account for a timing behavior which causes the width of the DLB to be off by 1 clock cycle. The value of  $DLBW_{\zeta}^{\beta}$  reported out in telemetry, and in ATL01, is the one which has been adjusted to account for this disparity. The correction must therefore be removed from the DLB width value when determining the actual width of the downlink band. The DLB width reported on the ATL02 product is the output of Equation 3-40.**

|                         |   |                          |
|-------------------------|---|--------------------------|
| $DLBW_{T\zeta}^{\beta}$ | $= \begin{cases} 0, & \text{when } DLBW_{\zeta}^{\beta} = 0 \\ \left( DLBW_{\zeta}^{\beta} + 1 \right) \cdot d_{USO} \cdot SF_{USO}^{\alpha}, & \text{when } DLBW_{\zeta}^{\beta} \neq 0 \end{cases}$ | <b>Equation<br/>3-40</b> |
|-------------------------|---|--------------------------|

### 3.8.5 Times of Flight Outside of DLB limits

Some times of flight computed in ATL02 are outside the downlink band boundaries computed in the previous section. At first glance, this is contrary to the definition of the flight software algorithms which indicate that events downlinked in the altimetric science packets occur within the confines of a DLB. However, the behavior is both acceptable and expected. This is due to the DLB boundaries being established purely in terms of coarse clocks whereas TOF measurements include both coarse and fine timing components. When considering the aggregate effect, this results in up to a 5ns and 10ns excursion of returns outside the beginning and end of a DLB respectively. Additional information about this behavior may be found in ICESat-2-SCI-TN-0953.

## 3.9 A Word on Zero Range Point

The times of flight reported in ATL02 are with respect to a zero range point that is left undefined in ATL02. The geometric coordinates of the zero range point are determined between ATL03, ATL03G, and the ISF by a process that uses ATL02 data and calibration data, and is seen in Figure 12. The process of computing return-point coordinates from times of flight is explained in ICESat-2-SCI-TN-0958.

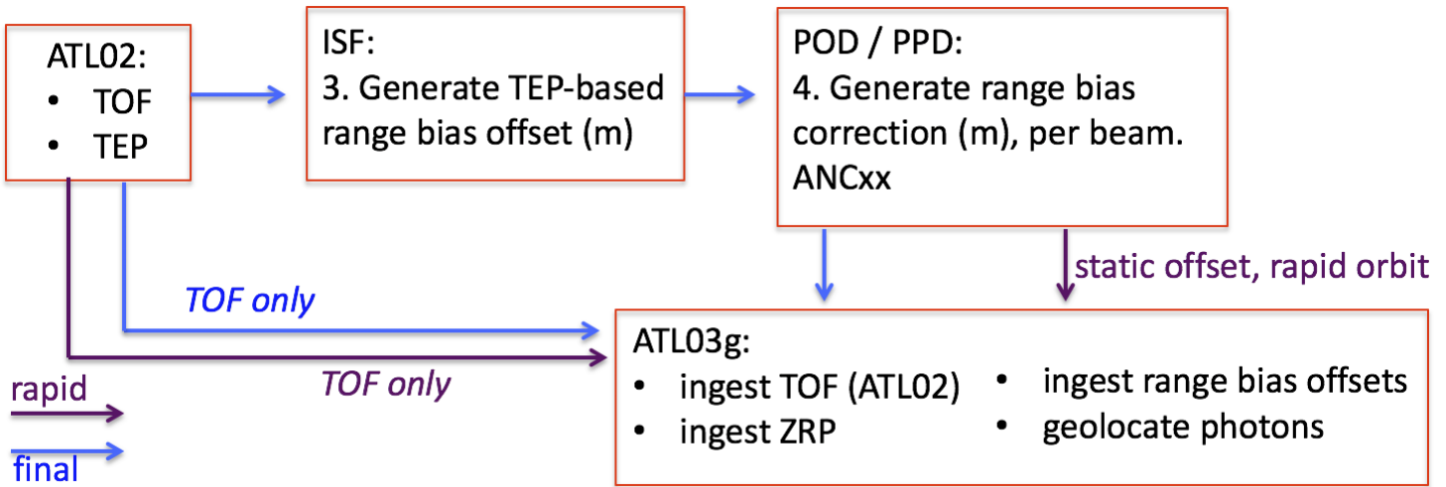


Figure 12: Schematic of the data flow to determine bias-corrected photon ranges.

### 3.10 Data Screening Mechanisms & Associated Responses

The computations outlined in this chapter will be assessed via the quality assessment parameters included in Table 25 below. (Some table contents are TBR-2)

Table 25: TOF Data Quality Monitoring Criteria

| Pre/Post Calculation | Check                        | Pass Criteria  | ATL02 Screening Parameter  | Method   | Failure Response  |
|----------------------|------------------------------|--|--|--|---|
| Pre                  | Coarse count values in range | CC less than or equal to 10,000                                  | <i>/quality_assessment<br/>/summary/pce{1-3}<br/>/qa_rx_coarse_count<br/>&amp;<br/>/qa_tx_coarse_count</i>                     | Compare coarse count for every TX + RX tag to the maximum number of intervals occurring between consecutive T0s. | Ignore this major frame of data on this PCE; likely corrupted. Write out error/warning flag in data product.                |
| Pre                  | Fine count values in range   | FC less than 75  | <i>/quality_assessment<br/>/summary/pce{1-3}<br/>/qa_rx_fine_count,<br/>/qa_tx_leading_fine &amp;<br/>/qa_tx_trailing_fine</i> | Compare fine count for every TX + RX tag to the maximum number of intervals occurring in the TDC delay chain.    | Ignore this major frame of data on this PCE; likely corrupted. Write out error/warning flag.                                |
| Pre                  | Channel Number Validity      | Value falls in range [1,20] or is special channel value [28, 29] | <i>/quality_assessment<br/>/summary/pce{1-3}<br/>/qa_rx_channel_id</i>   | Compare every RX tag channel to the range of allowable values.   | Ignore this major frame of data on this PCE; likely corrupted. Write out error/warning flag.                                |
| Post                 | # TX per Major Frame         | Nominal: [199, 201]<br>w/ DNF: < 201                             | <i>/quality_assessment<br/>/summary/pcex<br/>/qa_s_n_tx_oob</i>  | Compare the number of transmits in a frame to the expected value.  | Ignore this major frame of data on this PCE; likely corrupted. Write out number of Tx pulses not recorded in a major frame. |

| Pre/Post Calculation | Check                    | Pass Criteria  | ATL02 Screening Parameter                                   | Method  | Failure Response  |
|----------------------|--------------------------|--|---|---|---|
| Post                 | TX Jitter                | Nominal: (LL-T0) follows a sawtooth with 33.33 ns peak-to-peak | <i>/quality_assessment/summary/pce{1-3}/qa_ph_tx_ll</i>     | Compare positions of LL vs T0 for consecutive shots (n vs n+1).   | This may be an indication of laser instability. Issue warning via digest email.   |
| Post                 | Shot Index/Alignment     | Max period difference < 1ns                                    | TBD   | Construct a series of laser periods as observed by each PCE by taking the difference between LL time ( $TX_{CC\delta}^{\beta}$ ) of adjacent shots. Then compute the difference between the sequences for each pair of PCEs. If they are aligned, the maximum period difference absolute value will be less than 1 ns. If they are not aligned, the maximum will be larger than 5 ns. | This may be an indication poorly aligned data. Issue warning via digest email.  |
| Post                 | TOF                      | Within tolerance of range window and downlink band bounds      | <i>/atlas/pce{1-3}/altimetry/weak/photons/ph_tof</i>        | Compare TOF value to start + end time of downlink bands expressed relative to T0.   | This may be an indication of poorly chosen calibration value. Issue warning via digest email.   |
| Post                 | Duplicate ID             | By channel duplicates < 10%                                    | <i>/quality_assessment/summary/pce{1-3}/qa_dupe_percent</i> | Compare (as a percentage of total) the number of duplicate returns identified. Evaluate by channel. If percentage is greater than 10%, check fails.   | This may give indication of a dead time issue. Issue warning via digest email.  |
| Post                 | Missing Start Thresholds | No criteria  | ISF   | Provide summary of % of occurrences per scenario per granule using tof_flag   | Trend behavior and inspect periodically. If percentages vary drastically, indicates that laser behavior or settings may not be as expected. |

| Pre/Post Calculation | Check                     | Pass Criteria      | ATL02 Screening Parameter  | Method  | Failure Response   |
|----------------------|---------------------------|--------------------|--|---|--|
|                      |                           |                    |  |   | Additional investigation needed.   |
| Post                 | Relative Bias Per Channel | <i>No Criteria</i> | ISF  | Compute relative bias for all channels on a given spot + compare/trend. | If bias is changing drastically, then investigation of CAL-49 may be needed. |
| Pre                  | DNF                       | $>1$               | From ATL01:<br>/quality_assessment<br>/packet_counts/alt_sci<br>/qa_pce{1-3}_dnf | Identify how many major frames did not finish transferring.             | Report out as part of digest email.  |
| Post                 | Cal Value                 | <i>No Criteria</i> | /atlas/pce{1-3}<br>/altimetry/cal_fall_sm<br>& /cal_rise_sm                      | Report out min/max/mean of cal rising + falling values.                 | Report out as part of digest email. Gives a feel for system stability.       |
| Post                 | Fine counts switched      | $=0$               | qa_s_n_swapped_txfine  | Identify how many instances of fine count switching occurred            | Report out as part of digest email. May need to reset PCE.                   |

### 3.11 TOF-related Parameters Included in ATL02 Output File

The following TOF-related parameters are to be written to the ATL02 output file. These are provided for reference within the context of this document. More detailed descriptions of each value may be found in the ATL02 data product dictionary as well as the ATL02 verification matrix ICESat-2-SIPS-SPEC-0150. In the event of a conflict among sources, the verification matrix content will dictate. Note that additional parameters, such as pass-through or counter values, may also be present in the ATL02 product; these values are not captured here but are documented in the ATL02 verification matrix.

**Table 26: TOF-related parameters included in the ATL02 product (at 50Hz/major frame rate)**

| Parameter Path<br>Stored In<br><i>/atlas/pcex/altimetry/</i> | Equation      | Description   |
|--|---------------|---|
| <i>cal_{fall/rise}_sm</i>                                    | Equation 3-10 | Smoothed, calibrated value for the falling/rising edge used to convert cell counts to units of time. Expressed in seconds per cell. |
| <i>delta_time</i>  | Equation 2-16 | Time of first TX in major frame relative to SDP Epoch.  |
| <i>useflag</i>   | Table 20      | Science mode flag. Indicates what start components are present based on least significant digit of flag value.                      |
| <i>{strong/weak}/alt_rw_start</i>                            | Equation 3-37 | Range window start (RWS) time, relative to LL.  |
| <i>{strong/weak}/alt_rw_width</i>                            | Equation 3-38 | Range window width.   |
| <i>{strong/weak}/band{1/2}_offset</i>                        | Equation 3-39 | Downlink band offset time, relative to RWS.   |
| <i>{strong/weak}/band{1/2}_width</i>                         | Equation 3-40 | Downlink band width.  |

**Table 27: TOF-related parameters included in the ATL02 product (at 10kHz/shot rate)**

| Parameter Path<br>Stored In<br><i>/atlas/tx_pulse_width/</i> | Equation      | Description   |
|--|---------------|---|
| <i>delta_time</i>  | Equation 2-16 | Time elapsed since SDP Epoch, as measured by PCE1.  |
| <i>tx_pulse_skew_est</i>                                     | Equation 3-25 | The difference between the averages of the lower and upper threshold crossing times.          |
| <i>tx_pulse_width_lower</i>                                  | Equation 3-23 | The distance between the lower threshold crossing times measured by the start pulse detector. |
| <i>tx_pulse_width_upper</i>                                  | Equation 3-24 | The distance between the upper threshold crossing times measured by the start pulse detector. |

**Table 28: TOF-related parameters included in the ATL02 product (at variable/photon rate)**

| Parameter Path<br>Stored In<br><i>/atlas/pcex/altimetry/s_w/photons/</i> | Equation      | Description   |
|--|---------------|---|
| <i>delta_time</i>  | Equation 2-16 | Time elapsed since SDP Epoch.   |
| <i>ph_id_channel</i>   | Table 16      | Logical channel ID.   |
| <i>ph_tof</i>  | Equation 3-36 | Precise ground return time of flight (TOF), as measured from the start centroid to the return event   |
| <i>tof_flag</i>  | Table 20      | Flag indicating which start elements are missing from the start time calculation and if photon has been identified as a possible TE return.<br><br>Note: 10 is added to the value from Table 20 if the return is flagged as a possible TE return. More information can be found in Section 4.5. |
| <i>tx_ll_tof</i>   | Equation 3-21 | Time elapsed between T0 and the leading lower (LL).   |
| <i>tx_other_tof</i>  | Equation 3-20 | Time elapsed between LL and “other” start elements.   |

## 4 Transmitter Echo Path

The Transmitter Echo Path (TEP) is a design feature which allows for on-orbit calibration of the ATLAS instrument. The TEP takes a small fraction of the transmitted laser beam via the Laser Sampling Assembly (LSA), and feeds the light via fiber optics into the Optical Filter Module (OFM). The picked-off return is fed into the filters and detectors on Spots 1 and 3 (strong spots of PCE1 and PCE2). The resulting returns observed by the PCEs are referred to as the Transmitter Echo, or TE. When histogrammed in higher level data products like ATL03, the TE will show a bimodal distribution due to the reflection from both ends of the TEP fiber.

The TE is attenuated so that the mean number of TE events per laser shot is approximately 0.1 (~1 return per 10 shots). Although the TE return is relatively weak, there are two reasons to distinguish TE returns from the rest. First, whenever a TE return is detected within one of the DLBs, it may be used as an on-orbit calibration for timing stability and laser pulse-shape changes. Second, correctly identifying the TE returns within a downlink band allows higher-level data products to appropriately recognize the TE returns as TOF artifacts and not mistake them for geophysical signals.

ATLAS does not uniquely identify TE photons and instead treats all photons received by the detectors as if they are surface returns or solar background events. Because the transit time of the ground returns is on the order of three to four milliseconds, all TX information is “queued” by the FSW and is later associated with the appropriate RX. Since the transit time of a TE photon is significantly less (~100 ns vs a several microsecond RWS), using the same queuing technique for these picked off TE photons results in an incorrect TX-to-RX association. Thus, action must be taken to remediate this relationship in the case of TE photons in order to successfully compute a TE TOF (TE\_TOF).

The following sections present the calculations and heuristics used to identify the TE data and compute the TE TOF (TE\_TOF).

### 4.1 Ground Rules and Assumptions

The following “ground rules” and assumptions apply to the calculations outlined in this chapter:

- Only Spot 1 and Spot 3 have TE photons. Receive events in any of the other four spots can safely neglect the following considerations presented below.
- Ground processing software searches for TEP only on Spot 1 and Spot 3. This is a parameter defined in the ATL02 control file. Note that it possible to search for TEP on all 3 strong spots via manipulation of the ATL02 control file.
- In science mode, the TE will sometimes appear in the DLB that the flight software has defined to contain the surface return. At times, the flight software will define an additional DLB to contain the TE.
- At times, ATLAS will be commanded in manual mode to downlink a range window that is fixed around TE. In this case, the RWW typically defaults to a fixed ~17 coarse clock (~170ns) width.
- As the RWS and DLBO vary across major frames, the position of a TE within the DLB will also vary (if it appears at all).
- It is also possible that TE and actual surface returns will overlap. This product does not attempt to separate this information but instead will provide a flag for use by higher level data product authors to use if filtering is desired.

## 4.2 Variable Definitions and Notation Syntax

Before deriving the equations for TOF, shorthand notations and symbols for use in expressing generalized equations are established. Notation syntax is as follows:

$$\mathbf{Parameter}^{\mathbf{Hardware Identifier(s)}}_{\mathbf{Telemetry Type(s)}}$$

- Bolded parameters are values expressed in seconds
- Non-bolded parameters are dimensionless (i.e. clock cycles, channel, or ratios)
- Lower case parameters are uncalibrated
- Upper case parameters are calibrated
- Hardware identifiers include Hardware sides (A or B), PCE Identifiers (1, 2, or 3)
- Telemetry Types include Toggle values, Start Components, Downlink Band, Spot Type, Channels (Return Events)

**Table 29: Generalized TE-TOF Calculation Notation**

| Symbol     | Parameter               | Super or Subscript | Valid Values    |
|------------|-------------------------|--------------------|-----------------|
| $\alpha$   | Hardware Side           | Superscript        | A, B            |
| $\beta$    | PCE Identifier          | Superscript        | 1, 2, 3         |
| $\gamma$   | Toggle Value            | Subscript          | Rising, Falling |
| $\delta$   | Leading Start Component | Subscript          | LL1, LL2, LL3   |
| $\tau$     | Other Component         | Subscript          | LU, TU, TL      |
| $\xi$      | Spot Type               | Subscript          | Strong, Weak    |
| $\zeta$    | Downlink Band           | Subscript          | 1, 2, 3, 4      |
| $\epsilon$ | Channel                 | Subscript          | 1, 2, ..., 20   |
| $\beta$    | PCE Identifier          | Superscript        | 1, 2, 3         |
| $\delta$   | Leading Start Component | Subscript          | LL1, LL2, LL3   |
| $\epsilon$ | Channel                 | Subscript          | 1, 2, ..., 20   |

Because of the great degree of variety of notation in this document, a dictionary of utilized terms follows (in approximate order of appearance):

**Table 30: Dictionary of TE\_TOF Derivation Variables**

| Uncalibrated Notation | Calibrated Notation | Description   | Units        | Source                                    |
|-----------------------|---------------------|---|--------------|---|
| $cc/T0$               | n/a                 | Nominal number of ruler clocks per T0 interval (10,000).  | clock cycles | Defined in this document per Equation 4-6 |
| te_tol                | n/a                 | Tolerance value which takes up the maximum deviation of laser fires from 10,000 and the maximum expected time between laser fire and TE return. | clock cycles | Defined in this document per Equation 4-2 |
| N                     | n/a                 | Number of shots “apart” between the TE TX and the TX that the TEP return is associated with.  | T0 intervals | Calculated value per Equation 4-6         |



| Uncalibrated Notation | Calibrated Notation           | Description   | Units        | Source  |
|-----------------------|-------------------------------|---|--------------|---|
| n/a                   | $RWS_{\xi}^{\beta}$           | Range window start value, expressed relative to leading lower.<br><br><b>Note:</b> Value is corrected/calibrated by FSW and 1 coarse count does <b>not</b> need to be deducted.   | clock cycles | ATL01 parameter:<br><i>/atlas/pcex/a_alt_science/raw_alt_rw_start_{s/w}</i> |
| n/a                   | $DLBO_{\xi,\zeta}^{\beta}$    | Downlink band offset value, expressed relative to range window start.<br><br><b>Note:</b> The appropriate $DLBO_{\xi,\zeta}^{\beta}$ is selected from the array of 4 values appearing in the ATL01 product. This is done per Section 3.5.4. The values on the ATL01 product are corrected/calibrated by FSW prior to packetization and are used in the TE_TOF calculation as telemetered. | clock cycles | ATL01 parameter:<br><i>/atlas/pcex/a_alt_science/raw_alt_band_offset</i>    |
| n/a                   | $DLBW_{\zeta}^{\beta}$        | Downlink band width value.<br><br><b>Note:</b> The appropriate $DLBW_{\zeta}^{\beta}$ is selected from the array of 4 values appearing in the ATL01 product. This is done per Section 3.5.4. The values on the ATL01 product are corrected/calibrated by FSW prior to packetization and are used in the TE_TOF calculation as telemetered.  | clock cycles | ATL01 parameter:<br><i>/atlas/pcex/a_alt_science/raw_alt_band_width</i>     |
| n/a                   | $TX_{T\delta}^{\beta}$        | Time elapsed between T0 and LL for a given PCE and laser fire.  | seconds      | Calculated value per Equation 3-21  |
| n/a                   | $T_{center}$                  | Time elapsed between LL and the precise start time (centroid).  | seconds      | Calculated value per Equation 3-22  |
| n/a                   | $TX_{CENT_{T\delta}}^{\beta}$ | Start centroid time relative to T0.   | seconds      | Calculated value per Equation 4-7 and Equation 4-8                          |
| n/a                   | $Elapsed_{T\delta}^{\beta}$   | Time between T0s considered in TE_TOF calculation   | seconds      | Calculated value per Equation 4-9   |
| n/a                   | $TE_{TOF_{\epsilon}}^{\beta}$ | Precise TE Time of Flight.  | seconds      | Calculated value per Equation 4-10  |



### 4.3 Determining if the TE is Captured by a DLB

In order to compute the  $TE\_TOF$  of a return, it must first be determined whether or not a DLB, has the *potential* to contain returns originating from the TEP. Figure 13 depicts the two possible relationships between a TX, TE, and the DLB.

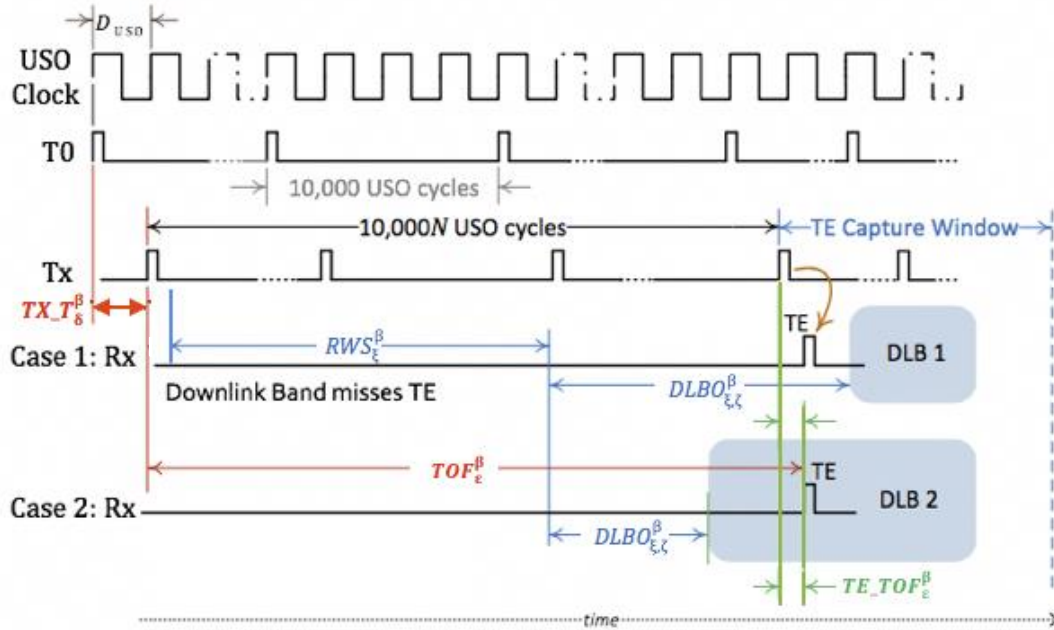


**Figure 13: Possible relationships between a TE and DLB**

Case 1 shows the case where the downlink band fails to include a TE time tag. This occurs when the bounds of the downlink band fall entirely between two TX events. Given that the TX events are spaced about 10,000 coarse clock cycles (100  $\mu$ s) apart, and a downlink band is typically on the order of 10  $\mu$ s in width, the odds that a TX event will fall within a downlink band are roughly 10/100, or 1 in 10.

Case 2 shows the case where a TE is included in a downlink band. When the downlink band contains a TX event, there is a high likelihood that the downlink band will also contain a TE event. This idea is predicated on TE events predictably occurring less than 100 ns after a TX event due to the physical geometry of the TEP.

To determine whether or not a TE is likely to be observed in a given DLB, the bounds of the DLB must be examined with respect to the shot interval. To begin, define the nominal number of coarse clock periods per  $T_0$ . Note that this value is insensitive to USO calibration:

|          |                                   |                     |
|----------|-----------------------------------|---------------------|
| $cc/T_0$ | $\stackrel{\text{def}}{=} 10,000$ | <b>Equation 4-1</b> |
|----------|-----------------------------------|---------------------|

Next, determine if there is some integer number of shots,  $N$ , whose corresponding number of coarse clock periods falls within the bounds of the DLB being examined. Because the laser has a jitter of a few clock cycles, additional tolerance must be considered. This jitter and the short delay between laser fire and TE arrival are taken up in the  $te\_tol$  parameter. Equation 4-3 determines the value of  $N$  which is needed to occur after the start of the DLB and Equation 4-4 determines the value of  $N$  which is needed to occur before the end of the DLB:

|            |  |                     |
|------------|--|---------------------|
| $te_{tol}$ | <sup>def</sup> tolerance value which takes up the maximum deviation of laser fires from 10,000 and the maximum expected time between laser fire and TE return. Nominally, this is set to 7 coarse clock periods (70 ns). | <b>Equation 4-2</b> |
|            | $RWS_{\xi}^{\beta} + DLBO_{\xi,\zeta}^{\beta} < (N * cc/T_0) + te_{tol}$   | <b>Equation 4-3</b> |
|            | $(N * cc/T_0) - te_{tol} < RWS_{\xi}^{\beta} + DLBO_{\xi,\zeta}^{\beta} + DLBW_{\zeta}^{\beta}$  | <b>Equation 4-4</b> |

However, since it is known that the DLBW will always be significantly less than  $cc/T_0$ , it can be concluded that for a TE to be observed in a DLB, Equation 4-3 and Equation 4-4 must return the same integer value of  $N$ :

|     |   |                     |
|-----|---|---------------------|
|     | $RWS_{\xi}^{\beta} + DLBO_{\xi,\zeta}^{\beta} - te_{tol} < N * cc/T_0 < RWS_{\xi}^{\beta} + DLBO_{\xi,\zeta}^{\beta} + DLBW_{\zeta}^{\beta} + te_{tol}$   | <b>Equation 4-5</b> |
| $N$ | $= \text{ceil} \left( \frac{RWS_{\xi}^{\beta} + DLBO_{\xi,\zeta}^{\beta} - te_{tol}}{cc/T_0} \right)$ $= \text{floor} \left( \frac{RWS_{\xi}^{\beta} + DLBO_{\xi,\zeta}^{\beta} + DLBW_{\zeta}^{\beta} + te_{tol}}{cc/T_0} \right)$ | <b>Equation 4-6</b> |

The existence of an integer  $N$  that satisfies the inequality seen in Equation 4-5 indicates that there may be TE events in the downlink band. Further, its value also indicates how many shots to move forward to match the TE events with their proper start and overcome the queuing disparity discussed earlier in this chapter. Note that this value is calculated once per major frame and thus should be considered applicable to all returns in that frame.

Conversely, if the ceil() and floor() seen in Equation 4-6 yield different integers values for  $N$ , then the down link band does not contain possible TE events and no further TE\_TOF analysis is needed for returns occurring within that particular DLB and major frame.

#### 4.4 Calculation of TEP Time of Flight (TE\_TOF)

As stated previously, the previously calculated TOF needs to be adjusted such that the TE returns are “re-associated” with the appropriate laser fire. Since the nominal TOF calculation establishes the time elapsed relative to the start centroid and not its T0 boundary, this may be leveraged to develop a relative correction to account for the jitter in start position using each shot’s T0 boundary as an origin point. A simplified view of this may be seen in Figure 14 below.

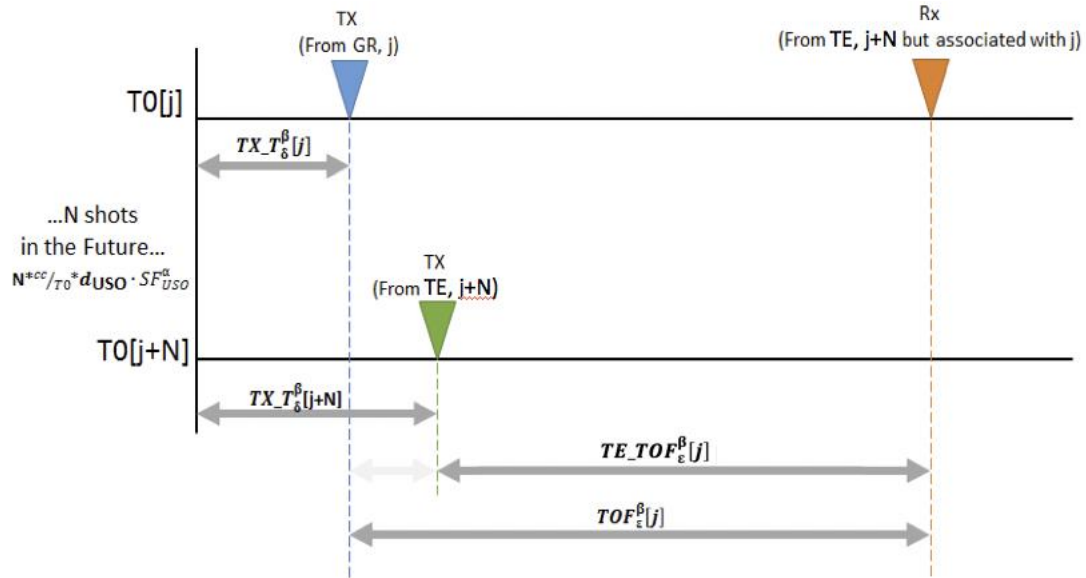


**Figure 14: Simplified TE\_TOF References**

To do so, begin by calculating the start centroid position for both the TX with which the TE return was incorrectly associated with in the telemetry ( $j^{th}$  shot) and the shot it actually came from (the  $j+N^{th}$  shot, in the “future”). Both calculations are relative to its TO and expressed in seconds:

|                                    |   |                     |
|------------------------------------|---|---------------------|
| $TX_{CENT_{T\delta}}^{\beta}[j]$   | $= TX_{T\delta}^{\beta}[j] + T_{center}[j]$     | <b>Equation 4-7</b> |
| $TX_{CENT_{T\delta}}^{\beta}[j+N]$ | $= TX_{T\delta}^{\beta}[j+N] + T_{center}[j+N]$ | <b>Equation 4-8</b> |

Then, the time elapsed between the shot which made the TE return and the one it was improperly associated with must also be accounted for. Using the value of  $N$  calculated previously, this duration may be found via:

|                             |  |                     |
|-----------------------------|--|---------------------|
| $Elapsed_{T\delta}^{\beta}$ | $= N * cc / T_0 * d_{USO} * SF_{USO}^{\alpha}$ | <b>Equation 4-9</b> |
|-----------------------------|--|---------------------|

Finally, all of these terms are put together to calculate  $TE_{TOF_{\epsilon}}^{\beta}[j]$  for each return as follows:

|                                  |   |                      |
|----------------------------------|---|----------------------|
| $TE_{TOF_{\epsilon}}^{\beta}[j]$ | $= TOF_{\epsilon}^{\beta}[j] - \{(TX_{CENT_{T\delta}}^{\beta}[j+N] - TX_{CENT_{T\delta}}^{\beta}[j]) - Elapsed_{T\delta}^{\beta}\}$ | <b>Equation 4-10</b> |
|----------------------------------|---|----------------------|

### 4.5 Flagging of TEP Photons

When the TE is present in downlinked data, it is observed in one of two scenarios: either in its own downlink band (whose RWW always defaults to a fixed ~170 ns), or alternatively, in a variable width downlink band which also contains the ground returns. In the latter case, it may or may not coincide with the ground

return. After the values of  $TE_{TOF}^B[j]$  are found via the methodology above, they must be further assessed for validity relative to the physical geometry of the TEP hardware:

- Events must occur within a major frame that satisfies the criteria outlined in Chapter 4.3.
- Events with a  $TE_{TOF}^B$  less than 0 ns or greater than 110 ns are discarded, as the transmit echo cannot arrive before or too long after the laser fires. (Note that a range of 0-100 ns was determined empirically during testing and is a result of the physical length of the TEP fibers. An extra 10 ns is added due to the screening being done on coarse times.)

Events which remain after the above criteria are applied are identified as possible TE events. To distinguish them from nominal ground returns, which have a *tof\_flag* of 1-8, 10 is added to the *tof\_flag* value. Thus, any TE events will have a *tof\_flag* of 11-18, preserving both the start time configuration as well as its status as a TE event. Assuming the expected TEP signal strength of about one photon per 10 shots, this process is expected to detect TE at a rate of about 20 TE events per major frame (of 200 shots each). Background events that occur between the TE bounds are treated the same as TE events, so they will add to the total.

**A word of warning: As designed, this methodology leads to a ~110 ns wide swath of TE signal being identified within any DLB which contains TE returns. In the case of an exclusively TE-seeking downlink band, this can result in the outer portions of the downlink band, which really contain background photons, being identified as ground returns. When plotted as a photon cloud, this will give the appearance of a thin, flat cloud with its middle portion missing. This is an expected outcome. If the presence of these additional background photons proves to be problematic, a heuristic to identify and ignore the downlink band may be implemented in higher level data products.**

## 4.6 Data Screening Mechanisms & Associated Responses

The computations outlined in this chapter will be assessed via the quality assessment parameters included in Table 31 below.

**Table 31: TEP Data Quality Monitoring Criteria**

| Pre/Post Calculation | Check                              | Pass Criteria                                | ATL02 Screening Parameter   | Method  | Failure Response                               |
|----------------------|------------------------------------|--|---|---|--|
| Post                 | Position of Return vs. Start Event | $TE_{TOF} > 0$<br>AND<br>$TE_{TOF} < 110$ ns | <i>/quality_assessment/summary</i><br><i>/pce{1-3}/qa_tep_tof</i> | Assess TE_TOF for all suspected TE returns. Valid values fall within the defined range. | Remove event from list of suspected TE values. |

## 4.7 Data Products

The following TE-related parameters are to be written to the ATL02 output file. These are provided for reference within the context of this document. More detailed descriptions of each value may be found in the ATL02 data product dictionary as well as the ATL02 verification matrix. In the event of a conflict among sources, the verification matrix content will dictate. Note that additional parameters, such as pass-through or counter values, may also be present in the ATL02 product; these values are not captured here but are documented in the ATL02 verification matrix.

Only events which have been identified as TE events are included in the */atlas/pcex/tep/*. All times and shot-specific information is referenced to the shot which the TE event originated from, not the one it was associated with in telemetry. Finally, returns which are identified as TE returns are included in both the */atlas/pcex/tep/* as well as the */atlas/pcex/altimetry/s\_w/photons/* groups, with different *delta\_time* values.

**Table 32: TE-related parameters included in the ATL02 product (at variable/photon rate)**

| Parameter Path<br>Stored In<br><i>/atlas/pcex/tep/</i> | Equation      | Description   |
|--|---------------|---|
| <i>delta_time</i>                                      | Equation 2-16 | Time Elapsed Since SDP Epoch. Time of the shot the event becomes associated with, not the place where it was recorded.  |
| <i>tep_pulse_num</i>                                   | Equation 4-6  | The number of laser pulses from the TEP laser pulse to the laser pulse for which ATLAS is currently receiving non-TEP photons.  |
| <i>tof_tep</i>   | Equation 4-10 | Precise Transmitter Echo (TE) return TOF values, as measured from the TE transmit start centroid to the TE return event.  |
| <i>tx_ll_tof_tep</i>                                   | Equation 3-21 | Time elapsed between T0 and the Leading Lower (LL). This information comes from the shot the event becomes associated with, not the place where it was recorded in telemetry.                 |
| <i>tx_other_tof_tep</i>                                | Equation 3-20 | Time elapsed between LL and “other” (LU, TU, or TL) start elements. This information comes from the shot the event becomes associated with, not the place where it was recorded in telemetry. |

## 5 Radiometry

ATL02 includes radiometric products related to transmitted laser energy and small-signal receiver sensitivity.

### 5.1 Data Products

The radiometric data products are

- Total transmitted energy per pulse in all six beams,
- Transmitted energy in each of the six beams, and
- Receiver sensitivity to small signals for each of the six active detectors.

### 5.2 Transmitted Energy

Two transmitted energy products are computed: the total transmitted energy and the individual beam energies.

The work/data flow is shown in Figure 15. The total transmitted energy is computed first, in three versions derived from data from each of three energy sensors: the SPD energy monitor, the laser internal energy monitor, and the Laser Reference System (LRS). From each of the total energy products, a set of values for each beam is computed.

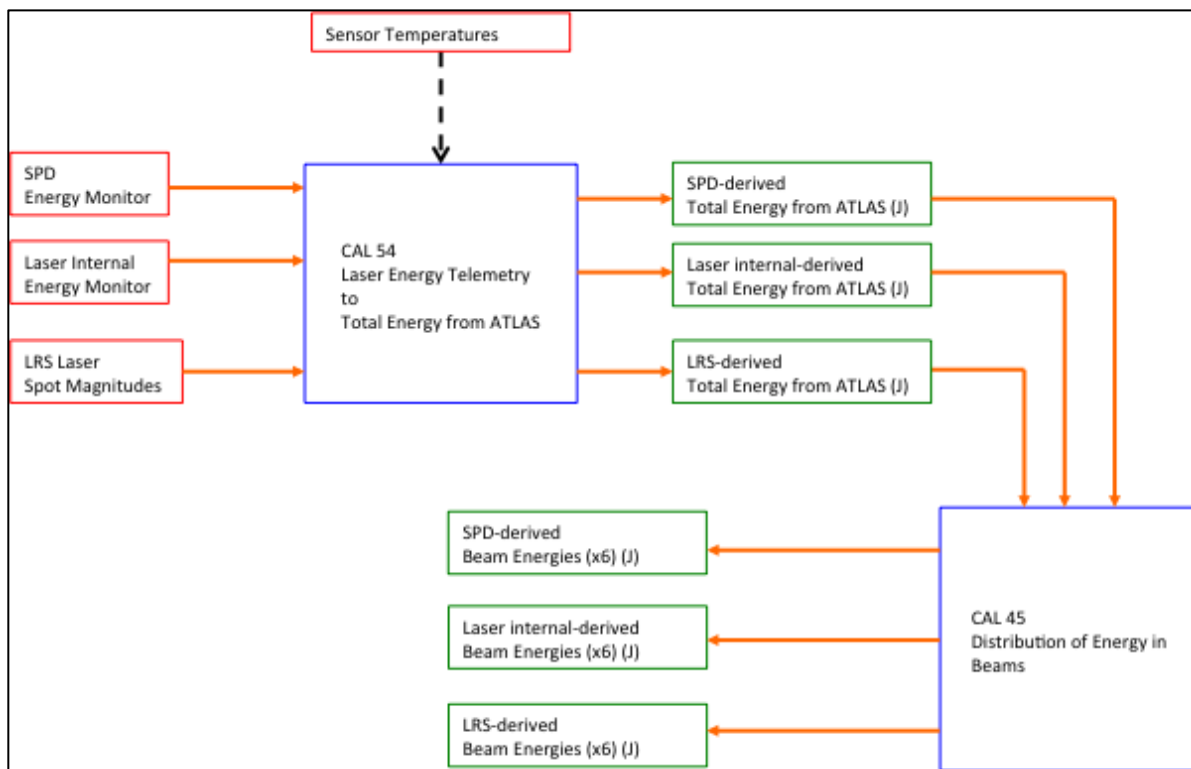


Figure 15: Transmitted Energy work/data flow

## 5.2.1 Total Transmitted Energy

### 5.2.1.1 Calculation

CAL-54 contains a table giving, for each sensor (SPD A, SPD B, Laser 1 Internal, Laser 2 Internal, LRS), a list of coefficients  $\{a, b_0, b_1, c_0, c_1\}_{sensor}$  for calculating total optical pulse energy leaving ATLAS as a function of sensor counts and sensor temperature.

ATL02 reports out three estimates of the total transmitted energy: one from the active SPD energy monitor, one from the active laser internal energy monitor, and one from the LRS.

For each sensor, the total energy is computed using the following equation, where  $S$  comes from the sensor reading from telemetry,  $T$  is the temperature from a telemetry point appropriate for that sensor,  $T_{0,sensor}$  is the reference temperature for that sensor from CAL-54 and  $\{a, b_0, b_1, c_0, c_1, d, e\}$  are the coefficients for that sensor from CAL-54.

For the SPD energy monitors,  $S$  is the raw telemetry value + 32768. For the laser internal energy sensor,  $S$  is the raw telemetry value. For the LRS,  $S$  is the sum of raw magnitudes for the 6 spots.

|                    |  |                     |
|--------------------|--|---------------------|
| $E_{total,sensor}$ | $= a + (b_0 + b_1 (T - T_0))S + (c_0 + c_1 (T - T_0)) S^2 + d S^3 + e S^4$ | <b>Equation 5-1</b> |
|--------------------|--|---------------------|

These values are reported out of ATL02 in `/atlas/`:

**Table 33: Total Transmitted Energy Values Reported on the ATL02 Product**

| Parameter Path Stored In<br><code>/atlas/housekeeping/</code> | Equation     | Description   |
|---|--------------|---|
| <code>laser_energy_internal/e_tx</code>                       | Equation 5-1 | Total laser energy derived from the internal laser energy monitor (APID 1032). Reported at 1 Hz.                            |
| <code>laser_energy_lrs/e_tx</code>                            | Equation 5-1 | Total laser energy from derived from LRS laser centroid magnitudes. Reported at 50 Hz.                                      |
| <code>laser_energy_spd/e_tx</code>                            | Equation 5-1 | Total laser energy from Analog HK Telemetry packet E (APID 1063). Recorded at 10 Hz but reported in segments of 10 at 1 Hz. |

### 5.2.1.2 Data sources

Data sources for  $S_{sensor}$  and  $T_{sensor}$  are given in this table. Note that:

- The selection of the SPD energy monitor should be made according to which SPD, *not laser*, is in use.
- Temperature data are reported at 1 Hz whereas energy monitor data are reported at 10 Hz; in cases where both temperature and energy data are used as input to an equation, the latest temperature data should be used for each of the 10 corresponding energy cases.
- Temperature data are converted prior to use in calculations. See Section 8.4.
- The energy monitor values are used as written on ATL01. They are not written to the ATL02 product.

**Table 34: Data Sources for the Total Transmitted Energy Calculation**

| Description   | Product | APID | Source  |
|---|---------|------|---|
| SPD energy monitor A                                      | ATL01   | 1063 | <b>Telemetry Mnemonic:</b> Chan 0-18 (evens): SPD PRI LSR ENERGY MON<br><b>ATL01 Path:</b><br><i>/atlas/a_hkt_e_1063/raw_pri_lsr_energy</i>                         |
| SPD energy monitor B                                      | ATL01   | 1063 | <b>Telemetry Mnemonic:</b> Chan 1-19 (odds): SPD RED LSR ENERGY MON<br><b>ATL01 Path:</b><br><i>/atlas/a_hkt_e_1063/raw_red_lsr_energy</i>                          |
| SPD temperature, A (Laser 1)                              | ATL01   | 1061 | <b>Telemetry Mnemonic:</b> Chan 82:<br>A_HKT_BEAMX_T<br><b>ATL01 Path:</b><br><i>/atlas/a_hkt_c_1061/raw_hkt_beamx_t</i>  |
| SPD temperature, B (Laser 1)                              | ATL01   | 1061 | <b>Telemetry Mnemonic:</b> Chan 82:<br>A_HKT_BEAMX_T<br><b>ATL01 Path:</b><br><i>/atlas/a_hkt_c_1061/raw_hkt_beamx_t</i>  |
| SPD temperature, A (Laser 2)                              | ATL01   | 1061 | <b>Telemetry Mnemonic:</b> Chan 74:<br>A_SPDA_THERM_T<br><b>ATL01 Path:</b><br><i>/atlas/a_hkt_c_1061/raw_spda_therm_t</i>  |
| SPD temperature, B (Laser 2)                              | ATL01   | 1061 | <b>Telemetry Mnemonic:</b> Chan 81:<br>A_SPDB_THERM_T<br><b>ATL01 Path:</b><br><i>/atlas/a_hkt_c_1061/raw_spdb_therm_t</i>  |
| Laser internal energy monitor (whichever laser is active) | ATL01   | 1032 | <b>Telemetry Mnemonic:</b> Chan 59:<br>A_HKT_CCHP_LAS1_T<br><b>ATL01 Path:</b><br><i>/atlas/a_sla_hk_1032/raw_energy_data_shg</i>                                   |
| Laser 1 interface temperature                             | ATL01   | 1061 | <b>Telemetry Mnemonic:</b> Chan 59: Laser 1 I/F TCS-14 (also: A_HKT_CCHP_LAS1_T)<br><b>ATL01 Path:</b><br><i>/atlas/a_hkt_c_1061/raw_hkt_cchp_las1_t</i>            |
| Laser 2 interface temperature                             | ATL01   | 5    | <b>Telemetry Mnemonic:</b><br>HT_ATL_TIB1_LSR2_IF01_Y07_T<br>(byte offset 146)<br><b>ATL01 Path:</b> 12 <sup>th</sup> value in the array<br><i>/sc1/hk/raw_at_t</i> |
| LRS magnitude, Spot 1                                     | ATL01   | 1123 | <b>Telemetry Mnemonic:</b> CMT[4].MAGNITUDE<br><b>ATL01 Path:</b> <i>/lrs/laser_centroid/raw_cent_mag</i>   |
| LRS magnitude, Spot 2                                     | ATL01   | 1123 | <b>Telemetry Mnemonic:</b> CMT[5].MAGNITUDE<br><b>ATL01 Path:</b> <i>/lrs/laser_centroid/raw_cent_mag</i>   |
| LRS magnitude, Spot 3                                     | ATL01   | 1123 | <b>Telemetry Mnemonic:</b> CMT[6].MAGNITUDE<br><b>ATL01 Path:</b> <i>/lrs/laser_centroid/raw_cent_mag</i>   |
| LRS magnitude, Spot 4                                     | ATL01   | 1123 | <b>Telemetry Mnemonic:</b> CMT[7].MAGNITUDE<br><b>ATL01 Path:</b> <i>/lrs/laser_centroid/raw_cent_mag</i>   |
| LRS magnitude, Spot 5                                     | ATL01   | 1123 | <b>Telemetry Mnemonic:</b> CMT[8].MAGNITUDE<br><b>ATL01 Path:</b> <i>/lrs/laser_centroid/raw_cent_mag</i>   |
| LRS magnitude, Spot 6                                     | ATL01   | 1123 | <b>Telemetry Mnemonic:</b> CMT[9].MAGNITUDE<br><b>ATL01 Path:</b> <i>/lrs/laser_centroid/raw_cent_mag</i>   |



| Description        | Product | APID | Source  |
|--------------------|---------|------|---|
| LRS temperature    | ATL01   | 1061 | <b>Telemetry Mnemonic:</b> APID 1120, A_LRS_HK, ANALOGHK channel 33, LRS Laser Detector Card Thermistor.<br><b>ATL01 Path:</b> /lrs/hk_1120/raw_ldc_t |
| Selected Laser     | ANC13   | N/A  |   |
| Laser Energy Level | ANC13   | N/A  |   |
| Selected SPD       | ANC13   | N/A  |   |

For the SPD energy monitors and the laser internal energy monitors, the sensor reading is the telemetry value. For the LRS, the sensor reading is the sum of all the spot magnitudes:

|           |  |                     |
|-----------|--|---------------------|
| $S_{LRS}$ | $= \sum_{spot = 1}^N Magnitude_{spot}$ | <b>Equation 5-2</b> |
|-----------|--|---------------------|

where  $N$  is the number of valid spot magnitudes reported in the LRS telemetry. The relation between window labels in the LRS telemetry and laser spot IDs is not necessarily constant, so LRS data cannot be used to calculate individual transmitted beam energies. The sum of the magnitudes is used to compute the total beam energy. Normally, there are six magnitudes, one for each spot, but it is possible that the LRS may fail to find one or more; in that case, the input data validity check fails.

### 5.2.1.3 Input data range

Acceptable input ranges for transmitted energy telemetry values are given in this table:

**Table 35: Acceptable Data Input Ranges for Transmitted Energy Calculation**

| Description   | Minimum | Maximum |
|---|---------|---------|
| SPD energy monitor A                                      | 0       | 30000   |
| SPD energy monitor B                                      | 0       | 30000   |
| SPD temperature, A (°C)                                   | -20     | +50     |
| SPD temperature, B (°C)                                   | -20     | +50     |
| Laser internal energy monitor (whichever laser is active) | 0       | 200     |
| Laser 1 interface temperature (°C)                        | +20     | +40     |
| Laser 2 interface temperature (°C)                        | +20     | +40     |
| Number of LRS spots                                       | 6       | 6       |
| LRS magnitude Sum   | 0       | 2000    |
| LRS individual spot magnitude                             | 0       | 500     |
| LRS temperature (°C)                                      | -20     | +50     |

### 5.2.1.4 Output data range

The expected output ranges for total transmitted energy:

**Table 36: Expected Output Ranges for Total Transmitted Energy Calculation**

| Laser Energy Level | Minimum (μJ) | Maximum (μJ) |
|--------------------|--------------|--------------|
| 1                  | 130          | 530          |
| 2                  | 160          | 650          |
| 3                  | 220          | 860          |
| 4                  | 240          | 980          |
| 5                  | 280          | 1120         |
| 6                  | 310          | 1250         |
| 7                  | 350          | 1400         |
| 8                  | 380          | 1500         |
| 9                  | 400          | 1610         |
| 10                 | 430          | 1740         |
| 11                 | 450          | 1800         |
| 12                 | 680          | 2700         |

These values were derived by multiplying measured mean pulse energies from the Flight 3 laser by 0.5 and 2.0 and rounding to the nearest 10 μJ. The ranges cover all expected variation between lasers and changes over time, barring some kind of failure.

## 5.2.2 Individual Transmitted Beam Energies

### 5.2.2.1 Calculation

CAL-45 contains a list of the fraction of the total transmitted energy in each of the six beams:

|        |  |                     |
|--------|--|---------------------|
| CAL-45 | $= \{EnergyFraction_{beam1}, \dots, EnergyFraction_{beam6} \}$ | <b>Equation 5-3</b> |
|--------|--|---------------------|

The beam energy fractions are a property of the diffractive optical element that splits the beam from the laser into multiple beams.

Equation 5-1 computes estimates of the total energy leaving ATLAS. In addition, ATL02 reports out three sets of estimates of the transmitted beam energies: one set of 6 beam energies for each of the three active sensors. These are computed by multiplying the total energy by the fraction in each beam:

|  |                               |                     |
|--|-------------------------------|---------------------|
| $\{E_{beam1}, \dots, E_{beam6}\}_{sensor}$ | $= CAL-45 * E_{total,sensor}$ | <b>Equation 5-4</b> |
|--|-------------------------------|---------------------|

These values are reported out of ATL02 in the following parameters:

**Table 37: Individual Transmitted Beam Energy Values Reported on the ATL02 Product**

| Parameter Path Stored In<br><i>/atlas/housekeeping/</i> | Equation     | Description   |
|---|--------------|---|
| <i>laser_energy_internal/e_tx_pce{1/2/3}_{s/w}</i>      | Equation 5-4 | Laser energy for a spot, derived from the internal laser energy monitor and split by calibration. Reported at 1Hz.                                |
| <i>laser_energy_lrs/e_tx_pce{1/2/3}_{s/w}</i>           | Equation 5-4 | Laser energy for a spot, derived from LRS laser centroids and split by calibration. Reported at 50Hz.   |
| <i>laser_energy_spd/e_tx_pce{1/2/3}_{s/w}</i>           | Equation 5-4 | Laser energy for a spot, derived from the analog HK telemetry and split by calibration. Recorded at 10 Hz but reported in segments of 10 at 1 Hz. |

### 5.2.2.2 Output data range

Individual beam energies are computed from the total beam energy by multiplying by a fixed factor, without any additional telemetry being involved. Therefore, no specific expected ranges are defined for individual beam energies.

## 5.3 Small-signal Receiver Sensitivity

This product is the small-signal receiver sensitivity, for each of the six active detectors, in terms of events at the receiver output per unit of optical input at the plane of the telescope aperture. It does not include any effects of receiver dead time.

The receiver sensitivity reported out of ATL02 takes into account all effects of optical throughput and aperture obstruction. It is meant to be used as if the entire aperture area within the aperture's outer boundary is unobstructed.

Receiver sensitivity is computed in two steps: 1) the maximum sensitivity is computed and 2) from that, the sensitivity to returns and sensitivity to background are computed. The overall work/data flow is shown in Figure 16.

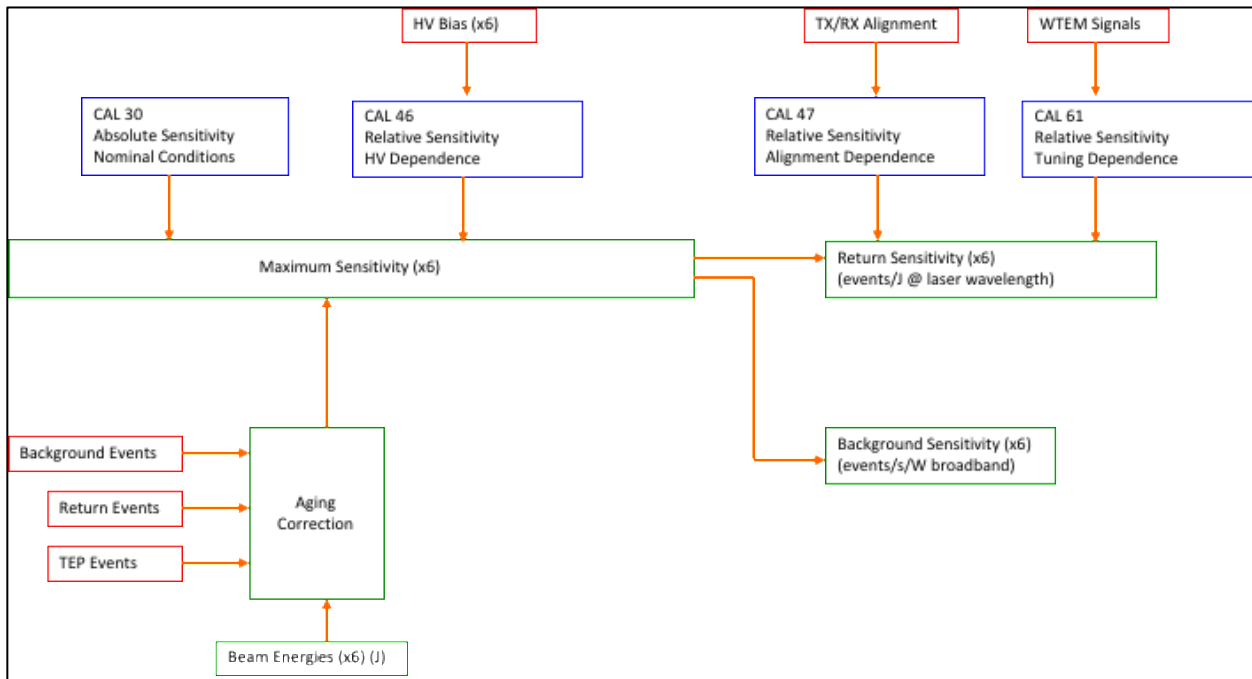


**Figure 16: Receiver Sensitivity work/data flow**

### 5.3.1 Maximum Sensitivity

Maximum receiver sensitivity  $S_{max}$  is an intermediate calculation that is used to produce two ATL02 outputs, background sensitivity and return sensitivity. It is not itself reported out.

The calculation of maximum sensitivity starts with a value under nominal conditions, which is retrieved from CAL-30. This value is then corrected for differences between the current conditions and the nominal conditions, as described in the following sections.

#### 5.3.1.1 Sensitivity under nominal conditions

CAL-30 contains slopes for each spot (1 through 6) on each side (A and B) of the receiver that, with intercept values of 0, calculate the small-signal event rate from optical power entering the spot's field of view under nominal conditions at the beginning of life:

|                        |                                |                         |
|------------------------|--------------------------------|-------------------------|
| CAL-30 <sub>side</sub> | $= \{m_1, \dots, m_6\}_{side}$ | <b>Equation<br/>5-5</b> |
|------------------------|--------------------------------|-------------------------|

The slopes  $\{m_1, \dots, m_6\}_{side}$  given in CAL-30 represent  $S_{max,nom}$ , the maximum small-signal receiver sensitivity in events/second per picowatt (events per picojoule) of optical energy entering the unobstructed portion of the aperture. These are used in ATL02.

The maximum small-signal receiver sensitivity under current conditions is calculated using other calibration products, taking into account the differences between the current conditions and the nominal conditions, as described in the following sections.

### 5.3.1.2 Variation of sensitivity with temperature

Results of thermal/vacuum testing indicate that the variation of receiver maximum sensitivity with temperature is insignificant over the relevant temperature range. Therefore, no computation needs to be done in ATL02 to correct for such an effect.

### 5.3.1.3 Variation of sensitivity with bias voltage

CAL-46 contains a set of nominal bias voltages  $V_{nom}$  and parameters  $(b, c)$  for a function that describes the relative change of receiver sensitivity with deviation from the nominal bias voltage:

|                        |  |                     |
|------------------------|--|---------------------|
| CAL-46 <sub>side</sub> | $= \{(V_{nom1}, c_1, b_1), \dots, (V_{nom6}, c_6, b_6)\}_{side}$ | <b>Equation 5-6</b> |
|------------------------|--|---------------------|

The ratio of receiver sensitivity at the current voltage  $V$  to the receiver sensitivity at the nominal voltage is:

|                     |   |                     |
|---------------------|---|---------------------|
| $\frac{S}{S_{nom}}$ | $= (c(V - V_{nom})^2 + b(V - V_{nom}) + 1)$ | <b>Equation 5-7</b> |
|---------------------|---|---------------------|

### 5.3.1.4 Combined Effects

Per the 24 October 2017 version of ICESat-2-ATSYS-TN-0660, a total of 18.7% of the receiver aperture is obstructed by the telescope secondary mirror, the TAMS LTR, and other hardware. Thus, the unobstructed fraction of the aperture is 0.813. Putting these together gives:

|                     |  |                     |
|---------------------|--|---------------------|
| $S_{max,side,spot}$ | $= m_{side,spot} \cdot \left( c_{side,spot} (V_{side,spot} - V_{nom,side,spot})^2 + b_{side,spot} (V_{side,spot} - V_{nom,side,spot}) + 1 \right) \cdot 0.813 \cdot \text{aging correction}$ | <b>Equation 5-8</b> |
|---------------------|--|---------------------|

Where  $m$  is from CAL-30 and  $b, c,$  and  $V_{nom}$  are from CAL-46 and  $S_{max}$  is computed for each of the 6 spots on the active side. Aging corrections have a default value of 1. Updated values will be supplied from the ISF in ANC27.

### 5.3.1.5 Data Sources

Data sources for bias voltages,  $V_{side,spot}$ , are given in

Table 38 and are converted via ITOS expressions, per Section 8.4, prior to use:

**Table 38: Data Sources for Maximum Sensitivity Calculation**

| Description      | Product | APID | Source   |
|------------------|---------|------|--|
| PMT HV bias A 1  | ATL01   | 1059 | <b>ATL01 parameter:</b> /atlas/a_hkt_a_1059/raw_pri_hvpc_mod_1 |
| PMT HV bias A 2  | ATL01   | 1059 | <b>ATL01 parameter:</b> /atlas/a_hkt_a_1059/raw_pri_hvpc_mod_2 |
| PMT HV bias A 3  | ATL01   | 1059 | <b>ATL01 parameter:</b> /atlas/a_hkt_a_1059/raw_pri_hvpc_mod_3 |
| PMT HV bias A 4  | ATL01   | 1059 | <b>ATL01 parameter:</b> /atlas/a_hkt_a_1059/raw_pri_hvpc_mod_4 |
| PMT HV bias A 5  | ATL01   | 1059 | <b>ATL01 parameter:</b> /atlas/a_hkt_a_1059/raw_pri_hvpc_mod_5 |
| PMT HV bias A 6  | ATL01   | 1059 | <b>ATL01 parameter:</b> /atlas/a_hkt_a_1059/raw_pri_hvpc_mod_6 |
| PMT HV bias B 1  | ATL01   | 1060 | <b>ATL01 parameter:</b> /atlas/a_hkt_b_1060/raw_red_hvpc_mod_1 |
| PMT HV bias B 2  | ATL01   | 1060 | <b>ATL01 parameter:</b> /atlas/a_hkt_b_1060/raw_red_hvpc_mod_2 |
| PMT HV bias B 3  | ATL01   | 1060 | <b>ATL01 parameter:</b> /atlas/a_hkt_b_1060/raw_red_hvpc_mod_3 |
| PMT HV bias B 4  | ATL01   | 1060 | <b>ATL01 parameter:</b> /atlas/a_hkt_b_1060/raw_red_hvpc_mod_4 |
| PMT HV bias B 5  | ATL01   | 1060 | <b>ATL01 parameter:</b> /atlas/a_hkt_b_1060/raw_red_hvpc_mod_5 |
| PMT HV bias B 6  | ATL01   | 1060 | <b>ATL01 parameter:</b> /atlas/a_hkt_b_1060/raw_red_hvpc_mod_6 |
| Aging correction | ANC27   |      | CAL46_Aging parameter  |

### 5.3.1.6 Input data range

Acceptable input ranges for bias voltages are given in this table:

**Table 39: Input Data Range for Maximum Sensitivity Calculation**

| Description     | Minimum (V) | Maximum (V) |
|-----------------|-------------|-------------|
| PMT HV bias A 1 | -699        | -826        |
| PMT HV bias A 2 | -677        | -797        |
| PMT HV bias A 3 | -729        | -859        |
| PMT HV bias A 4 | -723        | -870        |
| PMT HV bias A 5 | -714        | -861        |
| PMT HV bias A 6 | -718        | -859        |
| PMT HV bias B 1 | -734        | -862        |
| PMT HV bias B 2 | -708        | -852        |
| PMT HV bias B 3 | -740        | -862        |
| PMT HV bias B 4 | -662        | -790        |
| PMT HV bias B 5 | -667        | -788        |
| PMT HV bias B 6 | -711        | -852        |

CAL 46 models the dependence as a quadratic with a linear term. Maximum responsivity is near the nominal voltage, in most cases slightly more negative, so it incorrectly predicts reduced responsivity when the bias is much more negative than the nominal value. These limits are designed to avoid the region where CAL 46 is known to be invalid.

The maximum values are set 10 V more negative than the value at which CAL 46 gives responsivity of 0.

The minimum values are set 10 V more negative than the nominal voltage.

### 5.3.1.7 Output data range

Maximum receiver sensitivity is an intermediate calculation that is not reported in the ATL02 data product. It is effectively screened by the screening of the background sensitivity.

## 5.3.2 Background Sensitivity

### 5.3.2.1 Calculation

Background sensitivity is the receiver's response in (events/sec) per watt of continuous illumination in the receiver's passband from a diffuse source larger than the receiver's field of view, in the absence of any dead time effects. It is computed from maximum sensitivity by a scaling factor:

|                    |   |                         |
|--------------------|---|-------------------------|
| $S_{BG,side,spot}$ | $= \textit{scaling factor} \cdot S_{max,side,spot}$ | <b>Equation<br/>5-9</b> |
|--------------------|---|-------------------------|

The default value of the scaling factor is 1; it is a placeholder for any adjustment that may be needed.

About 10% of the background event rate is due to stray light from outside the receiver's field of view. CAL-30 is computed using measurements made with a light source that greatly overfills the field of view, so it accurately reflects the conditions of background light.

ATL02 reports background sensitivity for each of the 6 active spots, for the side that is in use, in the following location:

**Table 40: Output of Background Sensitivity Calculation**

| Parameter Stored In:  | Equation     | Description   |
|---|--------------|---|
| <code>/atlas/housekeeping/radiometry/bg_sensitivity_pce{1 2 3}_{s/w}</code> | Equation 5-9 | Receiver response per watt of continuous illumination in the passband from a diffuse source larger than the field of view, in the absence of any dead time effects. |

### 5.3.2.2 Output data range

The expected output range for background sensitivity:

**Table 41: Expected Output Range for Background Sensitivity Calculation**

| Parameter Stored In:  | Equation     | Description            | Minimum<br>(events/sec/watt) | Maximum<br>(events/sec/watt) |
|---|--------------|------------------------|------------------------------|------------------------------|
| <code>/atlas/housekeeping/radiometry/bg_sensitivity_pce{1 2 3}_{s/w}</code> | Equation 5-9 | Background Sensitivity | $5 \times 10^{17}$           | $2 \times 10^{18}$           |

## 5.3.3 Return Sensitivity

Return sensitivity is the receiver's response in (events/return pulse) per (joule/return pulse) in the receiver's field of view, in the absence of any dead time effects. It is affected by angular alignment of the transmitter to the receiver and by tuning of the transmitter's wavelength to the receiver's passband.

Note that the dimensions given for background sensitivity and return sensitivity both reduce to events per joule. They are expressed as they are to reflect the different quantities that are of interest in each case.



### 5.3.3.1 Variation of sensitivity with transmit/receive misalignment

CAL-47 describes the dependence of receiver sensitivity on transmit/receive misalignment. There are two versions, a radial version (which assumes circular symmetry and is available on the ICESat-2 Science Computing Facility) and an image version (included with science data products). The ATL02 product will be calculated using the image version.

CAL-47 (Image version) contains two-dimensional arrays of sample points of a function that describes the loss of return sensitivity as the transmitter is misaligned from the receiver by a pair of angles  $\theta$  and  $\phi$ :

|         |  |                      |
|---------|--|----------------------|
| CAL-47I | $= \left\{ \begin{array}{ccc} \eta_{\theta_1, \phi_1} & \cdots & \eta_{\theta_M, \phi_1} \\ \vdots & \ddots & \vdots \\ \eta_{\theta_1, \phi_N} & \cdots & \eta_{\theta_M, \phi_N} \end{array} \right\}_{spot, temperature}$ | <b>Equation 5-10</b> |
|---------|--|----------------------|

CAL-47 files are indexed by the temperature of the optical bench near the beam expander; the file nearest the current value of that temperature is used. If the temperature fails the valid input value test, the most recent valid value is used.

The ratio of receiver sensitivity at misalignment  $(\theta, \phi)$  to the receiver sensitivity at zero misalignment is calculated by:

|                 |  |                      |
|-----------------|--|----------------------|
| $\frac{S}{S_0}$ | = Interpolation[CAL-47I]( $\theta, \phi$ ) | <b>Equation 5-11</b> |
|-----------------|--|----------------------|

The ISF provides, in ANC27, a sequence values of transmit/receive misalignment angle  $(\theta_{misalign}, \phi_{misalign})$ , derived from the AMCS calibration procedure, with an effective date and time for each value. If the time,  $t$ , for which the calculation of sensitivity is being done is after the effective time of the last misalignment value in ANC27, the last value of  $(\theta_{misalign}, \phi_{misalign})$  is used for  $(\theta, \phi)$ . If  $t$  falls between two times  $t_N$  and  $t_{N+1}$  in the ANC27 sequence, then for a time  $t$  such that:

|  |                        |                      |
|--|------------------------|----------------------|
|  | $t_N < t \leq t_{N+1}$ | <b>Equation 5-12</b> |
|--|------------------------|----------------------|

The misalignment to be used is:

|                          |  |                      |
|--------------------------|--|----------------------|
| $\{\theta(t), \phi(t)\}$ | $= \{ \theta_{misalign, N}, \phi_{misalign, N} \} + \frac{t - t_N}{t_{N+1} - t_N} (\{ \theta_{misalign, N+1}, \phi_{misalign, N+1} \} - \{ \theta_{misalign, N}, \phi_{misalign, N} \})$ | <b>Equation 5-13</b> |
|--------------------------|--|----------------------|

This is a linear interpolation between misalignment values given at specific times in ANC27.

### 5.3.3.2 Variation of sensitivity with mistuning

Two wavelength deviation indicators,  $D_{\lambda S}$  and  $D_{\lambda A}$ , are used:

|                 |                                  |               |
|-----------------|----------------------------------|---------------|
| $D_{\lambda S}$ | $= \frac{D_{peak}}{D_{edge}}$    | Equation 5-14 |
| $D_{\lambda A}$ | $= \frac{D_{edge}}{W \cdot SPD}$ | Equation 5-15 |

where  $D_{peak}$  is the WTEM peak signal,  $D_{edge}$  is the WTEM edge signal,  $SPD$  is the SPD energy monitor reading as described above, and  $W$  has the value 1 at launch and is updated to reflect any changes in the relation between the maximum value of  $D_{edge}$  and the SPD.  $D_{\lambda S}$  is used when Standard Tuning is in effect, and  $D_{\lambda A}$  is used when Alternate Tuning is in effect.

CAL-61 contains sets of parameters of a function that relates loss of sensitivity to spectral mistuning as indicated by the WTEM edge signal ( $D_{edge}$ ), the WTEM peak signal ( $D_{peak}$ ), and the SPD energy monitor. Sets of parameters are included for Standard Tuning and Alternate Tuning and for several values of  $\Delta\lambda_{WTO M}$ .

|        |                                     |               |
|--------|-------------------------------------|---------------|
| CAL-61 | $= \{(h, D_{\lambda max})_{spot}\}$ | Equation 5-16 |
|--------|-------------------------------------|---------------|

where  $D_{\lambda max}$  is the value of  $D_{\lambda}$  when the laser is tuned to maximum transmittance of the OFMs. ANC27 contains a flag that indicates which tuning is in effect and the current value of  $\Delta\lambda_{WTO M}$ .

The ratio of receiver sensitivity at the current state of tuning to the receiver sensitivity at zero mistuning is calculated by:

|                 |  |               |
|-----------------|--|---------------|
| $\frac{S}{S_0}$ | $= 1 + h(D_{\lambda} - D_{\lambda max})^2$ | Equation 5-17 |
|-----------------|--|---------------|

### 5.3.3.3 Combined effects

Putting all this together gives:

|                     |  |               |
|---------------------|--|---------------|
| $S_{RET,side,spot}$ | $= \textit{scaling factor} \cdot S_{max,side,spot} \cdot \{ \textit{Interpolation}[CAL - 47I](\theta, \phi) \}_{spot} \cdot \{ 1 + h(D_{\lambda} - D_{\lambda max})^2 \}_{spot}$ | Equation 5-18 |
|---------------------|--|---------------|

The default value of the scaling factor is 0.9, reflecting the absence of return light from outside the field of view when the transmitter and receiver are aligned. CAL-30 is computed using measurements made with a light source that greatly overfills the field of view, so this correction is necessary to accurately reflect the conditions of return light.

ATL02 reports return sensitivity for each of the 6 active spots, for the side that is in use, in the following parameter:

**Table 42: Output of Return Sensitivity Calculation**

| Parameter Stored In:  | Equation      | Description  |
|---|---------------|--|
| /atlas/housekeeping/radiometry/ret_sensitivity_pce{1/2/3}_{s/w} | Equation 5-18 | Receiver response per joule/return pulse in the field of view, in the absence of any deadtime effects. |



### 5.3.3.4 Data sources

Data sources for quantities associated with alignment and tuning are given in Table 43. Note that:

- The selection of the SPD energy monitor should be made according to which SPD, *not laser*, is in use.
- Temperature data are reported at 1 Hz whereas energy monitor data are reported at 10 Hz; in cases where both temperature and energy data are used as input to an equation, the latest temperature data should be used for each of the 10 corresponding energy cases.
- Temperature data are converted prior to use in calculations. See Section 8.4.
- The energy monitor values are used as written on ATL01. They are not written to the ATL02 product.
- The WTEM peak and edge conversions are described in ATLAS-ALG-TN-0955.

**Table 43: Data Sources for Return Sensitivity Calculation**

| Description                                       | Product | APID | Source   |
|---|---------|------|--|
| Misalignment ( $\theta, \phi$ )                   | ANC27   |      | Bias_offset_X<br>Bias_offset_Y   |
| Misalignment Rate                                 | ANC27   |      | Bias_rate  |
| Time misalignment data is valid                   | ANC27   |      | Time stamp on Bias_offset_X  |
| Temperature for CAL47                             | ATL01   | 1061 | <b>Telemetry Mnemonic:</b> Chan 82: A_HKT_BEAMX_T<br><b>ATL01 parameter:</b> /atlas/a_hkt_c_1061/raw_hkt_beamx_t                       |
| WTEM peak signal ( $D_{peak}$ )                   | ATL01   | 1063 | <b>Telemetry Mnemonic:</b> Chan 21: A_PEAK_XMTNC_MV<br><b>ATL01 parameter:</b> /atlas/a_hkt_e_1063/raw_peak_xmtnc                      |
| WTEM edge signal ( $D_{edge}$ )                   | ATL01   | 1063 | <b>Telemetry Mnemonic:</b> Chan 20: A_EDGE_XMTNC_MV<br><b>ATL01 parameter:</b> /atlas/a_hkt_e_1063/raw_edge_xmtnc                      |
| SPD energy monitor A                              | ATL01   | 1063 | <b>Telemetry Mnemonic:</b> Chan 0-18 (evens): SPD PRI LSR ENERGY MON<br><b>ATL01 parameter:</b> /atlas/a_hkt_e_1063/raw_pri_lsr_energy |
| SPD energy monitor B                              | ATL01   | 1063 | <b>Telemetry Mnemonic:</b> Chan 1-19 (odds): SPD RED LSR ENERGY MON<br><b>ATL01 parameter:</b> /atlas/a_hkt_e_1063/raw_red_lsr_energy  |
| Tuning (Standard or Alternate)                    | ANC27   |      | WTOM_tuning_flag   |
| WTOM Wavelength Offset ( $\Delta\lambda_{WTOM}$ ) | ANC27   |      | WTOM_lambda_off  |
| Alternate Tuning Correction ( $W$ )               | ANC27   |      | WTOM_alt_tune_corr   |
| Selected SPD                                      | ANC13   |      | Second column  |

### 5.3.3.5 Input data range

Acceptable input ranges for quantities associated with alignment and tuning are given in this table:

**Table 44: Input Data Ranges for Return Sensitivity Calculation**

| Description                            | Minimum     | Maximum    |
|--|-------------|------------|
| Misalignment (each dimension)          | -70 $\mu$ R | 70 $\mu$ R |
| Temperature for CAL-47 ( $^{\circ}$ C) | -20         | +50        |
| WTEM peak signal ( $D_{peak}$ )        | >0          | Infinity   |
| WTEM edge signal ( $D_{edge}$ )        | >0          | Infinity   |
| SPD energy monitor A                   | 0           | 30000      |
| SPD energy monitor B                   | 0           | 30000      |

### 5.3.3.6 Output data range

The expected output range for return sensitivity:

**Table 45: Output Data Range for Return Sensitivity Calculation**

| Description        | Minimum<br>(events/Joule) | Maximum (events/Joule) |
|--------------------|---------------------------|------------------------|
| Return Sensitivity | 0                         | $2 \times 10^{18}$     |

## 5.4 Dead time effects on radiometry

The effects of dead time on receiver sensitivity, which are apparent at sufficiently high return strengths, are not treated in ATL02. They are calculated at the point of surface return analysis in higher-level science data products.

## 5.5 Data Screening Mechanisms & Associated Responses

The computations outlined in this chapter will be assessed via the quality assessment parameters listed in Table 46 below.

Data quality monitoring consists of input and output range checking.

Range checking is performed wherever range tables are given.

If a total transmitted energy value is flagged as suspect, then the individual beam energies calculated from it are also to be flagged as suspect.

**Table 46: Radiometry Data Quality Monitoring Criteria**

| Pre/Post Calculation | Check                  | Pass Criteria             | ATL02 Screening Parameter                     | Method                               | Failure Response   |
|----------------------|------------------------|---------------------------|---|--------------------------------------|--|
| <b>Pre</b>           | SPD Energy Monitor A/B | Value between 0 and 30000 | <i>/quality_assessment</i><br><i>/summary</i> | Check that values fall within range. | Total transmitted and individual beam energies are not computed, a |

|             |                                 |   |  |                                      |   |
|-------------|---------------------------------|---|--|--------------------------------------|---|
|             |                                 |   | <i>/qa_spd_energy</i>  |                                      | placeholder value is reported, and a flag is set to indicate input out of range.  |
| <b>Pre</b>  | SPD Temperature A/B             | Value between -20 and +50 degreesC                                      | <i>/quality_assessment<br/>/summary<br/>/qa_spd_temp</i>                                 | Check that values fall within range. | Total transmitted and individual beam energies are not computed, a placeholder value is reported, and a flag is set to indicate input out of range. |
| <b>Pre</b>  | Laser Internal Energy Monitor   | Value between 0 and 200   | <i>/quality_assessment<br/>/summary<br/>/qa_internal_energy</i>                          | Check that values fall within range. | Total transmitted and individual beam energies are not computed, a placeholder value is reported, and a flag is set to indicate input out of range. |
| <b>Pre</b>  | Laser 1/2 Interface Temperature | Value between +20 and +40 degreesC                                      | <i>/quality_assessment<br/>/summary<br/>/qa_internal_temp</i>                            | Check that values fall within range. | Total transmitted and individual beam energies are not computed, a placeholder value is reported, and a flag is set to indicate input out of range. |
| <b>Pre</b>  | Number of LRS Spots             | Value must be 6   | <i>/quality_assessment<br/>/summary<br/>/qa_lrs_inv_spot</i>                             | Check that value exactly 6.          | Total transmitted and individual beam energies are not computed, a placeholder value is reported, and a flag is set to indicate input out of range. |
| <b>Pre</b>  | LRS Magnitude Sum               | Value between 0 and 2000  | <i>/quality_assessment<br/>/summary<br/>/qa_lrs_inv_sum</i>                              | Check that values fall within range. | Total transmitted and individual beam energies are not computed, a placeholder value is reported, and a flag is set to indicate input out of range. |
| <b>Pre</b>  | LRS Individual Spot Magnitude   | Value between 0 and 500   | <i>/quality_assessment<br/>/summary<br/>/qa_lrs_inv_mag</i>                              | Check that values fall within range. | Total transmitted and individual beam energies are not computed, a placeholder value is reported, and a flag is set to indicate input out of range. |
| <b>Pre</b>  | LRS Temperature                 | Value between -20 and +50 degreesC                                      | <i>/quality_assessment<br/>/summary<br/>/qa_lrs_temp</i>                                 | Check that values fall within range. | Total transmitted and individual beam energies are not computed, a placeholder value is reported, and a flag is set to indicate input out of range. |
| <b>Post</b> | Total Transmitted Energy        | Laser energy-level dependant; range from 130-680 min to 530-2700 μJ max | <i>/quality_assessment<br/>/summary/qa_int_e_tx, /qa_lrs_e_tx &amp;<br/>/qa_spd_e_tx</i> | Check that values fall within range. | If a total transmitted energy value is flagged as suspect, then the individual beam energies calculated from it are also to be flagged as suspect.  |

|             |                               |                                       |   |                                      |   |
|-------------|-------------------------------|---------------------------------------|---|--------------------------------------|---|
| <b>Pre</b>  | PMT HV bias A/B 1-6           | Value between - values in Table 39    | <i>/quality_assessment<br/>/summary<br/>/qa_hpv_mod_{1-6}</i>                             | Check that values fall within range. | Maximum and background sensitivities are not computed, a placeholder value is reported, and a flag is set to indicate input out of range.                     |
| <b>Pre</b>  | Background sensitivity        | Value between 5e17 to 2e18            | <i>/quality_assessment<br/>/summary/pce{1-3}<br/>/qa_bg_sens_{s,w}</i>                    | Check that values fall within range. | If the maximum receiver sensitivity is flagged as suspect, then the background and return sensitivities calculated from it are also to be flagged as suspect. |
| <b>Pre</b>  | Misalignment (each dimension) | Value between -70 and 70 $\mu$ R      | <i>/quality_assessment<br/>/summary<br/>/qa_bias_offset_x &amp;<br/>/qa_bias_offset_y</i> | Check that values fall within range. | Return sensitivity is not computed, a placeholder value is reported, and a flag is set to indicate input out of range.  |
| <b>Pre</b>  | CAL-47 Temperature            | Value between -20 and +50 degreesC    | <i>/quality_assessment<br/>/summary<br/>/qa_cal47_temp</i>                                | Check that values fall within range. | Return sensitivity is not computed, a placeholder value is reported, and a flag is set to indicate input out of range.  |
| <b>Post</b> | Return sensitivity            | Value between 0 and 2e18 events/Joule | <i>/quality_assessment<br/>/summary/pce{1-3}<br/>/qa_ret_sens_{s,w}</i>                   | Check that values fall within range. | If return sensitivity is out of range, the computed value is reported, and a flag is set to indicate a suspect value.   |

## 6 Pointing and Geolocation

To meet ICESat-2's scientific requirement of computing elevation, each TOF measurement must be precisely geolocated. Computation of the geolocation and elevation of the laser altimeter bounce point relies primarily on:

- Position of ATLAS via Precise Orbit Determination (POD)
- Direction of the laser beam via Precise Pointing Determination (PPD)
- TOF of a surface return photon as measured by ATLAS

TOF calculations are documented in Chapter 3 of this ATBD and the resulting values are provided via the ATL02 data product. The POD and PPD components are calculated external to the ATL02 data product and are outside the scope of this ATBD. Detailed information about the computation of these components can be found in the ATL03G ATBD.

These higher level products rely on ATL02 to provide LRS, GPS receiver (gpsr), orbit (orbit\_info), and spacecraft (sc) information. Conversion of these data from their raw form to appropriate engineering units is described in Chapter 8 of this document.



## 7 Atmospheric Histograms

In addition to the altimetric data described in prior sections of this document, the ATL02 product also supplies atmospheric histograms. These atmospheric histograms are generated by the FSW for every major frame at a rate of 50 Hz (200 shots) for all six ground spots. Specifically, the atmospheric histograms span the lowest 14 km of the atmosphere with 467 vertical bins, each with a width of 200 ns (approximately 30 m). Consecutive histograms for each spot are combined to generate 400-shot histograms spanning a distance of 280 m along track.

Onboard, these 400-shot histograms are used by the flight software to determine the presence of thick clouds. In the telemetry, the atmospheric histogram associated with a major frame  $MF_n$ , contains the 200 shot histogram for consecutive major frames  $MF_m$  and  $MF_n$ , combined into a single 400 shot histogram. All 400 shot histograms are downlinked.

### 7.1 Atmospheric Histogram Nominal Calculations

The following terms are used in computing the parameters of the atmospheric histograms. In order of appearance:

**Table 47: Generalized Atmospheric Histogram Calculation Notation**

| Symbol     | Parameter               | Super or Subscript | Valid Values    |
|------------|-------------------------|--------------------|-----------------|
| $\alpha$   | Hardware Side           | Superscript        | A, B            |
| $\beta$    | PCE Identifier          | Superscript        | 1, 2, 3         |
| $\gamma$   | Toggle Value            | Subscript          | Rising, Falling |
| $\delta$   | Leading Start Component | Subscript          | LL1, LL2, LL3   |
| $\tau$     | Other Component         | Subscript          | LU, TU, TL      |
| $\xi$      | Spot Type               | Subscript          | Strong, Weak    |
| $\zeta$    | Downlink Band           | Subscript          | 1, 2, 3, 4      |
| $\epsilon$ | Channel                 | Subscript          | 1, 2, ..., 20   |

**Table 48: Dictionary of Atmospheric Histogram Derivation Variables**

| Uncalibrated Notation | Calibrated Notation        | Description   | Units         | Source  |
|-----------------------|----------------------------|---|---------------|---|
| $d_{USO}$             | n/a                        | Nominal USO period (10ns).  | Seconds       | DFC FPGA Spec   |
| n/a                   | $SF_{USO}^{\alpha}$        | USO scale factor.   | dimensionless | Calculated value per Equation 2-4                                     |
| n/a                   | $ATM_{RWS}_{\xi}^{\beta}$  | The number of coarse clock intervals between the transmit pulse and the start of the atmospheric range window.                                      | Clock cycles  | ATL01 parameter: <i>/atlas/pcex/a_atm_hist_x/raw_atm_rw_start</i>     |
| n/a                   | $ATM_{RWS}_{T\xi}^{\beta}$ | Time elapsed between the transmit pulse and the atmospheric range window.   | Seconds       | Calculated value per Equation 7-1                                     |
| n/a                   | $ATM_{RWW}_{\xi}^{\beta}$  | Atmospheric range window width expressed in coarse clock intervals.   | Clock cycles  | ATL01 parameter: <i>/atlas/pcex/a_atm_hist_x/raw_atm_rw_width</i>     |
| n/a                   | $ATM_{RWW}_{T\xi}^{\beta}$ | Time elapsed between the start and end of the altimetric range window.  | Seconds       | Calculated value per Equation 7-2                                     |
| n/a                   | $ATM\_bins$                | 467 element vector for the 400 shot atmospheric histogram. Each element represents the number of return events contained in the respective 30m bin. | Counts        | ATL01 parameter: <i>/atlas/pcex/a_atm_hist_x/raw_atm_bins</i>         |
| n/a                   | $ATM\_shift$               | The number of 30m bins that one of the two 200-shot histograms is shifted to align the histograms before adding them.                               | Counts        | ATL01 parameter: <i>/atlas/pcex/a_atm_hist_x/raw_atm_shift_amount</i> |

## 7.2 Construction of the Atmospheric Histogram

The atmospheric histogram represents the distribution of the apparent times of flight computed from all detected photon events. These histograms are passed through for use in the downstream workflow. Among other uses, these atmospheric histograms are used to detect clouds that may bias the range calculation or make the data unreliable, and to calculate thresholds for identifying signal photons. The atmospheric histograms are produced by the ATLAS flight software via the following method at a rate of 25 Hz:

- A 200 shot, 467 bin histogram, with bin widths of ~200 ns is computed for both  $MF_m$  and  $MF_n$ . This results in a resolution of ~30 m over a ~14 km range. The end (start + width) of each atmospheric range window is roughly aligned with the *end* of the corresponding altimetric range window. The boundaries of the altimetric range window change in steps of 20 ns while the boundaries of the atmospheric range window change in steps of 200 ns, so the alignment is rarely exact.
- Before summing two histograms from adjacent major frames, it may be necessary to shift one of the histograms slightly to account for any difference in the range window start times that might occur between the two major frames. Shifts are always done in single bin (200 ns or 30 m) increments so that the histogram bins can always be aligned between  $MF_m$  and  $MF_n$ . Figure 17 shows an example of this

alignment technique. The absolute value of the shift, *atm\_shift\_amount*, is recorded in ATL02 as an integer number of bins.

- Once the histograms of MF<sub>m</sub> and MF<sub>n</sub> are aligned, then their bins are summed and the resultant histogram is stored to the atm\_bins parameter in ATL02. After the summation, there may be bins at the ends of the histogram that do not overlap and therefore contain the original 200-shot values. The flight software discards the bins at the start of the histogram that do not overlap and keeps the bins at the end of the histogram that do not overlap, so the total length of the histogram remains 467 bins.

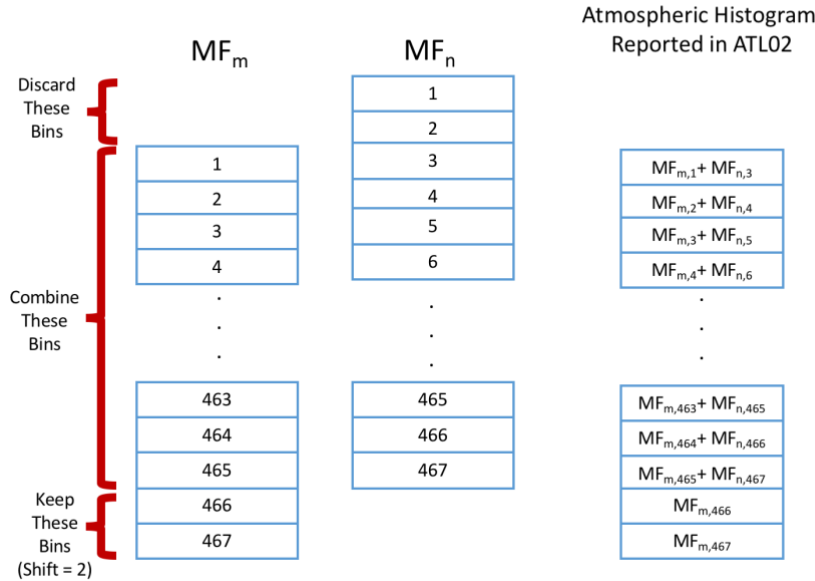


**Figure 17: Histogram alignment technique for Atmospheric Histogram Generation**

The atmospheric RWS and RWW of the 400 shot histograms are then calculated and the resultant values stored in ATL02. The atmospheric histogram range window start is calculated as:

|                        |   |                     |
|------------------------|---|---------------------|
| $ATM_{RWS_T\xi}^\beta$ | $= ATM_{RWS_\xi}^\beta \cdot d_{USO} * SF_{USO}^\alpha$ | <b>Equation 7-1</b> |
|------------------------|---|---------------------|

The atmospheric histogram range window width is calculated as:

|                        |   |                     |
|------------------------|---|---------------------|
| $ATM_{RWW_T\xi}^\beta$ | $= ATM_{RWW_\xi}^\beta \cdot d_{USO} * SF_{USO}^\alpha$ | <b>Equation 7-2</b> |
|------------------------|---|---------------------|

These values may in turn be used to determine the precise TOF of the top and bottom of the atmospheric histogram span.

### 7.3 Atmospheric Histogram Parameters Included in ATL02 Output File

The following values are written to the ATL02 output file and are provided for reference within the context of this document. More detailed descriptions of each value may be found in the ATL02 data product dictionary as well as the ATL02 verification matrix. In the event of a conflict among sources, the verification matrix content will dictate.

**Table 49: Atmospheric Histogram Parameters on the ATL02 Product (25Hz data rate)**

| Stored In<br><i>/atlas/pcex/atmosphere_sw/</i> | Equation<br>or Table | Description  |
|--|----------------------|--|
| <i>atm_bins</i>                                | N/A                  | The histogram bins for the Atmospheric beam. Summed once every 400 shots and expressed in units of counts.   |
| <i>atm_rw_start</i>                            | Equation<br>7-1      | Number of seconds between transmit pulse and start of atmospheric range window   |
| <i>atm_rw_width</i>                            | Equation<br>7-2      | Number of seconds between start and end of atmospheric range window  |
| <i>atm_shift_amount</i>                        | FSW<br>Supplied      | Shift between major-frame range windows, in 30 ns bins   |
| <i>delta_time</i>                              | Chapter<br>8.1       | The time of the first TX pulse considered in the 400-shot sum atmospheric histogram.   |
| <i>ds_hist_bin_index</i>                       | N/A                  | Dimension scale for atmosphere histogram bins. Default value is 467.   |
| <i>pce_mframe_cnt</i>                          | FSW<br>Supplied      | Frame number corresponding to, sequentially, the second of two major frames (i.e. MF <sub>n</sub> ) of data summed to generate the atmospheric histogram |
| <i>useflag</i>                                 | FSW<br>Supplied      | Flag which indicates the operational mode of the instrument.   |

## 7.4 Data Screening Mechanisms & Associated Responses

The computations outlined in this chapter will be checked via the quality assessment parameters included in Table 50 below.

**Table 50: Atmospheric Histogram Quality Monitoring Criteria**

| Check  | Pass Criteria                                   | ATL02 Screening<br>Parameter                                  | Method                               | Failure Response               |
|--|---|---|--------------------------------------|--------------------------------|
| <b>Number of ATM strong inputs processed.</b>  | Half of number of major frames +/- 1.           | <i>/quality_assessment/record_counts/pcex/qa_n_atm_hist_s</i> | Check that values fall within range. | Report via daily email digest. |
| Number of ATM weak inputs processed.   | Half of number of major frames +/- 1.           | <i>/quality_assessment/record_counts/pcex/qa_n_atm_hist_w</i> | Check that values fall within range. | Report via daily email digest. |
| <b>Summary statistics on the differences between successive <i>/atlas/pcex/atmosphere_strong</i> time of day values.</b> | 10 standard deviations from nominal mean 40 ms. | <i>/quality_assessment/summary/pcex/qa_s_tod_atm_hist_s</i>   | Check that values fall within range. | Report via daily email digest. |
| <b>Summary statistics on the differences between successive <i>/atlas/pcex/atmosphere_weak</i> time of day values.</b>   | 10 standard deviations from nominal mean 40 ms. | <i>/quality_assessment/summary/pcex/qa_s_tod_atm_hist_w</i>   | Check that values fall within range. | Report via daily email digest. |

## 8 Other Data & Data Pass-Throughs

In addition to the parameters outlined in previous sections, ATL02 acts as a “pass-through” for numerous other data. The majority of these are used by down-stream products for their processing; some, however, are included in order to provide context for the analysis performed within the ATL02 data product. In most cases, little to no manipulation of the data is performed apart from assigning a *delta\_time* value to the data. The following subsections outline all of the data for which ATL02 is a conduit.

### 8.1 Assignment of *delta\_time* for Non-Altimetric Science Data

The assignment of *delta\_time* values to non-altimetric science data varies according to the data type. The possible scenarios are as follows:

1. Any packets that reference the 1 PPS, the TOD of the associated 1 PPS is used
2. GPSR packets use the methodology described in DN-ICESat2-SYS-024
3. LRS packets use the methodology described in ICESat-2-LRS-IFACE-1794
4. All other packet times (i.e. those without a 1 PPS) are computed using the SIM\_HK CCSDS time and 1 PPS TOD interpolated to that packet’s CCSDS time. In the case of A\_HKT\_A-E, this is additionally supplemented by an additive offset.

The fourth scenario is not fully summarized in one document. An overview of this interpolation is provided in Section 8.1.1.

#### 8.1.1 Determining *delta\_time* for Packets without a 1 PPS Reference

The ATLAS HKT card performs 320 analog-to-digital conversions (ADCs) evenly spaced over a period of one second. The cycle repeats with the next full second, having been initiated by the subsequent internal 1 PPS from the ASC card. Thus, the sample period is found as:

|                      |  |                     |
|----------------------|--|---------------------|
| $T_{sample\_period}$ | $= \frac{1 \text{ sec}}{320 \text{ samples}}$ $= 3.125 \text{ msec}$ | <b>Equation 8-1</b> |
|----------------------|--|---------------------|

The sampled output of the HKT card is telemetered via five different packets (A\_HKT\_A-E). The collection order is documented in Table 6-3 ICESat-2-MEB-SPEC-0688. The time assigned to each packet is based on the time the lowest software channel contained in the packet was collected. A summary of channels by packet can be seen in Table 51: Housekeeping packet configurations.

**Table 51: Housekeeping packet configurations**

| Packet     | APID | HKT Telemetry Type          | HKT Channels (HKT_Channel_Number)  |
|------------|------|-----------------------------|--|
| A_HKT_A    | 1059 | PDU A Analog (Primary)      | 150 – 157<br>168 – 191<br>194 – 223<br>226 - 241   |
| A_HKT_B    | 1060 | PDU B Analog (Redundant)    | 158, 159<br>162 - 167<br>242 – 255<br>258 – 287<br>290 - 315   |
| A_HKT_C    | 1061 | Thermistor Analog           | 34 – 63<br>66 – 95<br>98 – 127<br>130 – 142  |
| A_HKT_D    | 1062 | MEB Analog                  | 2 - 31   |
| A_HKT_E    | 1063 | Laser                       | Laser energy levels:<br>0, 1<br>32, 33<br>64, 65<br>96, 97<br>128, 129<br>160, 161<br>192, 193<br>224, 225<br>256, 257<br>288, 289<br><br>Peak, Edge, and Threshold Info:<br>143 – 149 |
| Unassigned | N/A  | Unassigned / Spare Channels | 316 - 319  |

If the specific time of a particular telemetry sample is needed, the time elapsed between it and its associated internal 1 PPS may be found as:

|                      |  |                     |
|----------------------|--|---------------------|
| $T_{sample\_offset}$ | $= HKT_{ChannelNumber} * T_{sample\_period}$ | <b>Equation 8-2</b> |
|----------------------|--|---------------------|

In turn, the GPS time of the sample may be found by adding  $T_{sample\_offset}$  to the internal 1 PPS GPS time:

|              |   |                     |
|--------------|---|---------------------|
| $T_{sample}$ | $= T_{InternalPPSGPSTime} + T_{sample\_offset}$ | <b>Equation 8-3</b> |
|--------------|---|---------------------|

Where the value of  $T_{InternalPPSGPSTime}$  is obtained from `/atlas/a_sim_hk_1026/raw_gps_at_asc_1pps_secs` and `raw_gps_at_asc_1pps_sub_secs`.

In the flight telemetry, data will only be reported for the active PDU (i.e., A\_HKT\_A or A\_HKT\_B) and for only the *powered* laser in A\_HKT\_E. The active PDU and laser may be determined via the information

outlined in Section 1.5.1. Both primary and redundant values are reported for the MEB and Thermal HKT packets, A\_HKT\_D and A\_HKT\_C.

## 8.2 Ancillary Data (*/ancillary\_data*)

The following ATL02 groups contain calibration product information, instrument characteristics, and processing constants that support the calculations described in the TOD, TOF, and Radiometry chapters of this document. Data rates vary and content of these groups are not manipulated by the processing utilities. Description of field contents and rates may be found in the ATL02 data product dictionary.

This information applies to the following data group(s) on the ATL02 product:

- */ancillary\_data/* - Contains information ancillary to the data product. This may include product characteristics, instrument characteristics and/or processing constants. Populated by the ground processing software.
- */ancillary\_data/calibrations/\** - Parameters and tables read from the calibration products used to generate ATL02.
- */ancillary\_data/housekeeping/* - Instrument configuration flags as provided by APID 1065.
- */ancillary\_data/isf/* - Parameters supplied by ISF via ANC27.
- */ancillary\_data/tep/* - Parameters used to perform TEP identification. Content provided via ATL02 configuration file.
- */ancillary\_data/tod\_tof/* - Contains constants described in TOD and TOF chapters. Content provided via ATL02 configuration file.

## 8.3 Status HKT Data (*/atlas/housekeeping/status*)

This group contains flags parsed from the HKT Status Registers Housekeeping Packet, APID 1065. The data rate is nominally 1 Hz. No manipulation, beyond bit-wise unpacking of the data, is performed between the ATL01 and the ATL02 product.

This information applies to the following data group(s) on the ATL02 product:

- */atlas/housekeeping/status/*

## 8.4 Thermal & Electrical HKT Data (*/atlas/housekeeping/meb, pdu, thermal*)

The following ATL02 groups contain housekeeping data, including relevant voltage, current, temperature, and energy level telemetry points, as well as the *delta\_time* for each packet. The *delta\_time* of individual parameters may be determined per Section 8.1.

These housekeeping values are converted per the flight-delivered ITOS database and are reported as floats at a rate of 1 Hz. The information is derived from the 1059, 1060, 1061, and 1062 APID packets. Note that since telemetry point names in the ITOS database, the ATL01 product, and ATL02 do not display continuity, the authors of this ATBD have provided a rosetta stone which maps these parameters across the products. This document may be found at ATLAS-ALG-TN-0955.

This information applies to the following data groups on the ATL02 product:



- */atlas/housekeeping/meb/* - Includes ground check, currents, voltages, and temperatures.
- */atlas/housekeeping/pdu/* - Includes information on HVPC modules, currents, and voltages.
- */atlas/housekeeping/thermal/* - Includes temperature readouts from numerous thermistors.

**Note: The laser gives valid preamplifier voltage and current telemetry at energy level 0 and 6 or above. At levels 1 through 5, it gives 0 or previously valid stale values. This is a known and expected output of the FPGA card.**

## 8.5 MCE HKT Data (*/atlas/housekeeping/mce\_position*)

The following group contains the full-rate MCE position data, which appears in the telemetry when commanded. This information originates from the APID 1057 packet and is provided on the ATL02 product at its full rate of 200 Hz when present in the telemetry.

It is important to note that the *delta\_time* reported in this group is supplied at 200 Hz and corresponds to a packet which contains 50 azimuth/elevation samples. Thus, the time reported corresponds to the first sample in each of these packets. The size of the azimuth/elevation fields in this packet are 50x the length of the *delta\_time* vector, and are thus reported at a rate of 10 kHz. If desired, the time of each sample in this packet can be reconstructed using the count of azimuth/elevation pairs since the last 1 PPS of the last azimuth/elevation pair in the packet. Conversion information is provided in ATLAS-ALG-TN-0955.

The remaining parameters in this group are *mce\_total\_cycles* and *ds\_50*, which report the total number of MCE cycles and supply a dimension scale (for use in the ATL02 processing software), respectively.

This information applies to the following data groups on the ATL02 product:

- */atlas/housekeeping/mce\_position/*

## 8.6 Radiometry HKT Data (*/atlas/housekeeping/laser\_energy\_\**)

The following groups contain information about the laser energy, as measured from three points of reference (internal, LRS, SPD). The groups each contain pertinent temperature information and the total and individual spot energies as derived from the split of the energy monitor value by the calibration as seen in Chapter 5.2. Values are derived from APIDs 1032, 1123, and 1063 and are reported out as floats at rates of 1 Hz, 50 Hz, and 1 Hz (10 readings), for internal, LRS, and SPD laser energies, respectively. Some thermal values, as supplied via APID 1061, are used in the conversion equations. More information may be found in ATLAS-ALG-TN-0955.

This information applies to the following data groups on the ATL02 product:

- */atlas/housekeeping/laser\_energy\_internal/*
- */atlas/housekeeping/laser\_energy\_lrs/*
- */atlas/housekeeping/laser\_energy\_spd/*

## 8.7 Pointing, Position, & Velocity HKT Data (*/atlas/housekeeping/pointing, position\_velocity*)



The following groups contain information on the pointing, position, and velocity. The data contained in these groups are only downlinked on command. Pointing data originate in APID 1138 (variable rate) and position/velocity data in APID 1137 (1 Hz). Beyond unpacking data, conversion to SI units, and expressing flag values, these remain unmanipulated by the ATL02 processing. More information may be found in ATLAS-ALG-TN-0955.

This information applies to the following data groups on the ATL02 product:

- */atlas/housekeeping/pointing/*
- */atlas/housekeeping/position\_velocity/*

## **8.8 Time at the Tone (*/atlas/housekeeping/time\_at\_the\_tone/*)**

This group contains the spacecraft provided time of day message which includes the GPS time as well as the spacecraft time at the receipt of the 1PPS from the GPS receiver. Both time references are expressed in seconds and subseconds and originate APID 1136. No manipulation is performed between the ATL01 and the ATL02 product.

This information applies to the following data group(s) on the ATL02 product:

- */atlas/housekeeping/time\_at\_the\_tone/*

## **8.9 Algorithm Science Data (*/atlas/pcex/algorithm\_science/*)**

The following groups contain information on the pointing, position, and velocity, and algorithm control parameters. The data originates in APIDs 1137 and 1138 which is generated nominally at 1 Hz. Apart from *delta\_time* (which is computed per Section 8.1), the remainder of these groups' data are flags and counters. Beyond unpacking data, conversion to SI units, and expressing flag values, these remain unmanipulated by the ATL02 processing. More information may be found in ATLAS-ALG-TN-0955.

This information applies to the following data groups on the ATL02 product:

- */atlas/pcex/algorithm\_science/*
- */atlas/pcex/algorithm\_science/s\_w/*
- */atlas/pcex/pmf\_hk*
- */atlas/pcex/dfc\_hk*

## **8.10 PCE Background Data (*/atlas/pcex/background*)**

This group contains information on the total number of time tags, as counted by the ATLAS flight software, in 50 shot segments of a major frame. The data originates in APIDs 1162, 1164, and 1166 and is written to the ATL02 product at a rate of 50Hz. Each set of data in this group is assigned a *delta\_time* which is computed per Section 8.1 and is based on the *delta\_time* of the first shot in each 50-shot segment. In addition to this, the following information is also contained in this group:

- *bg\_cnt\_50shot\_{s/w}*: By-spot total of time tags in the range window, as recorded by the flight software, organized in sets of 50 laser pulses. The resultant data is a pass-through of the data present on ATL01, but in a flattened (i.e. 4n) form. The values reported are inclusive of duplicate tags as well as timetags downlinked via the downlink band.
- *pce\_mframe\_cnt*: Major frame counter value
- *useflag*: Flag indicating the instrument's operational mode.

This information applies to the following data group on the ATL02 product:

- */atlas/pcex/background*

## 8.11 SBC Extrapolation Task Telemetry (*/atlas/pcex/sxp\_ssr\_\**)

This group contains SBC (Single Board Computer) Extrapolation Task telemetry from APIDs 1152 through 1157 for the first set of PCE extrapolation data per major frame, stored at 1 Hz, and the parameters *cosb*, *error\_flags*, *latitude*, *longitude*, *range*, and *srn*, stored at 50 Hz (once per major frame). Each consecutive pair of APIDs is associated with a specific PCE and within the pairs s=strong beam, w=weak beam. The conversion factors for these data are described in ATLAS-ALG-TN-0955.

## 8.12 LRS Data (*/lrs*)

The ATL02 data product provides a pathway for the POD/PPD group to recover pertinent pointing information via the LRS. The following groups are provided for use by the PPD. The following LRS data is decommutated per its ICD (ICESat-2-LRS-IFACE-1794) and is stored in the following groups in the ATL02 data product.

- */lrs/laser\_centroid/*
- */lrs/laser\_image/*
- */lrs/laser\_image/window\_nn/*
- */lrs/laser\_window/*
- */lrs/stellar\_centroid/*
- */lrs/stellar\_image/*
- */lrs/stellar\_image/window\_nn/*
- */lrs/stellar\_window/*
- */lrs/tams\_window/*

The remaining parameters, which are contained in the */lrs/hk\_1120* group, are converted as follows:

- Currents and voltages are converted per the flight-delivered ITOS database (ICESat-2-IT-RPT-4005) and are reported as floats at a rate of 1Hz. Similar to the contents of the other HKT packets, more information on the conversions for these values may be found in ATLAS-ALG-TN-0955.
- Temperatures conversions are summarized in ATLAS-ALG-TN-0955.
- X, Y, Z components of the stellar rate pattern estimate, *srate\_{x/y/z}*, are converted from a 1:23:8 fixed point format (X and Y data) and a 1:15:16 fixed point format (Z data) to a standard number format. Units are pixels (X, Y) or radians (Z) and frame rate is 10Hz.
- All other parameters are flags or counters which remain unmanipulated.

With the exception of the */lrs/laser\_centroid/*, */lrs/stellar\_centroid/*, and */lrs/hk\_1120/* groups, all of the */lrs/\** groups are only telemetered on command.

## 8.13 Spacecraft Data (*/gpsr/\**, */orbit\_info*, */sc/\**)

ATL02 acts as a conduit for spacecraft provided data. This includes information on the GPS receiver, orbit info, and other spacecraft hardware groups. This information is decommutated, and in some cases converted, per ATLAS-ALG-TN-0955 and is stored in the following groups in the ATL02 data product.

This information applies to the following data groups on the ATL02 product:

- */gpsr/*
- */gpsr/carrier\_amplitude/*
- */gpsr/carrier\_phase/*
- */gpsr/channel\_status/*
- */gpsr/code\_phase/*
- */gpsr/hk/*
- */gpsr/navigation/*
- */gpsr/noise\_histogram/*
- */gpsr/time\_correlation/*
- */orbit\_info/*
- */sc/*
- */sc/attitude\_control\_system/*
- */sc/ephemeris/*
- */sc/hk/*
- */sc/inertial\_measurement\_unit/*
- */sc/inertial\_measurement\_unit/gyro\_abcd/*
- */sc/solar\_array/*
- */sc/star\_tracker/*
- */sc/star\_tracker/optical\_head\_1/*
- */sc/star\_tracker/optical\_head\_2/*

## 8.14 Quality assessment (*/quality\_assessment*)

The */quality\_assessment/* group and all of its subgroups contain the various flags and outputs of ASAS's internal QA code that is run as part of the ATL02 generation process. These subgroups include:

- */quality\_assessment/along\_track/\**: Along-track statistics. Includes count per interval of the number of duplicates, strong RX, weak RX, TEP, and TX events for each PCE. Also reports number of samples and summary statistics (i.e., min, max, average, and standard deviation) for TX LL and TX "other" elements listed on the ATL02 product.
- */quality\_assessment/record\_counts/*: Number of inputs, by packet type, processed during creation of ATL02.
- */quality\_assessment/record\_counts/pcex/*: Number of major frames, DFC HK, ATM strong/weak, and PMF related inputs processed during the creation of ATL02.
- */quality\_assessment/summary/*: Summary statistics of TOD periods for various packet types.
- */quality\_assessment/summary/pcex/*: Various counts and summary statistics related to the TOF and TOD computations outlined in this document.

In addition to the */quality\_assessment/\** groups written on the ATL02 product, the ASAS code also generates a QA file as part of its default processing efforts. As applicable for each parameter, the QA file provides information such as number of samples evaluated, basic statistics (min/max/mean/stddev), as well as error and counter values.

## Appendix A – Referenced Documents

The following documents were consulted in the writing of this ATBD:

**Table 52: Referenced Documentt**

| MIS/TDMS Doc #           | MIS/TDMS Alt Doc #                                 | Title  |
|--------------------------|--|--|
| ATLAS-ALG-TN-0955        | N/A  | Cross-Reference Table for ITOS, ATL01, and ATL02 Labels  |
| DN-ICESat2-SYS-024       | N/A  | Ancillary Telemetry Packet Description (Spacecraft)  |
| ICESat-2-OSCI-TN-0953    | N/A  | Behavior of the Return Event Population at the Boundaries of the Downlink Band                                     |
| ICESat-2-ALG-PROC-0675   | ICESat-2-ALG-PROC-3899                             | ATLAS Flight Science Receiver Algorithms   |
| ICESat-2-ATSYS-HDBK-0023 | ICESat-2-ATSYS-HDBK-3431                           | ATLAS Flight Software User Guide   |
| ICESat-2-ATSYS-TN-0044   | ICESat-2-ATSYS-TN-0502                             | ATLAS Architecture Description Document  |
| ICESat-2-ATSYS-TN-0073   | ICESat-2-ATSYS-TN-0660                             | ATLAS Monthly Technical Budget Report  |
| ICESat-2-ATSYS-TN-0090   | ICESat-2-ATSYS-TN-0910                             | ATLAS Spots, Channels and Redundancy Assignments   |
| ICESat-2-ISF-ANYS-0209   | ICESat-2-ISF-ANYS-5400                             | Computation of start time correction coefficients  |
| ICESat-2-LRS-ICD-0054    | ICESat-2-LRS-IFACE-0744<br>ICESat-2-LRS-IFACE-1794 | ATLAS LRS Command and Data ICD   |
| ICESat-2-MEB-SPEC-0031   | ICESat-2-MEB-SPEC-0688                             | ICESAT-2 ATLAS MEB Housekeeping and Thermal Field Programmable Gate Array Specification                            |
| ICESat-2-MEB-SPEC-0063   | ICESat-2-MEB-SPEC-0875                             | ATLAS MEB Photon Counting Electronics (PCE) Data Flow Controller (DFC) Field Programmable Gate Array Specification |
| ICESat-2-SCI-TN-0958     | N/A  | Computation of the ICESat-2 Range Vector   |
| ICESat-2-SCSYS-CDRL-0151 | 6145510000R0<br>ICESat-2-SCSYS-CDRL-1258           | [CDRL SE-9A] 1553 Interface Control Document (ICD)   |
| ICESat-2-SIPS-SPEC-0139  | ICESat-2-SIPS-SPEC-1595                            | SIPs: Precision Pointing Determination (PPD) Products Level 5 Specification Document                               |
| ICESat-2-SIPS-SPEC-0141  | ICESat-2-SIPS-SPEC-1601                            | SIPs: Level 1A Products L5 Specification Document (ATL01)  |
| ICESat-2-SIPS-SPEC-0142  | ICESat-2-SIPS-SPEC-1602                            | SIPs: Level 2A Products L5 Specification Document (ATL03)  |
| ICESat-2-SIPS-SPEC-0213  | ICESat-2-SIPS-SPEC-2325                            | ATLAS Science Algorithm Software Design Description (SDD) – Volume 6 (atlas_11b)                                   |
| ICESat-2-SIPS-TN-0957    | N/A  | Summary of "Effective T0" Determination Technique  |
| N/A - Accessible via ISF | N/A  | ATL01 Data Dictionary  |
| N/A - Accessible via ISF | N/A  | ATL02 Data Dictionary  |
| N/A - Accessible via ISF | N/A  | ATL03 Data Dictionary  |

## Appendix B –Construction of Unique Photon Identifiers

Occasionally, it may be desired to trace the heritage of a specific RX entry in ATL02 to a specific entry on ATL01 or ATL03. The ATL02 product stores all data necessary to accomplish this in both the */atlas/pcex/altimetry/s\_w/photons* and */atlas/pcex/tep* groups, both of which are written out at the photon rate. The relevant parameters are as follows:

**Table 53: ATL02 Parameters Used to Provide Unique Photon Identification**

| Parameter             | Description               | Provides Heritage of...   |
|-----------------------|---------------------------|---|
| <b>pce_mframe_cnt</b> | Major frame counter       | Major frame; value is common to strong and weak spots, rolling over every ~2.7 years                            |
| <b>ph_id_channel</b>  | Logical return channel ID | Aggregate of Spot, Detector Side, Channel, and Toggle. A summary of ph_id_channel mappings is seen in Table 16. |
| <b>ph_id_pulse</b>    | Laser pulse counter       | TX within major frame   |
| <b>ph_id_count</b>    | Photon event counter      | # of RX for a given TX on a per channel basis   |

When viewed in aggregate, the *pce\_mframe\_cnt*, *ph\_id\_channel*, *ph\_id\_count*, and *ph\_id\_pulse* parameters provide a unique identifier for an RX. Because of this, this information is maintained in the ATL01 and ATL03 products as well. A mapping of equivalent fields across the three products can be seen in Table 54: Mapping of Equivalent Data Parameters Across ATL01, ATL02, and ATL03.

**Table 54: Mapping of Equivalent Data Parameters Across ATL01, ATL02, and ATL03**

| Parameter<br>Description         | ATL01 Path<br><i>/atlas/pcex/a_alt_science_ph/</i> | ATL02 Path<br><i>/atlas/pcex/altimetry/s_w/photons/</i> | ATL03 Path<br><i>/gtx/heights/</i> |
|----------------------------------|--|---|------------------------------------|
| <b>Major frame counter</b>       | <i>raw_pce_mframe_cnt</i>                          | <i>pce_mframe_cnt</i>                                   | <i>pce_mframe_cnt</i>              |
| <b>Logical return channel ID</b> | <i>ph_id_channel</i>                               | <i>ph_id_channel</i>                                    | <i>ph_id_channel</i>               |
| <b>Laser pulse counter</b>       | <i>ph_id_pulse</i>                                 | <i>ph_id_pulse</i>                                      | <i>ph_id_pulse</i>                 |
| <b>Photon event counter</b>      | <i>ph_id_count</i>                                 | <i>ph_id_count</i>                                      | <i>ph_id_count</i>                 |

Finally, note that while every photon event in ATL03 has a history back to the corresponding ATL01 and ATL02 files, not all events in ATL01 appear in ATL02 or ATL03. This is due to successively higher level products utilizing checks which result in data being excluded from the product due to a failed QA or similar check.